FUNCTIONS OF SINGLE-CHAIN VARIABLE FRAGMENTS IN *IN VITRO* VISUALIZATION AND *IN VIVO* MODULATION OF PLANT CELL WALL POLYSACCHARIDES

by

SI ZHANG

(Under the Direction of Michael G Hahn)

ABSTRACT

Plant cell walls are known as a highly complex and dynamic structure that encloses each cell in a plant. As of now, most research on cell walls is performed using biochemical analysis of fractionated walls and immunolabeling of fixed tissues. These techniques are difficult to apply to the study of temporal and developmental changes in plant cell walls. Antibodies that recognize plant cell wall polysaccharides have been developed as probes for cell wall analysis *in vitro* because they are intrinsically specific toward polysaccharides structures. If the genes encoding the antibodies can be obtained, they should be easy for heterologous expression and simple for modification with fluorescent protein markers.

ScFvs are single polypeptide fragments of antibodies that are composed of the variable regions of the heavy (V_H) chain and the light (V_L) chain with a flexible peptide linker between. ScFvs may be more easily applied to the labeling of plant cell walls *in vitro* if they are able to retain the binding specificity and affinity of their parent antibody. In the work reported here, scFvs were generated from genes encoding several plant cell wall glycan-directed monoclonal antibodies. Enzyme-linked immunosorbent assay, or ELISA showed

that twelve of the heterologously expressed scFvs have largely similar binding specificities, although perhaps weaker binding affinity than their parent antibodies. One expressed scFv had no activity at all. The expressed scFv genes also yielded proteins that could be used to label cell walls in sectioned plant tissues. The immunolabeling results confirmed the weaker binding affinity of scFvs.

Heterologous expression of scFvs *in planta* resulted in modulations of polysaccharide functions in plant cell walls. The *in vivo* expression of scFv-M1:YFP in *Arabidopsis* plants resulted in hypoplasia at the stages of seedling and/or vegetative growth, and withering in the early stage of floral budding. Transgenic scFv-M140:YFP plants displayed a stem-lodging phenotype, suggesting that although the scFv-M140:GFP displayed no activities *in vitro* it still affected the plant cell wall polysaccharides network to effect plant growth and developmental processes. These results indicate that expression of a specific scFv in *Arabidopsis* may lead to changes in the composition and/or structure of the cell wall, which consequently, may cause an impact on the development and/or morphological phenotype of the plant.

INDEX WORDS: single-chain variable fragment (scFv), plant cell wall, *in vitro* visualization tool, immunolabeling,

FUNCTIONS OF SINGLE-CHAIN VARIABLE FRAGMENTS IN *IN VITRO* VISUALIZATION AND *IN VIVO* MODULATION OF PLANT CELL WALL POLYSACCHARIDES

By

SI ZHANG

B.S. Sichuan University, China, 2006

M.S. Oklahoma State University, Oklahoma, United States, 2011

A Dissertation Submitted to the Graduate Faculty of The University of Georgia in Partial Fulfillment of the Requirements for the Degree

MASTER OF SCIENCE

ATHENS, GEORGIA

2019

FUNCTIONS OF SINGLE-CHAIN VARIABLE FRAGMENTS IN *IN VIVO* VISUALIZATION AND *IN VIVO* MODULATION OF PLANT CELL WALL POLYSACCHARIDES

by

SI ZHANG

Major Professor: Michael G Hahn

Committee: Alan G Darvill

Will S York

Electronic Version Approved:

Suzanne Barbour
Dean of the Graduate School
The University of Georgia
May 2019

DEDICATION

This dissertation is dedicated to my parents and my wife for their forever love and unconditional support.

ACKNOWLEDGEMENTS

First and most importantly, I would like to express my gratitude and appreciation to my mentor, Dr. Michael G Hahn, for giving me the opportunity to study and work in his group with an extraordinary environment. I am sincerely grateful to his constant guidance, support and encouragement throughout all the years of my graduate study.

I would like to thank my committee, Dr. Alan G Darvill and Dr. William S York for their invaluable time and expertise. I would also like to thank Dr. Kelley Moremen and Dr. Debra Mohnen, for their countless help.

I would like to thank Dr. Jeong-Yeh Yang for her support in expressing scFvs, and Stefan Eberhard for his great help in plant growing tissue harvesting, fixation, embedding and sectioning plant issue.

I also would like to give my thanks to the past and present members of the Complex Carbohydrate Research Center: Yingzhen Kong, Sivakumar Pattathil, Utku Avci, Fangfang Fu, Claudia L. Cardenas, Ron Clay, Christina Hopper, Sivasankari Venketachalam, Sindhu Kandemkavil, Ann (Zhangyin) Hao, Li Tan, Angelo Peralta, Maria Soto, Hsin-Tzu Wang. Best wishes in their future endeavors.

Last but not least, I would like to thank my family and all my friends for their love and support.

TABLE OF CONTENTS

LIST OF TABLES

Page

LIST OF FIGURES

Page

CHAPTER I

INTRODUCTION

Plant Cell Wall

The plant cell wall is the extracellular matrix which surround plant cells. It is semi-rigid and complex and largely composed of polysaccharides, many of which have complex structures (Hayashi, Koyama et al. 1988). One of its known functions is to defines the shape and size of the cell (McNeil, Darvill et al. 1984). It has different physical and chemical properties, which are important in many plant developmental processes, such as growth, proliferation, and fruit and vegetable ripening (Bauer, Talmadge et al. 1973, Keegstra, Talmadge et al. 1973, Talmadge, Keegstra et al. 1973). It is also reliable sources for natural textile fibers, paper and wood products, human nutrition, animal feedstock, and raw materials for biofuel production (Somerville 2007).

Plant cell walls are typically classified into two types: primary cell walls and secondary cell walls. Previous studies found that both primary and secondary cell walls are mainly composed of cellulose, hemicelluloses and pectins, in different proportions. Secondary cell wall also contains some lignin. They have different structures and functions. Primary cell walls surround growing and expanding cells. Usually, the main components of primary cell walls in plant tissues and cells are polysaccharides. In addition, there are some other components, such as proteins (e.g. enzymes), glycoproteins (e.g. hydroxyproline-rich extensins), phenolic esters (e.g. ferulic and coumaric acids),and ionically and covalently bound minerals (e.g. calcium and boron) (Selvendran and O'Neill 1985). These minor components are important for cell functions. For

example, protein expansins are supposed to regulate wall expansion (Cosgrove 2001). The main functions of primary cell wall are: i) providing structural and mechanical support to the cell; ii) defining and maintaining shape and size of cell; iii) resisting internal expanding pressure to cell; iv) controlling rate and direction of growth; v) determination for plant architecture and form; vi) regulation of material diffusion through apoplast; vii) storage for carbohydrate - walls of seeds could be metabolized if necessary; viii) protection against pathogens, dehydration and other environmental factors; ix) producing and transferring biologically active signals; and x) - interaction between cells. It is also known that plant-derived foods contain much primary cell walls, or the polysaccharides which are the major components of primary cell walls (Albersheim 1976).

Secondary cell walls are much stronger and thicker than primary cell walls. They are the main constituent of plant biomass (Albersheim 1976). Their main function is to provide mechanical support. Thus, secondary walls are usually found in specialized cells, such as tracheary elements, fibers and other sclerenchymatous cells. Previous studies suggest lignin and xylan are associated by different types of covalent bonds in the secondary cell wall. The formed network eliminates water from the cell wall to make secondary cell wall hydrophobic (Niklas, Cobb et al. 2017). These covalent bonds include ester linkages between glucuronoxylans and lignin via benzyl ester bonds with the carboxylate group of 4-O-methylglucuronic acid. The second-most reported type of covalent bonds between xylan and lignin are ether linkages that involve L-arabinofuranose side chains or xylose units. Other covalent linkages likely to interconnect xylan with lignin in the cell wall are oxygen-containing bonds, acetals, and glycosides (Joseleau, Cartier et al. 1992).

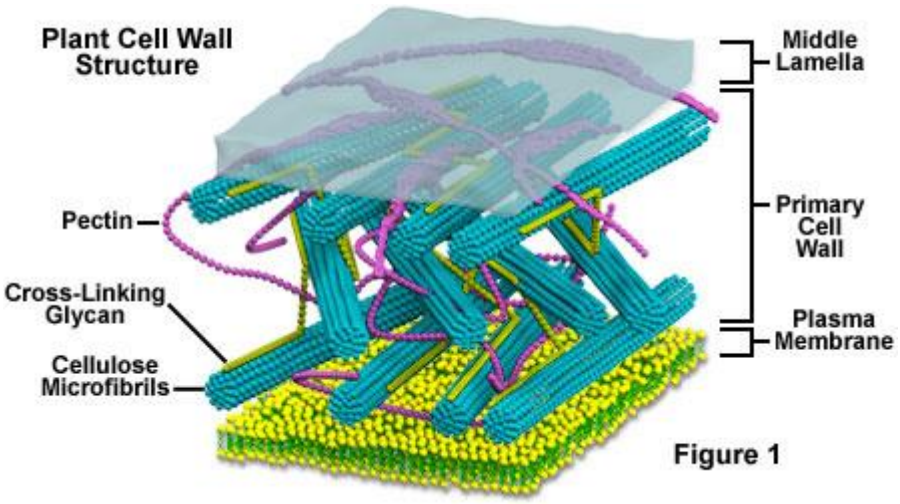

Figure 1.1 Plant cell wall structure.

Cartoon of plant cell wall structure. Adapted from

https://micro.magnet.fsu.edu/cells/plants/cellwall.html

The following sections provide a brief overview of the structural complexity of several important classes of non-cellulosic plant cell wall polysaccharides that will be the focus of the studies reported here.

Xyloglucan

Xyloglucans consist of a β-1,4-linked glucan backbone, with substitution of xylosyl residues. In different plant families and specific tissues, the xylosyl residues can be further substituted with different glycosyl and/or non-glycosyl substituents (Pauly and Keegstra 2016). Xyloglucans compose approximately 20% of leaf cell walls in dicots, which makes it the most abundant hemicellulosic polysaccharide in these plants (Zablackis, Huang et al. 1995). Previous studies found xyloglucan works as a structurally important glycan (Carpita and Gibeaut 1993). It is thought to cross-link and tether cellulose microfibrils. These features have led to the

hypothesis that xyloglucans and cellulose form the basic load-bearing framework of type I cell walls (Carpita 1996). Xyloglucan exists in different locations at different developmental stages, such as cell plates in dividing cells (Moore and Staehelin 1988), the primary walls in growing cells, and completely differentiated secondary walls.

Previous studies suggested that xyloglucan synthesis occurs in the Golgi apparatus (Hayashi 1989, Zhang and Staehelin 1992, Perrin, DeRocher et al. 1999, Chevalier, Bernard et al. 2010, Davis, Brandizzi et al. 2010, Chou, Pogorelko et al. 2012). However, the exact locations of the several xyloglucan biosynthetic enzymes within the Golgi apparatus is still vague. And there are different opinions about where the backbone synthesis occurs. Chou suggested it occurs in the *trans*-Golgi compartment (Chou, Pogorelko et al. 2012), while some other scientists indicated it begins in the *cis*-Golgi compartment (Brummell, Camirand et al. 1990, Davis, Brandizzi et al. 2010). After the synthesis in the Golgi apparatus, xyloglucan is packaged into secretory vesicles and transported to the plasma membrane, where xyloglucan is released into the extracellular matrix. (Figure 1.2)

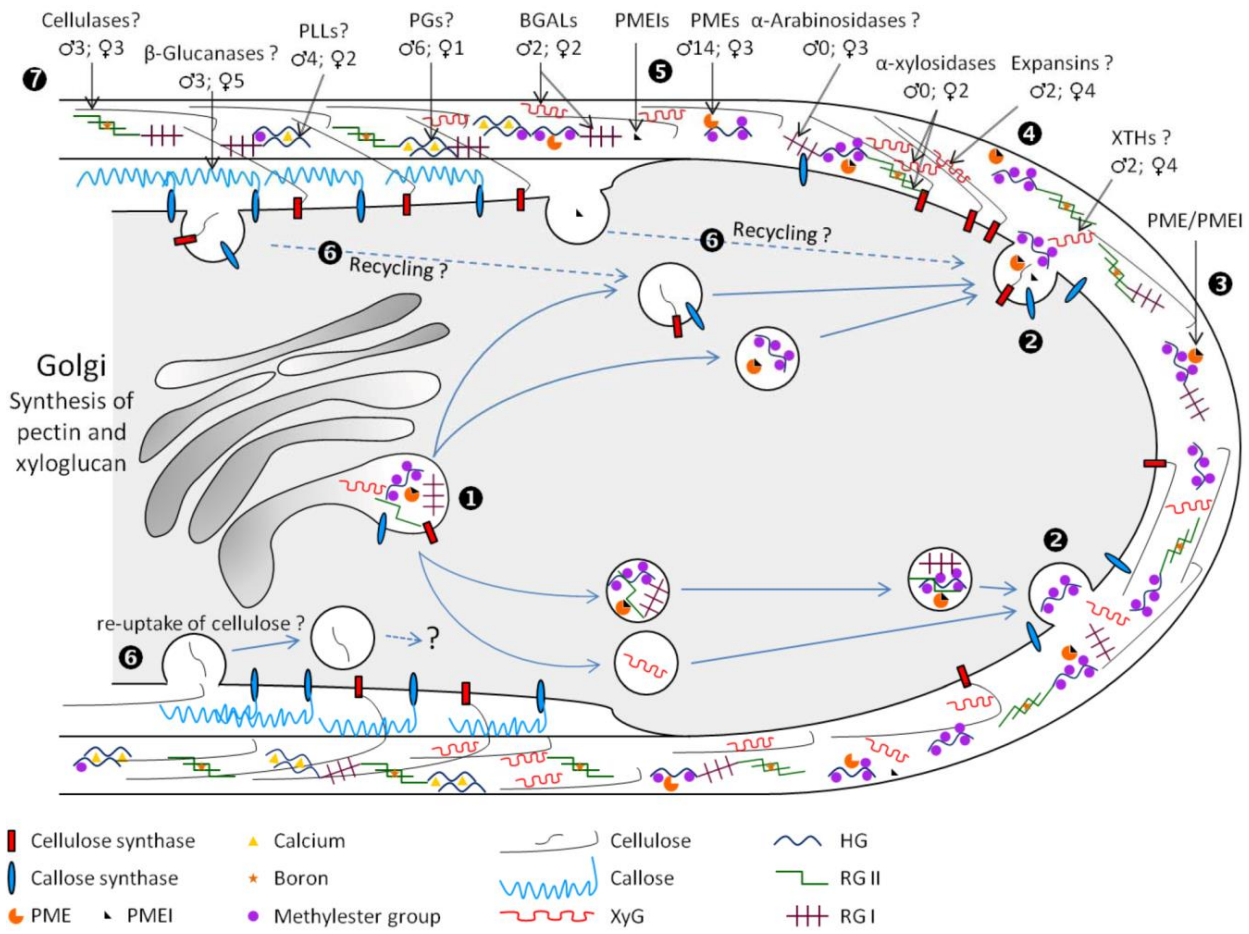

Figure 1.2 Overview of xyloglucan and pectin biosynthesis

Adapted from Figure 4 of (Mollet, Leroux et al. 2013)

Xylan

All land plant xylans are composed of a β-1,4-linked D-xylopyranosyl main chain with a variable number of neutral or uronic monosaccharide substituents or short oligosaccharide side chains (Bajpai 1997). Xylans of marine algae show different chemical structure based on a ß-1,3-linked D-xylosyl backbone. The structure becomes more complex with increases in the number of substituting mono- and oligosaccharides attached to the β-1,4-linked xylosyl main chain. The substitutions of monosaccharide residues include α-1,2-linked glucuronic acid (GlcA), α-1,2-

linked 4-O-methylglucuronic acid (MeGlcA), and α-1,2 and/or α-1,3-linked arabinose (Ara) (Ebringerova 2000). Unbranched linear xylan homopolysaccharides from land plants are very rare to find. In the secondary cell wall of dicots, xylan is the predominant hemicellulose, but little is found in primary cell walls. Dicot xylan molecules possess reducing-end sequences of the tetrasaccharide 4-β-D-Xyl-(1–4)-β-D-Xyl-(1–3)-α-L-Rha-(1–2)-α-D-GalA-(1–4)-D-Xyl, which is believed to act as either as an initiator or terminator of xylan backbone synthesis (York and O'Neill 2008).

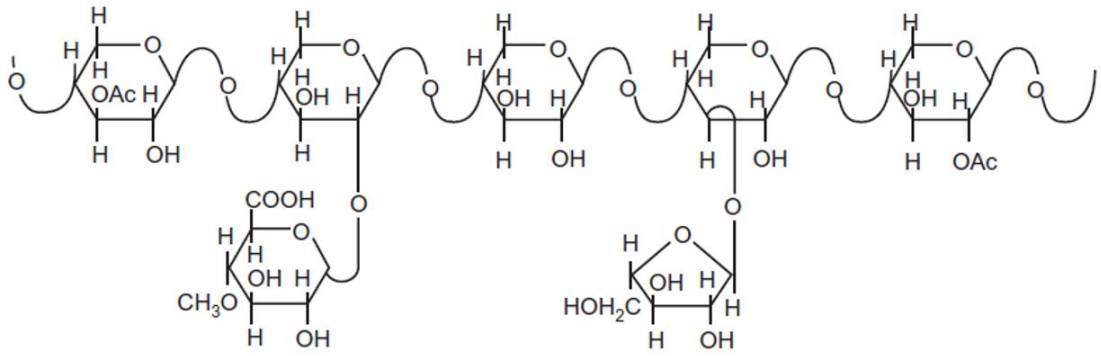

Figure 1.3 A hypothetical structure of plant xylan.

Adapted from *Xylanolytic Enzymes* (Bajpai 2014)

Synthesis of the xylan backbone requires *Irregular Xylem (IRX) 9* and *IRX14*, both of which belong to the Glycosyltransferase Family 43 (GT43), and *IRX10*, which is a member of GT47 encoding putative xylosyltransferases. Some other genes *IRX9-like (IRX9-L)*, *IRX10-L*, and *IRX14-L* appear to encode functionally redundant paralogs (Brown, Goubet et al. 2007, Lee, O'Neill et al. 2007, Wu, Hornblad et al. 2010). Previous studies suggested that *IRX10* and *IRX14* exist in the same xylan synthase complex (Zeng, Jiang et al. 2010). Two members of the GT8 family, Glucuronic Acid Substitution of Xylan (GUX) 1 and GUX2 are required for the GlcA substitutions on xylans in the *Arabidopsis* secondary cell wall (Mortimer, Miles et al. 2010,

Oikawa, Joshi et al. 2010, Rennie, Hansen et al. 2012). GXMT1, a protein containing a Domain of Unknown Function 579 (DUF579), transferred 4-*O*-Methyl groups from S-adenosyl-methionine to GlcA residues (Lee, Teng et al. 2012, Urbanowicz, Pena et al. 2012). Previous studies indicated GT61 family that are likely to add arabinosyl residues to the xylan backbone (Anders, Wilkinson et al. 2012). Another GT61 enzyme, a xylosyltransferase is responsible for xylose linked to O-2 of feruloylated arabinosyl residues (Chiniquy, Sharma et al. 2012), as well as some acyltransferases of the BAHD family (Piston, Uauy et al. 2010, Bartley, Peck et al. 2013). A number of additional glycosyltransferases known as IRX7/FRA8 (and the homolog IRX7L/F8H), IRX8/ GAUT12, and PARVUS/GATL1 may also be involved in synthesis of xylan by synthesizing the reducing end which may function as a type of terminator (York and O'Neill 2008).

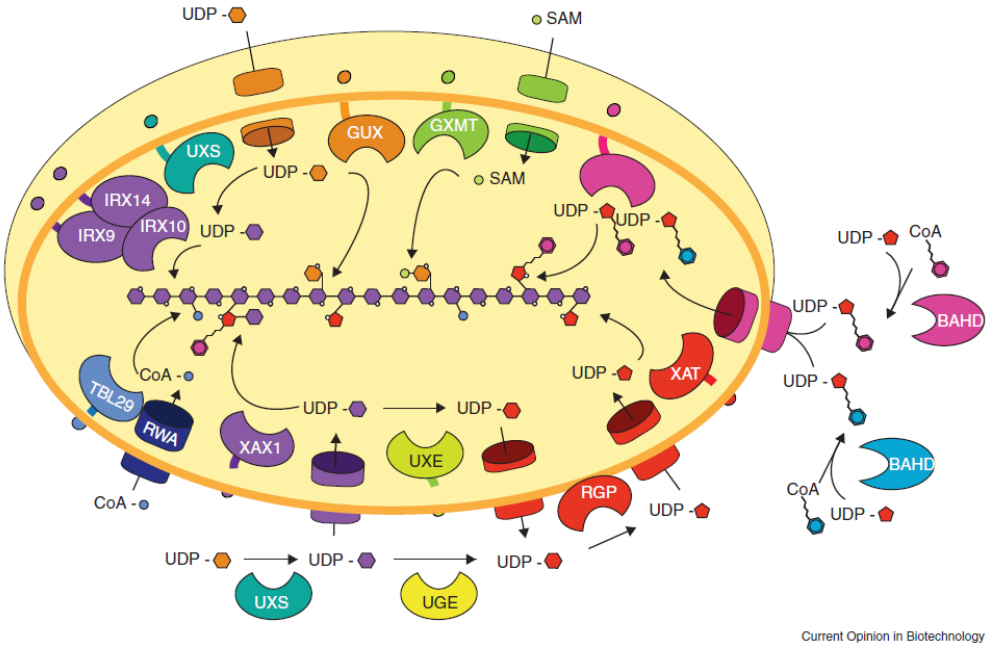

Figure 1.4 General view of xylan synthesis.

Adapted from *Xylan Biosynthesis* (Rennie and Scheller 2014).

Rhamnogalacturonan-I

Rhamnogalacturonan-I (RG-I) comprises 20-35% of pectic polysaccharides. This term refers to a group of closely related cell wall pectic polysaccharides that have a backbone composed of the repeating disaccharide (1-2)-α-L-rhamnosyl-(1-4)-α-D-galacturonic acid (GalA)(McNeil, Darvill et al. 1980, Lau, McNeil et al. 1985). Usually the O-2 and O-3 positions of the GalA residue on the backbone are acetylated (Komalavilas and Mort 1989), while various neutral sugars branches of mainly D-galactose and L-arabinose are attached to O-4 of rhamnose (Lau, McNeil et al. 1985, Stevenson, Darvill et al. 1988). The nature of the sidechains depends on the origin of the pectin (Buchanan, Gruissem et al. 2000), the stage of cell growth, and tissue development (Oomen, Doeswijk-Voragen et al. 2002). The function of RG-I is still little known and no RGI has been fully characterized (Ridley, O'Neill et al. 2001, Willats, McCartney et al. 2001).

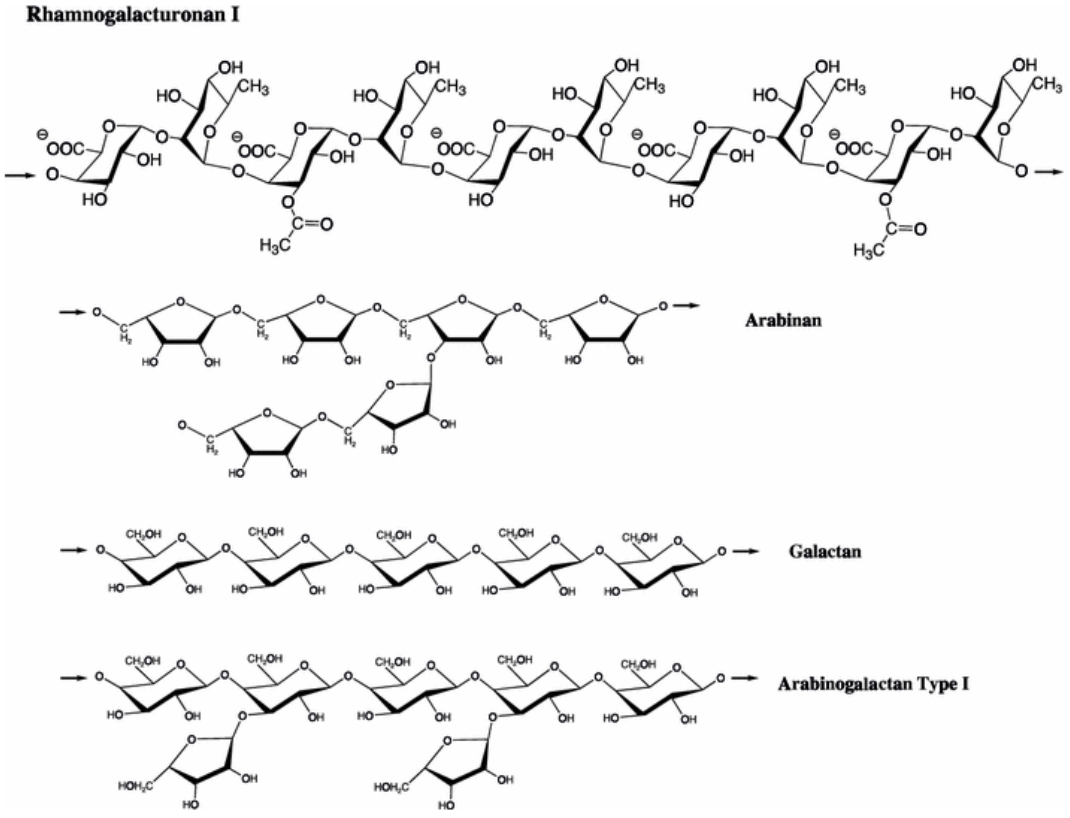

Figure 1.5 Three types of rhamnogalacturonan I side chains.

Side groups attached to the C4 position of the rhamnopyranosyl residue: (1→5)-α-L-arabinans, (1→4)-β-D-galactan, and arabinogalactan Type I (Wong 2008)

Homogalacturonan

Homogalacturonan is a linear chain composed of 85-320 α-1-4-D galactosyluronic acid residues. Though it is simple and smooth, it is the most abundant pectic structural domain and composes nearly 65% of the pectin in plant cell walls. Up to 80% of the carboxyl groups of the GalA residues are esterified with methanol at C-6 while the O-2 and O-3 position of hydroxyl groups could be acetylated (Ishii 1997, O'Neill, Albersheim et al. 1990, Pauly and Scheller 2000).

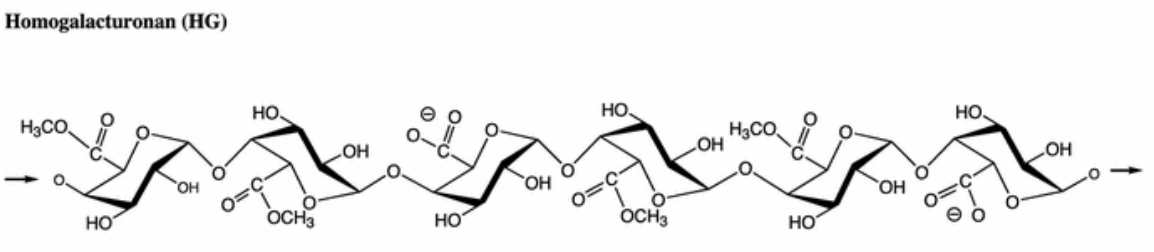

Figure 1.6 Homogalacturonan with methyl esterification (Wong 2008)

Monoclonal Antibodies against Polysaccharides

The defense system of animals employs antibodies to identify and neutralize foreign objects. The most significant feature of an antibody is the antigen-binding site, which recognizes a specific structure unique to its target. The antigen-binding sites, also known as the paratope, binds specifically to an epitope which is from the antigen (Ahmad, Yeap et al. 2012). The immune system directs an antibody to tag a microbe or an infected cell and also to directly neutralize its target (C. A. Janeway 2001).

In the past decades, the genetic manipulation of antibody fragments has advanced. The development not only helps us understand the structure and functional organization of immunoglobulins, but impels the technology of engineered antibody molecules for research, diagnosis, and therapy. Having the immunoglobin gene sequence can also allow for the improvement of the affinity and specificity of antigen binding by mimicking somatic hypermutation (Gram, Marconi et al. 1992).

Previous studies found that monoclonal antibodies (mAbs) can be generated against polysaccharides from multiple source, including bacteria capsular polysaccharides (Robbins, Parke et al. 1973), plant polysaccharides such as starch and ulvan (Rydahl, Krac Un et al. 2017),

and fungal polysaccharides (Drouhet and Latge 1988). The most popular application is using the antibodies as protections against detrimental bacteria, such as *Haemophilus influenzae* Type b and *Streptococcus pneumoniae* (Mikolajczyk, Concepcion et al. 2004), *Streptococcus suis* (Gottschalk, Xu et al. 2010). The efficacy of protection of the different immunoglobulin (Ig) classes against bacterial infection is determined by the specificity and affinity with the targeted antigen and on their biological functions. IgG2b, IgG2c, and IgG3 in mice are categorized as "type 1 IgG subclasses" because they are associated with gamma interferon (IFN-γ)-dominant Th1 immune responses The type 1 IgG subclasses are particularly effective at mediating bacterial lysis by triggering the complement cascade directly at the surface of the pathogen or by activating bacterial opsonophagocytosis (Calzas, Lemire et al. 2015).

MAbs and scFvs as Tools for Cell Wall Characterization

Because of their high structural complexity, research on polysaccharides requires the development of novel probes for further insight. There are two types of important molecular probes to detect and dissect cell wall structures in plant material, mAbs (Pennell and Roberts 1995) and carbohydrate-binding modules (CBMs) (Hervé, Marcus et al. 2010). Previous research in recent years revealed that mAbs against cell wall polysaccharides have become important tools in the study of plant cell wall structure and function (Knox 2008, Pattathil, Avci et al. 2015). In 2010, the Hahn Lab reported the generation of ~170 plant cell wall glycan-directed monoclonal antibodies to facilitate in-depth analysis of cell wall glycans (Pattathil, Avci et al. 2010). These mAbs were grouped based on the polysaccharide recognition patterns observed, including arabinogalactans (both protein- and polysaccharide-linked), pectins (homogalacturonan, rhamnogalacturonan I), xyloglucans, xylans, mannans, and glucans. Most of

these mAbs displayed epitope-specific binding patterns. Thus, the more than 200 glycan-directed antibodies from various laboratories are able to serve as a large and diverse set of probes for studies of plant cell wall structure, function, dynamics, and biosynthesis (Pattathil, Avci et al. 2015). Indeed, these tools have been used by many laboratories to monitor changes in primary wall composition and organization at the cellular and sub-cellular level (Knox 1997, Bush and McCann 2002, Freshour, Bonin et al. 2003).

ScFvs, single-chain variable fragments, are known as the smallest immunoglobulin molecules having the ability of antigen-binding. They are made up of the variable regions of heavy (V_H) chain and light (V_L) chain, with a flexible peptide linker expressed between them to link them together. The flexible peptide linker is quite important in determining the properties of the scFv, e.g. affinity and binding specificity (Griffiths and Duncan 1998). Its length is critical in correct folding of the mature peptide. Previous studies estimated that the length must be at least 3.5 nm in order for the heavy and light chains to form an intact binding site (Huston, Mudgett-Hunter et al. 1991). The amino acid composition of peptide linker is also important because the peptide linker must be hydrophilic to avoid intercalation during the protein folding process (Argos 1990). Currently, the most common sequences used for peptide linkers mainly contains Gly and Ser which are for flexibility (J. S. Huston 1988). The order of domain, which is V_L-linker-V_H or V_H-linker-V_L, has been studied in both ways. The expression of ScFv in *Pichia pastoris* has been found to prefer the V_L-linker-V_H configuration (Luo, Mah et al. 1995), while other expression systems prefer V_H-linker-V_L, including mammalian and yeast cells (Ho, Nagata et al. 2006), plant cells (Galeffi, Lombardi et al. 2006) and insect cells (Choo, Dunn et al. 2002). Some scFv antibody can be expressed as correctly folded and directly active proteins while

others aggregate in cells, which requires refolding to become active. The most popular expression system for scFvs is *E. coli* (Baneyx 1999).

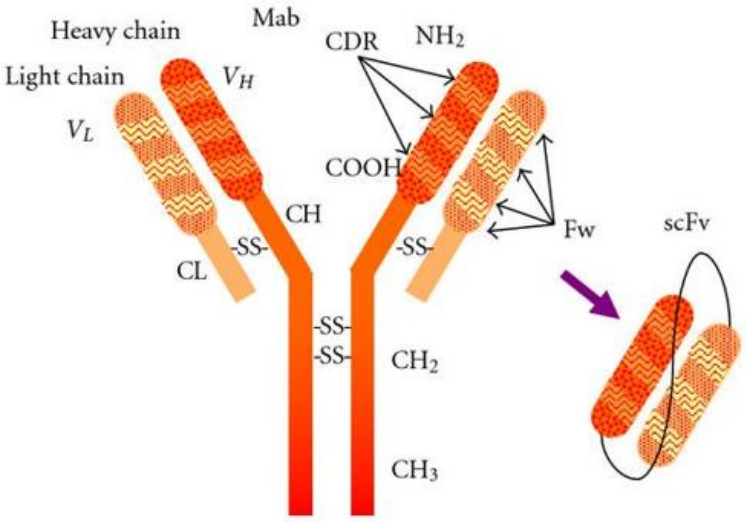

Figure 1.7 The structure of antibody and scFv.

The scFv is generated of V_H and V_L with a linker between. Adapted from *scFv Antibody: Principles and Clinical Application* (Ahmad, Yeap et al. 2012)

ScFv are generated from antibodies produced by hybridoma cells (J. S. Huston 1988, Chaudhary, Batra et al. 1990, Deng, Nesbit et al. 2003, Galeffi, Lombardi et al. 2006), spleen cells from immunized mice (Chaudhary, Queen et al. 1989, Clackson, Hoogenboom et al. 1991, Finlay, Shaw et al. 2006), and B lymphocytes from human (Marks, Hoogenboom et al. 1991, Shadidi and Sioud 2001, Zhang, Gou et al. 2006). Nowadays, scFvs are popular tools against hapten (Kobayashi, Ohtoyo et al. 2005), protein (Dai, Zhu et al. 2003, Guo, You et al. 2003), carbohydrate (Ravn, Danielczyk et al. 2004, Sakai, Shimizu et al. 2007), receptor (Galeffi, Lombardi et al. 2006), tumor (Shadidi and Sioud 2001, He, Zhou et al. 2002) and virus (Hu, O'Dwyer et al. 2005) antigens.

The Hahn lab has generated a library of more than 170 monoclonal antibodies, using plant polysaccharides as the immunogens. One disadvantage of the monoclonal antibodies is their size, particularly for IgMs (which are frequently generated when using glycan immunogens) that have a molecular mass of about 10^6 Daltons. In order to get a smaller molecule while maintain the antigen-binding functions, we decided to generate scFvs for 49 antibodies that represent a broad cross-section of binding specificities across the entire antibody toolkit that had been generated in the Hahn lab.

The basic strategy to produce scFvs from a given antibody is to clone the V_H and V_L domains separately and then to generate a gene fusion using a sequence encoding a linker peptide of 15 or 16 amino acids to connect the two immunoglobin domains. The linker of length shorter than 12 amino acid would impact the V_H domain's binding ability to its attached V_L domain in the Fv orientation (Atwell, Breheney et al. 1999).

CHAPTER II

MATERIALS AND METHODS

pDONR221

pDONR221 is a commercial plasmid from Invitrogen. It is a highly efficient as a donor plasmid for Gateway cloning technology. The map is available below, and the sequence is also available online. It has a pUC origin for high plasmid yield, around 500~700 copies per cell (Lin-Chao, Chen et al. 1992). pDONR221 has a Kanamycin resistance gene for selection in *E. coli*. For sequencing, it has universal M13 Forward and Reverse priming sites. The recombination sites are *att*P1 and *att*P2. The *ccd*B locates between these two *att*P sites for negative selection. The *ccd*B gene interferes with the activity of DNA gyrase by forming a covalent GyrA-DNA complex that cannot be resolved, thus promoting breakage of plasmid and chromosomal DNA. Thus, the *ccd*B gene is lethal to wild type *E. coli* (Bernard and Couturier 1992). As a result, the pDONR221 cannot be propagated in standard *E. coli* which is widely used for cloning, such as DH5α or TOP10. Instead, a special strain, such as DE3.1 or *ccd*B Survival^{TM} (Invitrogen) is used because it contains a mutant version of DNA gyrase (gyrA462) which is resistant to the toxic effects of *ccd*B.

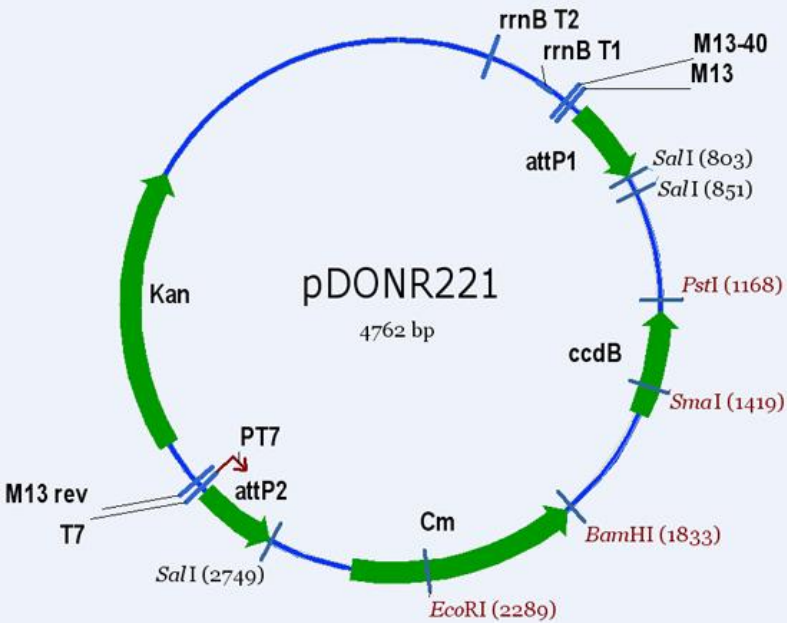

Figure 2.1 map of pDONR221

Map of pDONR221. Adapted from

https://cnrgv.toulouse.inra.fr/Media/Images/images_vecteurs/pDONR221.

pGEc2-DEST

pGEc2-DEST is a gift from Dr. Kelley Moremen, Carbohydrate Complex Research Center, Department of Biochemistry and Molecular Biology, University of Georgia. It is a mammalian expression vector with a CMV promoter and C-terminal Superfolder GFP, AviTag and 10xHis tag. Its parent plasmid is pXKM, a derivative of pMA. The map is available below, and the sequence is available online (http://dnasu.org/DNASU/GetVectorDetail.do?vectorid=550). It has an Ampicillin resistance gene for selection in *E. coli*. The recombination sites are *att*R1 and *att*R2. The *ccd*B locates between these two *att*R sites for negative selection. So like pDONR221, some special *E. coli* strain such as DE3.1 is used for propagation.

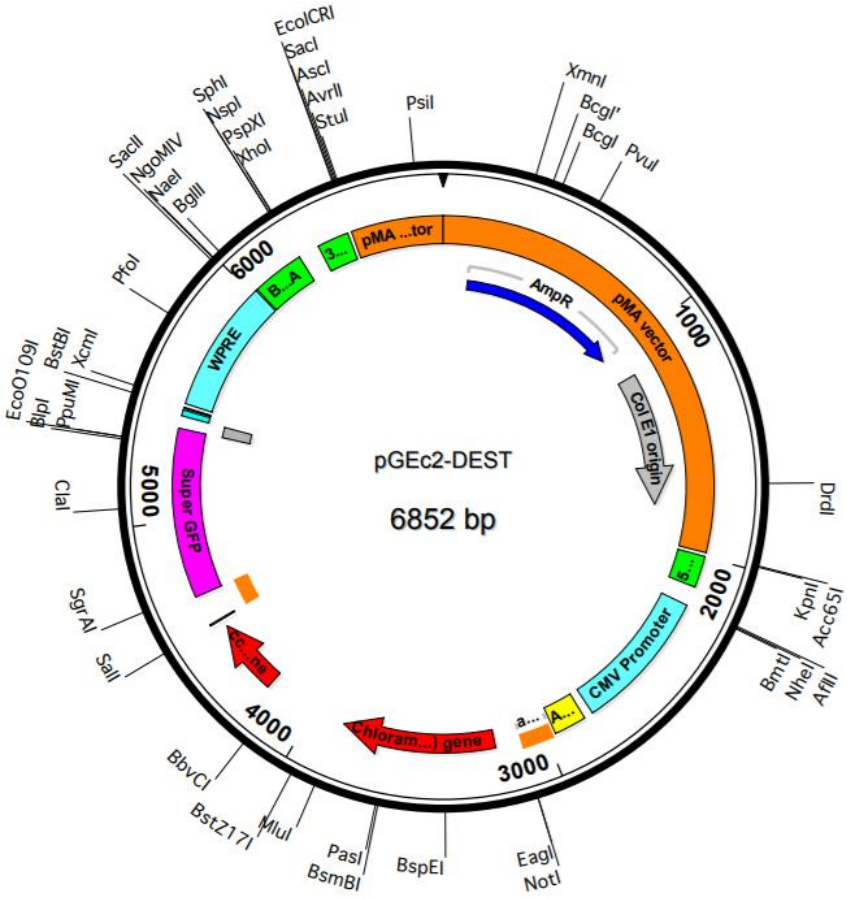

Figure 2.2 map of pGEc2-DEST

Map of pGEc2-DEST. Adapted from

http://dnasu.org/DNASU/GetCloneDetail.do?cloneid=534627.

Gateway Cloning Technology

The Gateway cloning technology was developed by Invitrogen in 1990s. Instead of using restriction enzymes to integrate DNA of interest into expression plasmid, the Gateway cloning technology employs and modifies integration and excision recombination reactions that take place when lambda phage infects bacteria. The first step is the BP Reaction. In the recombination reaction, the PCR product is flanked by *attB1* and *attB2*, and there are *attP* attachment sites on

the donor vector. With the catalysis of BP clonase enzyme mix, the Entry Clone is generated, which contains the DNA of interest. However, the DNA of interest on the Entry Clone is flanked by *attL* sites. The excision of *ccdB* gene is the byproduct of this reaction. The *ccdB* gene is a lethal gene, which codes for *ccdB* protein. The *ccdB* protein is toxic through acting as DNA gyrase poison. It causes cell death by locking up DNA gyrase. So the Donor Vector without recombination is lethal for cells after transformation. It is an efficient selection method (Bernard 1996). The second step is LR Reaction. Catalyzed by LR Clonaser, the generated Entry Clone integrates the DNA of interest into the Destination Vector, which will be used for expression later. The product, Expression Clone has the DNA of interest flanked by *attB* sites, while the byproduct is the Entry Clone carrying the *ccdB* gene which excised from the Destination Vector.

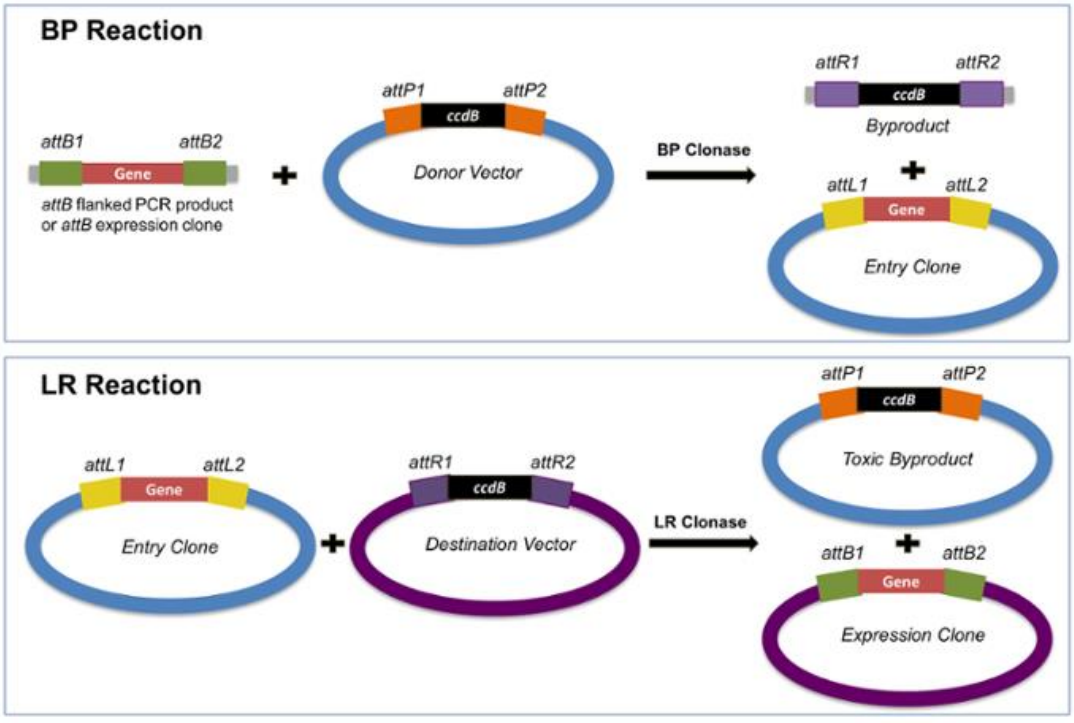

Figure 2.3 The two-step process of Gateway cloning technology.

The two-step process of Gateway cloning technology. Adapted from https://blog.addgene.org/plasmids-101-gateway-cloning.

scFv expression and purification

We chose 49 parent antibodies from the antibody library generated in the Hahn laboratory; these antibodies were representative of the broad diversity of binding specificities against plant polysaccharide structures. They are listed in table 2.1. In order to get the scFvs of these antibodies, fusion PCR was performed to obtain the scFv DNA fragments. The template was cDNA which was reverse-transcribed from mRNA extracted from hybridoma cells. The first round of fusion PCR was used to amplify V_H and V_L, separately. For the V_H fragment, the forward primer is composed of 3 parts: 5` - *att*B1 site - signal peptide sequence – pair region to 5` end of V_H, and the reverse primer is composed of 2 parts: 5` - linker peptide DNA sequence – pair region to 3` end of V_H. The signal peptide sequence used is the secretion signal from the V-J2-C region of the mouse Ig kappa-chain for efficient secretion of recombinant proteins (Coloma, Hastings et al. 1992). The peptide sequence of the linker is GGGGSGGGGSGGGGS. For the V_L fragment, the forward primer is composed of 2 parts: 5` - linker peptide DNA sequence – pair region to 5` end of V_L, and the reverse primer is composed of 2 parts: 5` - *att*B2 site – pair region to 3` end of V_L. There is no stop codon at the 3` end of V_L because there is Superfold GFP, AviTag and 10x histidine after. The second round of fusion PCR was assembling the two fragments of first round PCR products (Figure 2.4).

Table 2.1 List of expressed antibodies

CCRC-M1	IgG1(κ)	Fuc XG
CCRC-M5	IgG1(κ)	RG-Ia
CCRC-M14	IgM(κ)	RG-I Backbone
CCRC-M17	IgG1(κ)	RG-Ic
CCRC-M21	IgG3(κ)	RG-I/AG
CCRC-M23	IgG1(κ)	RG-Ic
CCRC-M30	IgM(κ)	RG-Ib
CCRC-M33	IgM(κ)	RG-I/AG
CCRC-M35	IgM(κ)	RG-I Backbone

CCRC-M38	IgG1(κ)	HG Backbone-1
CCRC-M48	IgG1(κ)	Non-Fuc XG-5
CCRC-M52	IgG1(λ)	Non-Fuc XG-4
CCRC-M55	IgG1(λ)	Non-Fuc XG-4
CCRC-M58	IgG1(κ)	Non-Fuc XG-4
CCRC-M70	IgM(κ)	Galactomannan-1
CCRC-M75	IgM(κ)	Galactomannan-1
CCRC-M78	IgM(κ)	AG-4
CCRC-M80	IgG1(κ)	RG-I/AG
CCRC-M85	IgM(κ)	AG-3
CCRC-M87	IgG1(λ)	Non-Fuc XG-2
CCRC-M90	IgM(λ)	Non-Fuc XG-6
CCRC-M92	IgM(κ)	AG-4
CCRC-M95	IgG1(λ)	Non-Fuc XG-1
CCRC-M96	IgG3(λ)	Non-Fuc XG-5
CCRC-M98	IgG1(κ)	Physcomitrella Pectin
CCRC-M102	IgM(κ)	Fuc XG
CCRC-M103	IgM(κ)	Non-Fuc XG-3
CCRC-M104	IgG1(λ)	Non-Fuc XG-2
CCRC-M106	IgG1(κ)	Fuc XG
CCRC-M108	IgG1(λ)	Xylan-1/XG
CCRC-M113	IgG1(κ)	Xylan-3
CCRC-M116	IgM(κ)	Xylan-3
CCRC-M126	IgG3(κ)	RG-I/AG
CCRC-M131	IgG1(κ)	HG Backbone-1
CCRC-M133	IgM(κ)	AG-2
CCRC-M134	IgG3(κ)	RG-I/AG
CCRC-M137	IgM(κ)	Xylan-7
CCRC-M140	IgG1(κ)	Xylan-6
CCRC-M141	IgG_{2b}(κ)	Linseed Mucilage RG-I
CCRC-M144	IgG1(κ)	Xylan-5
CCRC-M147	IgM(κ)	Xylan-6
CCRC-M150	IgG3(κ)	Xylan-4
CCRC-M152	IgM(κ)	Xylan-7
CCRC-M156	IgM(κ)	Xylan-6
CCRC-M160	IgG1(κ)	Xylan-7
CCRC-M165	IgM(κ)	Linseed Mucilage RG-I
CCRC-M169	IgM(κ)	Acetyl Mannan
CCRC-M174	IgM(κ)	Galactomannan-2
CCRC-M175	IgM(κ)	Galactomannan-2

Abbreviations: HG - homogalacturonan; Fuc XG - fucosylated xyloglucan; AG - arabinogalactan; RG-I - rhamnogalacturonan-I.

Table 2.2 Sequences of primers.

	5` primer sequences	3` primer sequences
V_H	5' GGGGACAAGTTTGTACAAAA AAGCAGGCTTCATGGAGACA GACACACTCCTGCTATGGGTACTG CTGCTCTGGGTTCCAGGTTCCACTGGTT TATTGCTAGCGGCTCAGCCTTATTGCTA GCGGCTCAGCC 3`	5` AGAACCACCACCACCGGA GCCGCCGCCGCCAGAACCACC ACCACCCTTGAAGCTTGCTGCA GAGAC 3`
V_L	5` GGTGGTGGTGGTTCTGGCGG CGGCGGCTCCGGTGGTGGTGGTTCT CCGGCCATGGCGGATATT 3`	5' GGGGACCACTTTGTA CAAGAAAGCTGGGTG TGGTGCGGCCGCAGTAC 3`

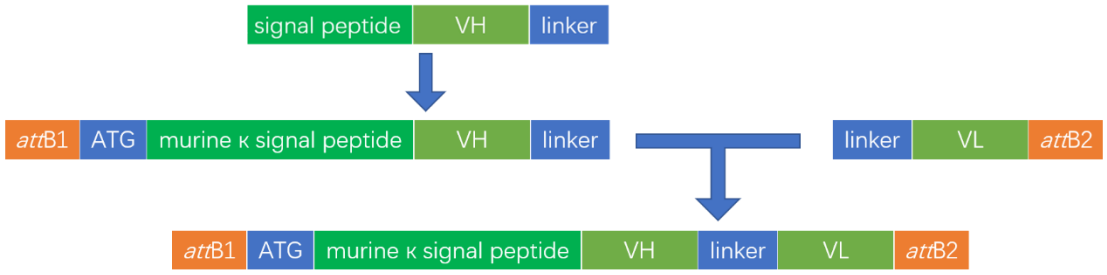

Figure 2.4 Structure of DNA fragment for donor plasmid.

Figure 2.4 displayed the fusion PCR process. The first step was cloning V_H with part of the signal peptide at the 5` end and linker at the 3` end. The second step was adding *att*B1 site, ATG and the rest of the signal peptide at the 5` end. Meanwhile, the $V_L$ with linker at the 5` end and *att*B2 site at the 3` end was also cloned. The third step was fusing the two products of the second step. Table 2.2 listed the sequences of the primers used for amplifying the DNA fragment for pDONR221. The colors used in the Table are the same as in Figure 2.4. The sequence in orange is from *att*B1/*att*B2; the green is from signal peptide; the dark green is from V_H/V_L; the blue is ATG/linker.

The BP and LR reactions were performed to obtain the pGEc2-DEST with scFv gene carried. The sequences of correct recombinants were confirmed (Macrogen, USA). The recombinant plasmids were propagated by DH5α and extracted using MaxiPrep Kit (PureLink™ HiPure Plasmid Filter Maxiprep Kit, Thermo Fisher, Waltham, Massachusetts). With the assistance of Dr. Jeong-Yeh Yang, a post-doc research scientist of Dr. Kelley Moremen's lab, the recombinants of pGEc2-DEST were transformed into HEK293-6E for expression. After 4~5 days, the cells with medium were collected. The expression and secretion was confirmed by fluorescence strength measurement using Gemini Fluorescence Microplate Readers from Molecular Devices LLC.

In order to purify the expressed scFvs, we centrifuged the cell and medium three times using Coulter Allegra X-22R Centrifuge of Beckerman Coulter, at temperature of 4°C and speed of 1000RPM, 2000RPM and 3000RPM, separately. The supernatant was collected and concentrated by using ultrafiltration (Vivaspin 20, 50000 MWCO PES, Sartorius, Gottingen, Germany). The concentrated supernatant was applied to nickel column for purification. The nickel column was pre-washed and washed by washing buffer (50 mM NaH_2PO_4, 300 mM NaCl, 20 mM imidazole, pH=8.0). The scFvs which bound to the nickel beads were eluted using elution buffer (50 mM NaH_2PO_4, 300 mM NaCl, 250 mM imidazole, pH=8.0). The elution process was performed at 4°C. The eluted scFvs were dialyzed using 0.1X Tris-Buffered Saline (TBS) buffer (5 mM Tris-Cl, 15 mM NaCl, pH 7.6) overnight and stored at 4°C for further use. The final concentration of scFvs was ~0.5mg/ml.

Preparation of Polysaccharides

Our polysaccharide samples from various plant sources were obtained from commercial sources (Megazyme, Sigma, and Sunkist) and the lab stocks. Detailed information about these polysaccharides is available in Table 2.3. Polysaccharides were dissolved at 1mg/mL in deionized water to make 100X stock solutions. Stock solutions were stored at -20°C for further use.

Enzyme-Linked Immunosorbent Assay (ELISA)

We coated 96-well plates by applying polysaccharides (50 ul of 10 ug/ml in deionized water per well) and dried the plates by evaporation overnight at 37°C. Control wells were coated with D.I. water. In the next morning the plates were blocked with 200 ul of TBS with 3% (w/v) non-fat dry milk for 1 h. Then the blocking agent was removed by aspiration. Next, we added 50 ul of hybridoma supernatant or fluorescent protein tagged scFv proteins (~50ug/ml) to each well and incubated for 1 hour. Then the wells were washed three times with 300 ul of TBS with 0.1% (w/v) non-fat dry milk. Then we added 50 ul of peroxidase-conjugated goat anti-mouse antibodies to CCRC antibodies or mouse anti-his antibodies (Sigma-Aldrich, diluted in TBS by 1:3000) to scFvs and incubated for 1 hour. Before we added substrate, the wells were washed five times with 300 ul of TBS with 0.1% (w/v) non-fat dry milk. 50 ul fresh TMB (3,3',5,5'-Tetramethylbenzidine, Sigma-Aldrich) as substrate solution was added to each well. After 15 minutes, we stopped the reactions by adding 50 ul of 1 N sulfuric acid to each well. The OD was read from each well in A450 and A655 using a model 680 microplate reader (Bio-Rad). All the aspiration and washing steps were performed using an ELx405 Microplate Washer (Bio-Tek Instruments).

Plasmid Construction and Plant Transformation

The scFv DNA fragments were amplified using iProof Polymerase. The forward primer contained XmaI restriction enzyme site and the reverse primer contained XhoI restriction enzyme site. PCR products were digested by the XmaI and XhoI (FastDigest, Thermo) and ligated into the modified pBI121-YFP vector (Clontech). The modified pBI121-YFP carried the *AtExpansin10* signal peptide (At1g26770) (Cho and Cosgrove 2000) All constructs were confirmed by sequencing (Macrogen, USA) and individually transformed into *Agrobacterium tumefaciens* GV3101 competent cells by electroporation. Transformation of *Arabidopsis* was conducted by floral dipping (Bent 2006). First the transformed *Agrobacterium tumefaciens* were inoculated into LB medium with Kanamycin (50ug/ml) and Rifampicin (25ug/ml), and shaken at 28°C for 72 hours. Then medium was centrifuged at 4000 RPM (Coulter Allegra X-22R, Beckerman Coulter) and the pellet was resuspended in transformation solution (1/2 MS, 5% (w/v) Sucrose, 0.02% Silwet L-77). Inflorescences of 6-8 weeks old *Arabidopsis* were dipped into transformation solution with transformed *Agrobacterium tumefaciens*. Then the *Arabidopsis* were covered by clear plastic dome for 48 hours to maintain the humidity, followed by returned to normal growth chamber. Seeds were harvested when they were brown.

Growth of Plant

Both *Arabidopsis* wild type and transgenic plant lines generated were in the ecotype Columbia (Col-0) background. For sterilization, seeds of *Arabidopsis* were washed by 95% (v/v) ethanol for 5 minutes and rinsed by D.I. water for 5 times. Then seeds were cold treated at 4°C for 48 hours and germinated on 1/2 MS medium in a growth chamber (light intensity 120 umol/m^2*s, relative humidity 70%.) under a cycle of 16-h-light 19°C /8-h-dark 15°C. For screen

of individual with T-DNA insertion, the G2 seeds were germinated on 1/2 MS medium with 50ug/ml Kanamycin. Two-week-old seedlings were transferred to soil and grown in growth chambers under the same conditions.

DNA Confirmation of Homozygous Plants

To identify homozygous plants with T-DNA insertions in the G2 *Arabidopsis*, genomic DNA was extracted using DNeasy Plant Mini Kit (Qiagen). T-DNA insertions were confirmed using the flanking primers of scFvs. The primers are generated using the T-DNA verification primer design website: http://signal.salk.edu/tdnaprimers.2.html. The sequences are below:

LP: TTATTGCTAGCGGCTCAGCC

RP: TGGTGCGGCCGCAGTAC.

RNA Isolation and Reverse Transcript (RT)-PCR

Fresh plant stems were frozen immediately in liquid nitrogen and RNA was isolated using RNeasy plant mini kit (Qiagen) and treated with RNase-free DNase (Qiagen) to remove contaminating genomic DNA. Total RNA (500 ng) was reverse-transcribed using Superscript® III Reverse Transcriptase (Invitrogen). PCR was performed using Taq DNA Polymerase (Thermo). Actin2 (At3g18780) was used as internal control.

Tissue Fixation

Arabidopsis was planted for 4 days. For the dehydration, roots were cut and washed in D.I. water for 2 hours, followed by 15% (v/v) ethanol for 2 hours, 30% (v/v) ethanol for 3 hours, 50% (v/v) ethanol for 3 hours, 70% (v/v) ethanol for overnight, 80% (v/v) ethanol for 2 hours, 95% (v/v) ethanol for 1.5 hours and 100% ethanol for 40 minutes, 100% ethanol:

dimethylbenzene =3:1 for 1.5 hours, 100% ethanol: dimethylbenzene =1:1 for 1 hour and dimethylbenzene for 0.5 hour twice. The dehydrated tissue was moved to 4°C and gradually infiltrated with cold LR White embedding resin (Ted Pella) using 33% (v/v) and 66% (v/v) resin in 100% dimethylbenzene for 4 hours and 12 hours separately, followed by 24-hour infiltration in 100% resin for three times. The infiltrated tissue was transferred to gelatin capsules containing 100% resin for embedding, and the resin was exposed to 365-nm UV light at 4°C for 48 hours for polymerization. The plant growing, tissue harvesting, fixation, embedding and sectioning were performed by Stefan Eberhard of Carbohydrate Complex Research Center of University of Georgia.

Direct fluorescence labeling by fluorescent protein tagged scFvs

Thick sections (250nm) were prepared using a Leica EM UC6 ultramicrotome (Leica Microsystems) and mounted on glass slides (Fisher Scientific). Sections were blocked with PBS with 3% (w/v) non-fat dry milk for 20 minutes and washed with PBS for 5 minutes. 20 ul fluorescent protein-tagged scFv proteins (~0.5 mg/ml) were applied and incubated for 1 hour. Sections were washed with PBS three times for 5 minutes and D.I. water for 5 minutes. Before covering a coverslip, Citifluor antifade mounting medium AF1 (Electron Microscopy Sciences) was applied to the sections. The whole process of labeling was performed at room temperature. The immunolabeling images were captured by microscopy on an Eclipse 80i microscope (Nikon) equipped with epifluorescence optics. Images were captured with a Nikon DS-Ri1 camera lens using NIS-Element Basic Research software.

Table 2.3 List of 55 plant polysaccharides

	Antigens Name	Heat Map Name	Group	Source and Reference(s)/Website for Structural Studies	Sugar Composition (Mol %)
A01	Tamarind Xyloglucan	Tam XG	Xyloglucans	CCRC, UGA; (York, Harvey et al. 1993); Hahn lab data (Pattathil, Avci et al. 2010)	Glc (43), Xyl (37), Gal (17) and Ara (3)
A02	Tomato Xyloglucan	Tom XG	Xyloglucans	CCRC, UGA; (Jia, Qin et al. 2003); Hahn lab data (Pattathil, Avci et al. 2010)	Glc (44), Xyl (32), Gal (14) and Ara (10)
A03	Sycamore Maple Xyloglucan	Syc XG	Xyloglucans	CCRC, UGA; (Stevenson, McNeil et al. 1986); Hahn lab data (Pattathil, Avci et al. 2010)	Glc (42), Xyl (31), Gal (10), Man (9), Fuc (4) and Ara (4)
A04	Wheat Arabinoxylan	Wh Araxyl	Xylans	Megazyme, Bray, Ireland; Hahn lab data (Pattathil, Avci et al. 2010),http://secure.megazyme.com/Arabinoxylan-Wheat-Flour-Insoluble	Ara (37), Xyl (61) and traces of other sugars
A05	4-O-Methyl-D-glucurono-D-xylan	MeGLA Xy	Xylans	Sigma-Aldrich, St. Louis, MO; Hahn lab data (Pattathil, Avci et al. 2010)	Xyl (82.8) and Methyl GlcA (17.2)
A06	Birch Wood Xylan	BW Xyl	Xylans	Sigma-Aldrich, St. Louis, MO; Hahn lab data (Pattathil, Avci et al. 2010)	Xyl (100)
A07	*Phormium tenax* Partially Hydrolysed	PT Xyl PH	Xylans	IRL, New Zealand; Hahn lab data (Pattathil, Avci et al. 2010)	Xyl (94) and Gluc (6)
A08	*Phormium tenax* Low Arabinose Xylan	PT Xyl LA	Xylans	IRL, New Zealand; Hahn lab data (Pattathil, Avci et al. 2010)	Xyl (87), Ara (8) and Glc (5)
A09	*Phormium tenax* cookianum High Arabionose Xylan	PC Xyl	Xylans	IRL, New Zealand; Hahn lab data (Pattathil, Avci et al. 2010)	Xyl (70), Ara (27) and Glc (3)
A10	Corn Xylan	Corn Xyl	Xylans	National Renewable Energy Lab, Golden, CO; Hahn lab data (Pattathil, Avci et al. 2010)	Xyl (100)
A11	Tomato Glucomannan	Tom GlucM	Mannans	CCRC, UGA; Hahn lab data (Pattathil, Avci et al. 2010)	Glc (61) and Man (39)
B01	Guar Galactomannan	Guar GalM	Mannans	Megazyme, Bray, Ireland; Hahn lab data (Pattathil, Avci et al. 2010), http://secure.megazyme.com/Galactomannan-Guar-Medium-Viscosity	Man (62) and Gal (38)
B02	Gum Guar	Gum Guar	Mannans	Sigma-Aldrich, St. Louis, MO; Hahn lab data (Pattathil, Avci et al. 2010)	Man (63), Gal (36) and Ara (1)
B03	Locust Bean Gum	Loc Bean G	Mannans	Sigma-Aldrich, St. Louis, MO; Hahn lab data (Pattathil, Avci et al.	Man (81) and Gal (19)

				2010)	
B04	(1,3)(1,4)-β-Glucan	1314 Gluc	β-Glucans	Megazyme, Bray, Ireland; Hahn lab data (Pattathil, Avci et al. 2010)	Glc (97), Man (2) and Ara (1)
B05	(1,3)(1,6)-β-Glucan	1315 Gluc	β-Glucans	CCRC, UGA; (Hahn, Darvill et al. 1992); Hahn lab data (Pattathil, Avci et al. 2010)	Glc (91), Man (7) and Ara (2)
B06	Pachyman	Pachyman	β-Glucans	Megazyme, Bray, Ireland; Hahn lab data (Pattathil, Avci et al. 2010), http://secure.megazyme.co m/Pachyman	D-glucose essentially all of which is 1,3-ß-linked (>98)
B07	Lichenan	Lichena n	β-Glucans	Megazyme, Bray, Ireland; Hahn lab data (Pattathil, Avci et al. 2010), http://secure.megazyme.co m/Lichenan-Icelandic-Moss	Glc (98) and Ara (2)
B08	Lupin Galactan	Lup Gal	Galactans	Megazyme, Bray, Ireland; Hahn lab data (Pattathil, Avci et al. 2010), http://secure.megazyme.co m/Galactan-Lupin	Gal (83), GalA (5), Rha (5), Ara (3), Xyl (2) and traces of Glc
B09	Potato Galactan	Pot Gal	Galactans	Megazyme, Bray, Ireland; Hahn lab data (Pattathil, Avci et al. 2010), http://secure.megazyme.co m/Galactan-Potato	Gal (88), GalA (6), Ara (3) and Rha (3)
B10	Larch Arabinogalactan	Lar Ara Gal	Arabinogalactans	Megazyme, Bray, Ireland; Hahn lab data (Pattathil, Avci et al. 2010), http://secure.megazyme.co m/Arabinogalactan-Larch- Wood	Gal (81), Ara (14) and traces of other sugars
B11	Gum Arabic	Gum Arabic	Arabinogalactans	Sigma-Aldrich, St. Louis, MO (Stephen, Phillips et al. 2006); Hahn lab data (Pattathil, Avci et al. 2010)	Ara (37), Gal (40), Rha (20) and traces of Glc
C01	Gum Ghatti	Gum Ghatti	Arabinogalactans	Sigma-Aldrich, St. Louis, MO(Stephen, Phillips et al. 2006); Hahn lab data (Pattathil, Avci et al. 2010)	Ara (49), Gal (31), Man (10), GlcA (8) and Xyl (2)

C02	Gum Tragacanth	Gum Trag	Arabinogalactans	Sigma-Aldrich, St. Louis, MO (Stephen, Phillips et al. 2006); Hahn lab data (Pattathil, Avci et al. 2010)	Gal (32.3), Ara (31.7), Xyl (12), Glc (12.3), Fuc (8.4) and Rha (3.3)
C03	Arabinan	Arabina n	Arabinogalactans	Megazyme, Bray, Ireland; Hahn lab data (Pattathil, Avci et al. 2010), http://secure.megazyme.co m/Arabinan-Sugar-Beet	Ara (88), Gal (3), Rha (2) and GalA (7)
C04	Linear Arabinan	Linear Arabina n	Arabinogalactans	Megazyme, Bray, Ireland; Hahn lab data (Pattathil, Avci et al. 2010), http://secure.megazyme.co m/Linear-1-5-alpha-L-Arabinan-Sugar-Beet	Ara (97.5), GalA (2), Gal (0.4) and Rha (0.1)
C05	Sycamore Maple Pectic Polysaccharides	Syc PecP	RG-I	CCRC, UGA; (Stevenson, McNeil et al. 1986); Hahn lab data (Pattathil, Avci et al. 2010)	Gal (52.4), GlcA (15), GalA (11), Xyl (7.9), Ara (7.5), Glc (2.6), Rha (2), Man (1.3) and traces of Fuc
C06	Tomato Pectic Polysaccharides	Tom PecP	RG-I	CCRC, UGA; (Jia, Qin et al. 2003); Hahn lab data (Pattathil, Avci et al. 2010)	Gal (57.4), Ara (25.2), GalA (6.5), Rha (4.4), Xyl (4.3) and Fuc (2.2)
C07	Physcomitrella patens Pectin Polysaccharides	PhyscPe cP	RG-I	CCRC, UGA; (Pena, Darvill et al. 2008); Hahn lab data (Pattathil, Avci et al. 2010)	GalA (46.7), Rha (24), Gal(17.4), Ara (8.1), Glc (2.3) and Xyl (1.5)
C08	Gum Karaya	Gum Karaya	RG-I	Sigma-Aldrich, St. Louis, MO; Hahn lab data (Pattathil, Avci et al. 2010)	GalA (57), GlcA (8), Gal (17), Rha (16) and traces of Glc
C09	Potato RG-I	Pot RG- I	RG-I	Megazyme, Bray, Ireland; Hahn lab data (Pattathil, Avci et al. 2010), http://secure.megazyme.co m/Rhamnogalacturonan-I- Potato	GalA (51), Rha (28.6), Gal (14), Ara (5.4) and Xyl (1)
C10	Soybean RG-I	Soy RG-I	RG-I	Megazyme, Bray, Ireland; Hahn lab data (Pattathil, Avci et al. 2010), http://secure.megazyme.co m/Rhamnogalacturonan-Soy-Bean	GalA (51), Xyl (13), Gal (11), Rha (10), Fuc (9) and Ara (6)

C11	Arabidopsis thaliana RG-I	At RG-I	RG-I	CCRC, UGA; (Zablackis, Huang et al. 1995); Hahn lab data (Pattathil, Avci et al. 2010)	GalA (34), Rha (27), Gal (17), Ara (14), Xyl (5), Fuc (1), GlcA (1) and GalA (1)
D01	Green Tomato Fruit RG-I	GrTomF rR	RG-I	CCRC, UGA; Hahn lab data (Pattathil, Avci et al. 2010)	GalA (49.5), Gal (43.8), Rha (4.7), GlcA (1), Ara (0.5) and traces of Xyl and Glc
D02	Lettuce RG-I	Let RG- I	RG-I	CCRC, UGA; Hahn lab data (Pattathil, Avci et al. 2010)	Gal (54.9), GalA (23.4), Rha (6.9), GlcA (5.7), Ara (4.9) and Xyl (4.2)
D03	Arabidopsis Seed Mucilage	At Seed Mu	Mucilages	CCRC, UGA; Hahn lab data (Pattathil, Avci et al. 2010)	Rha (69), GalA (27.7), Gal (1.8) and Xyl (1.5)
D04	Sinapus Seed Mucilage	Sin Seed Mu	Mucilages	CCRC, UGA; Hahn lab data (Pattathil, Avci et al. 2010)	GalA (57), Gal (19), Rha (12), GlcA (10) and traces of Man and Glc
D05	Peppergrass Seed Mucilage	Pep Gr S Mu	Mucilages	CCRC, UGA;(Deng, O'Neill et al. 2009); Hahn lab data (Pattathil, Avci et al. 2010)	GlcA (22.2), GalA (22.1), Gal (18.9), Xyl (9.8), Rha (8), Glc (7), Fuc (5.2), Ara (5) and Man (1.8)
D06	Citrus Pectin	Citrus Pectin	HG	Hercules, Wilmington, DE; Hahn lab data (Pattathil, Avci et al. 2010)	GalA (85), Rha (13) and Gal (2)
D07	73% Me Pectin	73% MePec	HG	Hercules, Wilmington, DE; Hahn lab data (Pattathil, Avci et al. 2010)	GalA (81), Gal (7), Rha (6.5), Ara (4.6) and Glc (0.9)
D08	55% Me Pectin	55% MePec	HG	Hercules, Wilmington, DE; Hahn lab data (Pattathil, Avci et al. 2010)	GalA (81), Gal (10), Rha (9)

D09	33% Me Pectin	33% Me Pec	HG	Hercules, Wilmington, DE; Hahn lab data (Pattathil, Avci et al. 2010)	GalA (89), Gal (7), Rha (4)
D10	Jatoba Xyloglucan of Hymenaea courbaril	Znone	Xyloglucans	CCRC, UGA; Hahn lab data (unpublished)	
D11	High-acetyl Sugarbeet β-Pectin	HAcSB Pec	HG	Hercules, Wilmington, DE; Hahn lab data (Pattathil, Avci et al. 2010)	GalA (56.2), Rha (21.3), Gal (15) and Ara (7.5)
E01	Poplar Xylan	Pop Xyl	Xylans	National Renewable Energy Lab, Golden, CO; Hahn lab data (Pattathil, Avci et al. 2010)	Xyl (94), GalA (4) and Rha (2)
E02	Camelina Seed Mucilage	Cam Seed	Mucilages	CCRC, UGA; Hahn lab data (Pattathil, Avci et al. 2010)	Rha (57.1), GalA (24.4), Gal (13.3), Xyl (2.2), Ara (2.3) and Man (0.8)
E03	Potato Arabinogalactan	Pot Ara Gal	Arabinogalactans	Dr. Henk Schols, Laboratory of Food Chemistry, Wageningen, The Netherlands; personal communication	Gal (63), Ara (20) and UA (17)
E04	Arabinogalactan II	Ara Gal II	Arabinogalactans	Dr. Henk Schols, Laboratory of Food Chemistry, Wageningen, The Netherlands; personal communication	Gal (84) and Gal (16)
E05	RG-I from Okra	Okra RG-I	RG-I	Dr. Henk Schols, Laboratory of Food Chemistry, Wageningen, The Netherlands; personal communication	Gal (53), GalA (26), Rha (14), GlcA (4), Glc (2.5) Ara (1) and Man (1)
E06	Eucalyptus KOHss	Eucal KOH	Xylans	Dr. Henk Schols, Laboratory of Food Chemistry, Wageningen, The Netherlands; personal communication	Xyl (81), UA (13), Gal (3), Rha (2), Ara (1), Glc (1) and Man (1)

E07	Sugar Beet Linear Arabinan	SB Lin Ara	Arabinogalactans	Dr. Henk Schols, Laboratory of Food Chemistry, Wageningen, The Netherlands; personal communication	Ara (74), UA (14) and Gal (12)
E08	Sugar Beet Branched Arabinan	SB Branch	Arabinogalactans	Dr. Henk Schols, Laboratory of Food Chemistry, Wageningen, The Netherlands; personal communication	Ara (>80)
E09	Sorghum BE1	Sorg BE1	Xylans	Dr. Henk Schols, Laboratory of Food Chemistry, Wageningen, The Netherlands; personal communication	Ara (45.8), Xyl (40.9), UA (9.8), Gal (1.8), Glc (1.7) and Man (0.2)
E10	Corn BE1	Corn BE1	Xylans	Dr. Henk Schols, Laboratory of Food Chemistry, Wageningen, The Netherlands; personal communication	Ara (38.4), Xyl (48.3), UA (8.3), Gal (4.3), Glc (0.7) and Man (0.1)
E11	Linseed Mucilage	Lin Seed Mu	Mucilages	CCRC, UGA; Hahn lab data (Pattathil, Avci et al. 2010)	Rha (44.2), GalA (18.5), Xyl (15.8), Gal (11.1), Fuc (3), Ara (4.6) and Glc (2.9)

Abbreviations: HG - homogalacturonan; RG-I - rhamnogalacturonan-I; Me – methoxyl; BE - base extract (taken from the Supplemental Materials attached to Pattathil, Avci et al. 2010).

CHAPTER III

RESULTS

Fluorescent protein tagged scFvs expression and purification

The 49 scFvs (Table 2.1) were expressed as fusion proteins joined to fluorescent protein Superfold GFP at the C-terminus of the scFvs. At the C-terminus of Superfold GFP domain, there is an Avi-Tag and a 10x histidine tag. The recombinant proteins were expressed in HEK293-6E and purified by immobilized Ni-column affinity chromatography. It was expected that the molecular weight of these 49 GFP tagged scFvs would be between 50 KD and 55 KD, based on their amino acid sequences. However, only 13 of the 49 scFvs could be obtained as secreted proteins from the HEK expression system. The other scFv fusion proteins were either not well expressed or failed to be secreted from the HEK cells (see Discussion Chapter). SDS-PAGE electrophoresis was performed to confirm if the purified GFP tagged scFvs were homogenous (Figure 3.1). The purified proteins electrophoresed as single bands with the expected sizes under typical SDS-PAGE conditions. The binding of expressed scFv fusion proteins to cell wall polysaccharides was explored in more detail as follows.

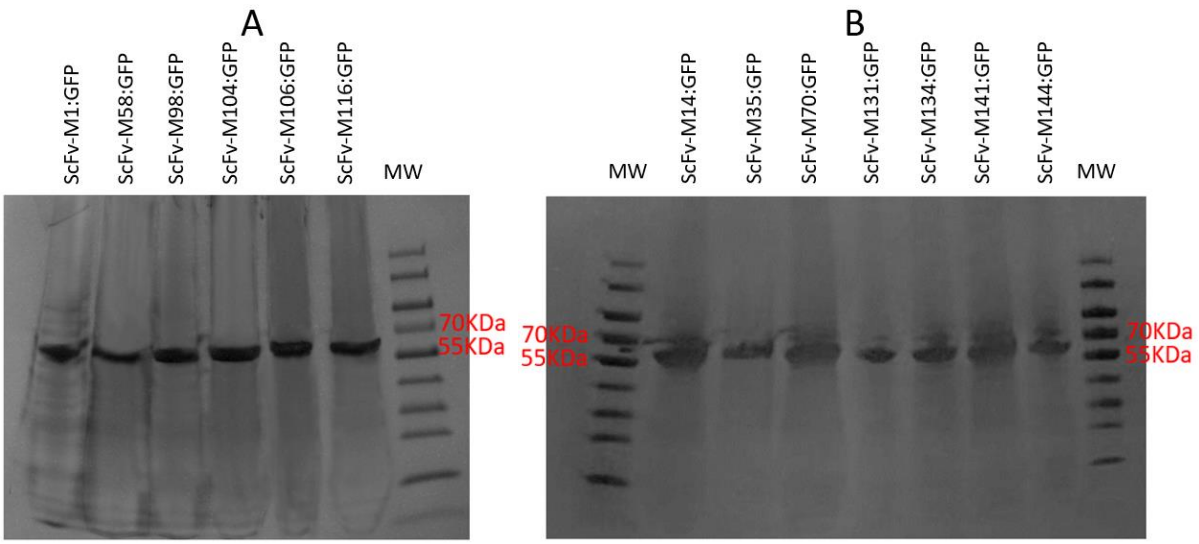

Figure 3.1 SDS-PAGE of purified GFP tagged scFvs

(A) From left to right: purified scFv-M1:GFP, purified scFv-M58:GFP, purified scFv-M98:GFP, purified scFv-M104:GFP, purified scFv-M106:GFP, purified scFv-M116:GFP, MW - protein marker (PageRuler Prestained Protein Ladder, purchased from Thermo Fisher).

(B) From left to right: MW - protein marker, unpurified scFv-M14:GFP, purified scFv-M35:GFP, purified scFv-M70:GFP, purified scFv-M131:GFP, purified scFv-M134:GFP, purified scFv-M141:GFP, purified scFv-M144:GFP, MW - protein marker

Secretion of ScFvs

Because of the secretion signal from the V-J2-C region of the mouse Ig kappa-chain at N-terminus, the GFP tagged scFvs were supposed to be secreted into the culture medium after appropriate post-translational modifications in HEK293-6E cells. However, the fluorescence signal strengths of GFP from cell+medium were stronger than those from medium-only after centrifugation. 13 of the expressed GFP tagged scFvs showed signal from the medium-only. The other ones did not have any signal from medium-only while the fluorescence signals were only

found in the cell pellets (Table 3.1 and Table 3.2). The 13 successfully secreted GFP tagged scFvs are listed below. The secretion efficiency of these 13 GFP tagged scFvs varied from 21%-100%.

Table 3.1 List of secreted GFP tagged scFvs and their corresponding fluorescence strengths.

scFv	Fluorescence Strength Cell & Medium*	Fluorescence Strength Medium-only after Centrifuge*	Secretion Efficiency
scFv-M1:GFP	570	580	102%
scFv-M14:GFP	380	200	49%
scFv-M35:GFP	440	190	39%
scFv-M58:GFP	460	180	35%
scFv-M98:GFP	340	170	45%
scFv-M104:GFP	560	380	66%
scFv-M106:GFP	160	130	77%
scFv-M116:GFP	540	600	112%
scFv-M131:GFP	410	190	42%
scFv-M134:GFP	540	310	55%
scFv-M140:GFP	380	100	20%
scFv-M141:GFP	500	240	47%
scFv-M144:GFP	500	270	51%

*The medium itself has a signal with strength of ~30. So the formula of Secretion Efficiency is (Fluorescence strength of medium only-30)/(Fluorescence strength of cell&medium-30)*100%

Table 3.2 Examples of non-secreted GFP tagged scFvs.

scFv	Fluorescence Strength Cell & Medium*	Fluorescence Strength Medium-only after centrifuge*	Secretion Efficiency
scFv-M5:GFP	180	30	0%
scFv-M21:GFP	340	30	0%
scFv-M87:GFP	180	30	0%
scFv-M147:GFP	450	40	2%
scFv-M152:GFP	380	40	3%

*The medium itself has a signal with strength of ~30. So the formula of Secretion Efficiency is (Fluorescence strength of medium only-30)/(Fluorescence strength of cell&medium-30)*100%

Binding of fluorescent protein tagged scFvs to a diverse panel of 55 plant polysaccharides

ELISAs were performed to identify the binding characteristics of all the secretable fluorescent protein GFP tagged scFvs against 55 diverse plant polysaccharide preparations, whose detailed chemical compositions have been previously studied (Pattathil, Avci et al. 2010). Based on their compositions and structures, the 55 plant polysaccharide preparations were categorized into groups of Xyloglucans, Xylans, Mannans, β-Glucans, Galactans, Arabinogalactans, Rhamnogalacturonans, Mucilages, and Homogalacturonans.

Xyloglucan-binding Group (scFv-M1:GFP, scFv-M58:GFP, scFv-M104:GFP, scFv-M106:GFP)

The ELISA results showed that the fluorescent protein GFP tagged scFv-M1:GFP had similar specific binding activity for xyloglucan compared with its parent antibody, CCRC-M1. First, scFv-M1:GFP, as well as CCRC-M1, could not effectively bind to most samples of hemicellulose or pectin in this polysaccharide panel (Figure 3.2, 3.3). Second, scFv-M1:GFP displayed binding capacity to Sycamore Xyloglucan and Sycamore Maple (*Acer pseudoplatanus*) Pectic Polysaccharides as did CCRC-M1. However, scFv-M1:GFP was able to bind to Poplar Xylan to which CCRC-M1 did not show significant binding ability. Additionally, the signal strength of scFv-M1:GFP was lower than CCRC-M1. It has been suggested that scFvs, being the shorter fragment of antibodies, have weaker affinity than the whole antibody molecules (Cai, Fu et al. 2013).

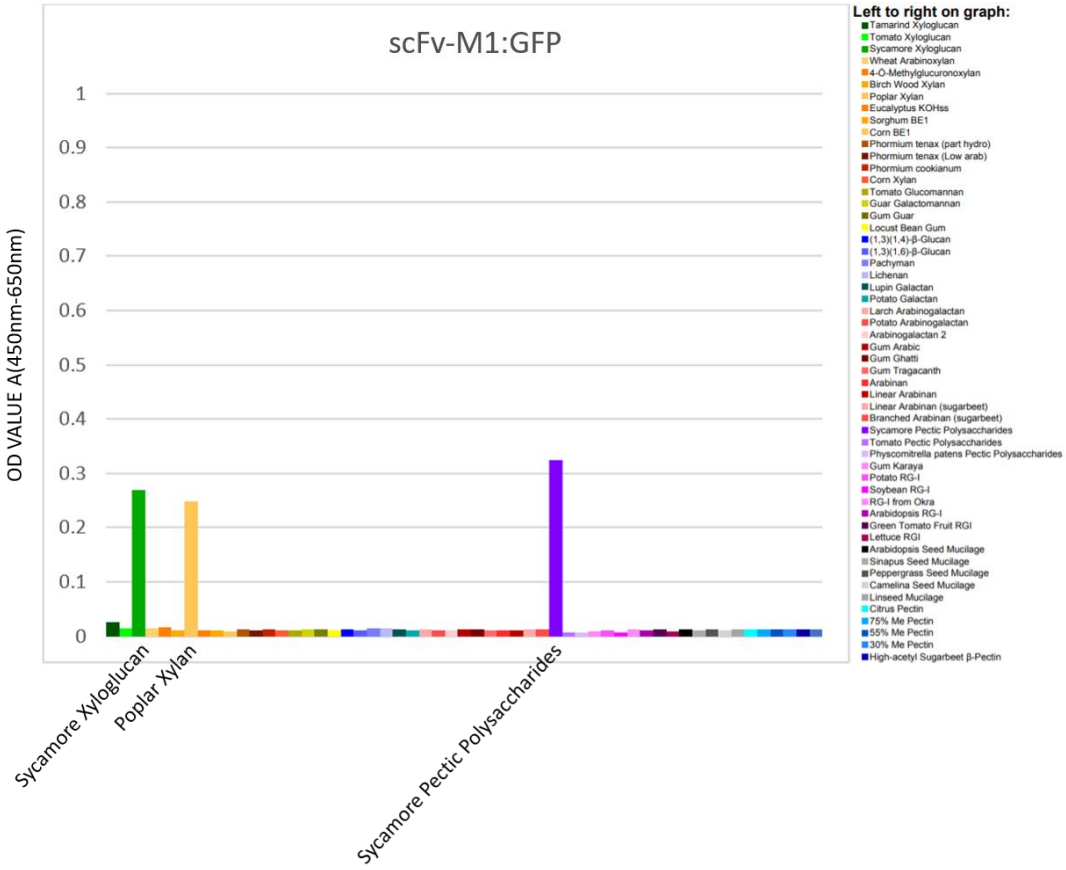

Figure 3.2 Binding specificity of scFv-M1:GFP toward 55 plant polysaccharides.

The specificity of scFv-M1:GFP is revealed by its polysaccharide recognition pattern in the ELISA. Each column reflects the binding strength of scFv-M1:GFP against an immobilized polysaccharide in the corresponding well. ELISA of each scFv was performed in triplicate and the values are the mean.

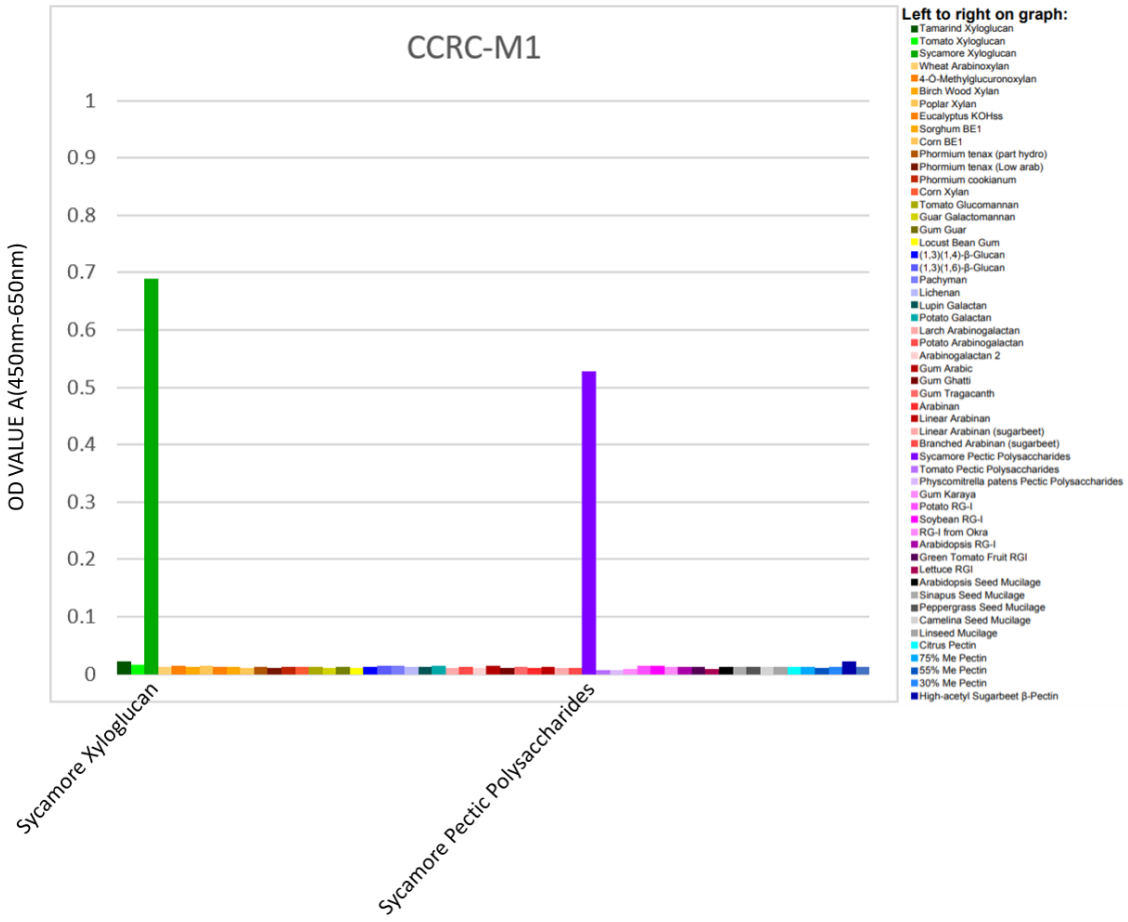

Figure 3.3 Binding specificity of CCRC-M1 toward 55 plant polysaccharides.

The specificity of CCRC-M1 is revealed by its polysaccharide recognition pattern in the ELISA. Each column reflects the binding strength of CCRC-M1 against an immobilized polysaccharide in the corresponding well. The ELISA of each CCRC parental antibody was performed once.

The ELISA results showed that the fluorescent protein GFP tagged scFv-M106:GFP had similar specific binding activities of CCRC-M106 for xyloglucan. First, scFv-M106:GFP, as well as CCRC-M106 , could not effectively bind to most samples of hemicellulose or pectin in this panel (Figure 3.4, 3.5). Second, like CCRC-M106, scFv-M106:GFP displayed binding capacity to Sycamore Xyloglucan. Different from CCRC-M106, scFv-M106:GFP showed low binding

ability to Lupin Galactan and Larch Arabinogalactan, although it is not certain that these signal are significantly above background. Additional testing would be required to determine if these latter binding results are significant. Noticeably, the signal strength of scFv-M106:GFP was lower than CCRC-M106.

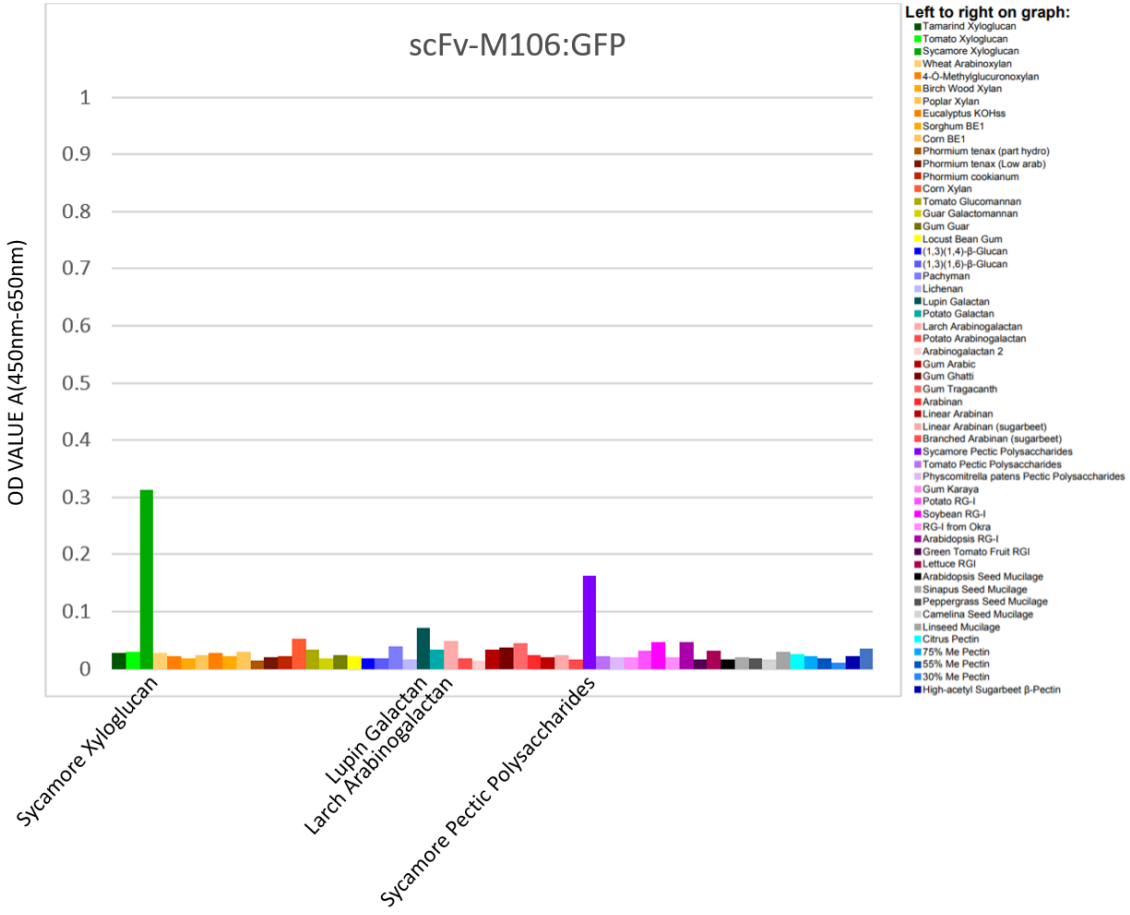

Figure 3.4 Binding specificity of scFv-M106:GFP toward 55 plant polysaccharides.

The specificity of scFv-M106:GFP is revealed by its polysaccharide recognition pattern in the ELISA. Each column reflects the binding strength of scFv-M106:GFP against an immobilized polysaccharide in the corresponding well. Each ELISA of scFv was performed in triplicate and the values were the mean.

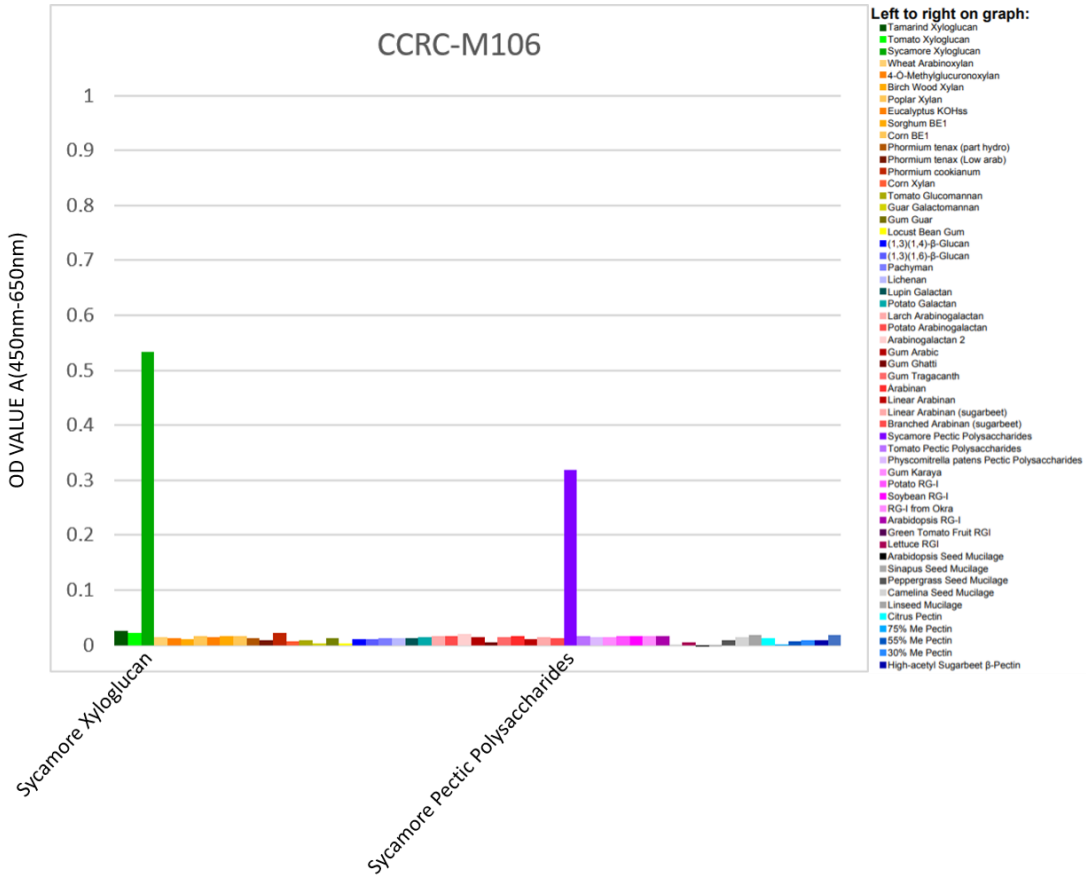

Figure 3.5 Binding specificity of CCRC-M106 toward 55 plant polysaccharides.

The specificity of CCRC-M106 is revealed by its polysaccharide recognition pattern through ELISA. Each column reflects the binding strength of CCRC-M106 against an immobilized polysaccharide in the corresponding well. ELISA of each CCRC parental antibody was performed once.

Xyloglucan has a β-1-4 glucan backbone. Up to 75% of the backbone could be substituted with xylose units, which also could be decorated with galactose and fucose units. The xyloglucans without any fucose on side chains is defined as non-fucosylated xyloglucan. The ELISA results showed that the fluorescent protein GFP tagged scFv-M58:GFP had similar

specific binding activities of CCRC-M58 for non-fucosylated xyloglucan. First, scFv-M58:GFP, as well as CCRC-M58, could not effectively bind to most samples of hemicellulose or pectin in this panel (Figure 3.6, 3.7). Second, like CCRC-M58, scFv-M58:GFP displayed binding capacity to Tamarind Xyloglucan, Tomato Xyloglucan, Sycamore Xyloglucan and Sycamore Pectic Polysaccharides, which are rich in non-fucosylated xyloglucans (Buckeridge 2010). Additionally, the signal strength of scFv-M58:GFP was lower than CCRC-M58.

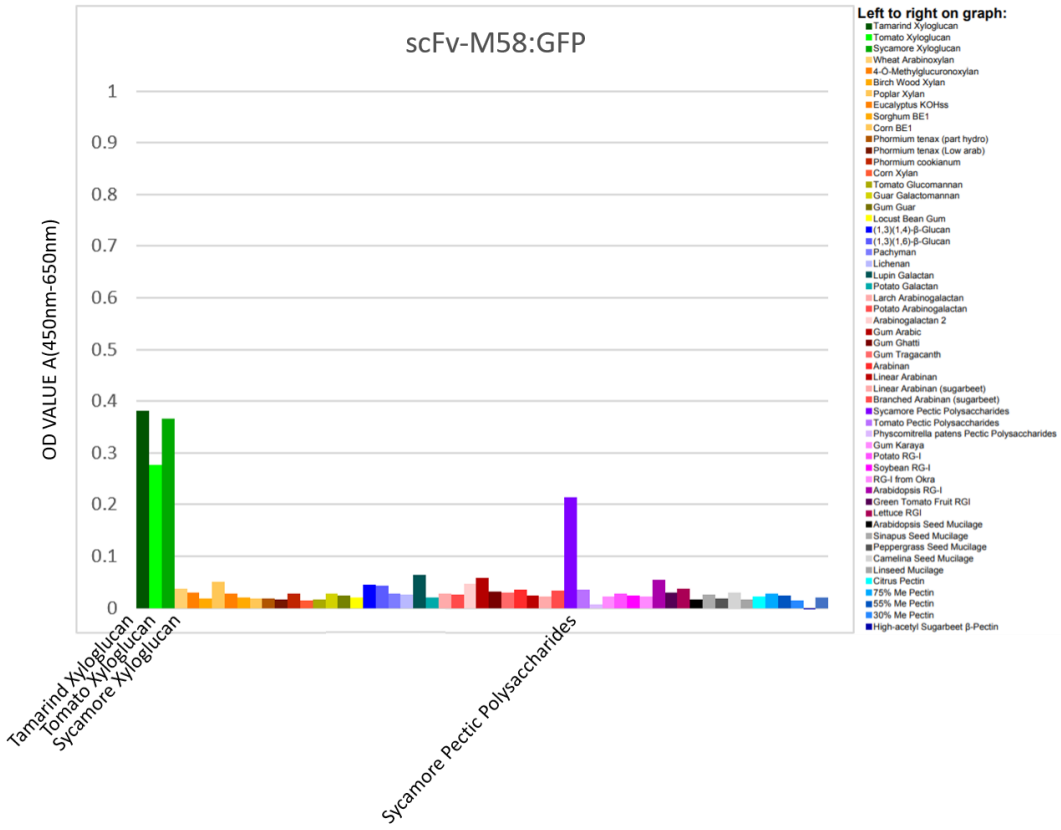

Figure 3.6 Binding specificity of scFv-M58:GFP toward 55 plant polysaccharides.

The specificity of scFv-M58:GFP is revealed by its polysaccharide recognition pattern in the ELISA. Each column reflects the binding strength of scFv-M58:GFP against an immobilized polysaccharide in the corresponding well. ELISA of each scFv was performed in triplicate and the values are the mean.

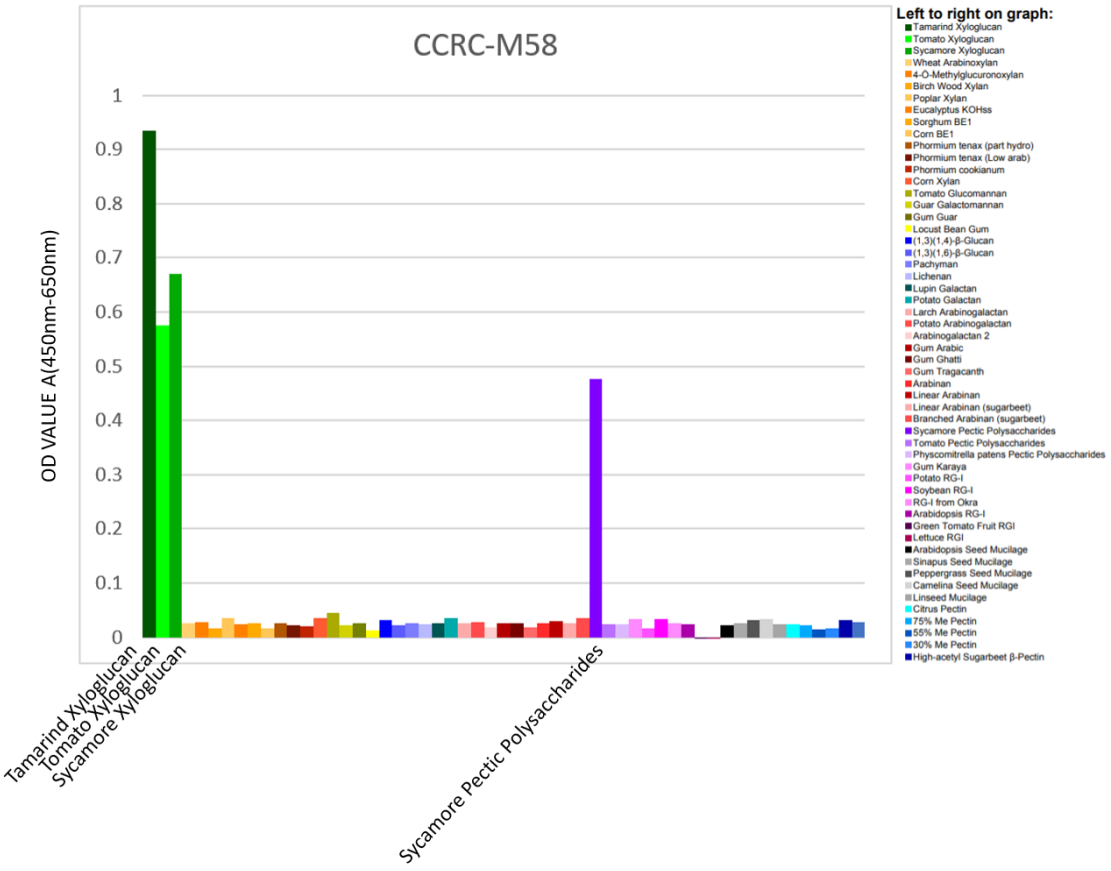

Figure 3.7 Binding specificity of CCRC-M58 toward 55 plant polysaccharides.

The specificity of CCRC-M58 is revealed by its polysaccharide recognition pattern through ELISA. Each column reflects the binding strength of CCRC-M58 against an immobilized polysaccharide in the corresponding well. ELISA of each CCRC parental antibody was performed once.

The ELISA results showed that the fluorescent protein GFP tagged scFv-M104:GFP had similar specific binding activities of CCRC-M104 for non-fucosylated xyloglucan. First, scFv-M104:GFP as well as CCRC-M104, could not effectively bind to most samples of hemicellulose or pectin in this panel (Figure 3.8, 3.9). Second, like CCRC-M104, scFv-M104:GFP displayed binding capacity to Tamarind Xyloglucan, Tomato Xyloglucan, Sycamore Xyloglucan,

Sycamore Pectic Polysaccharides and Green Tomato Fruit RG-I. Noticeably, the signal strength of scFv-M104:GFP was lower than CCRC-M104.

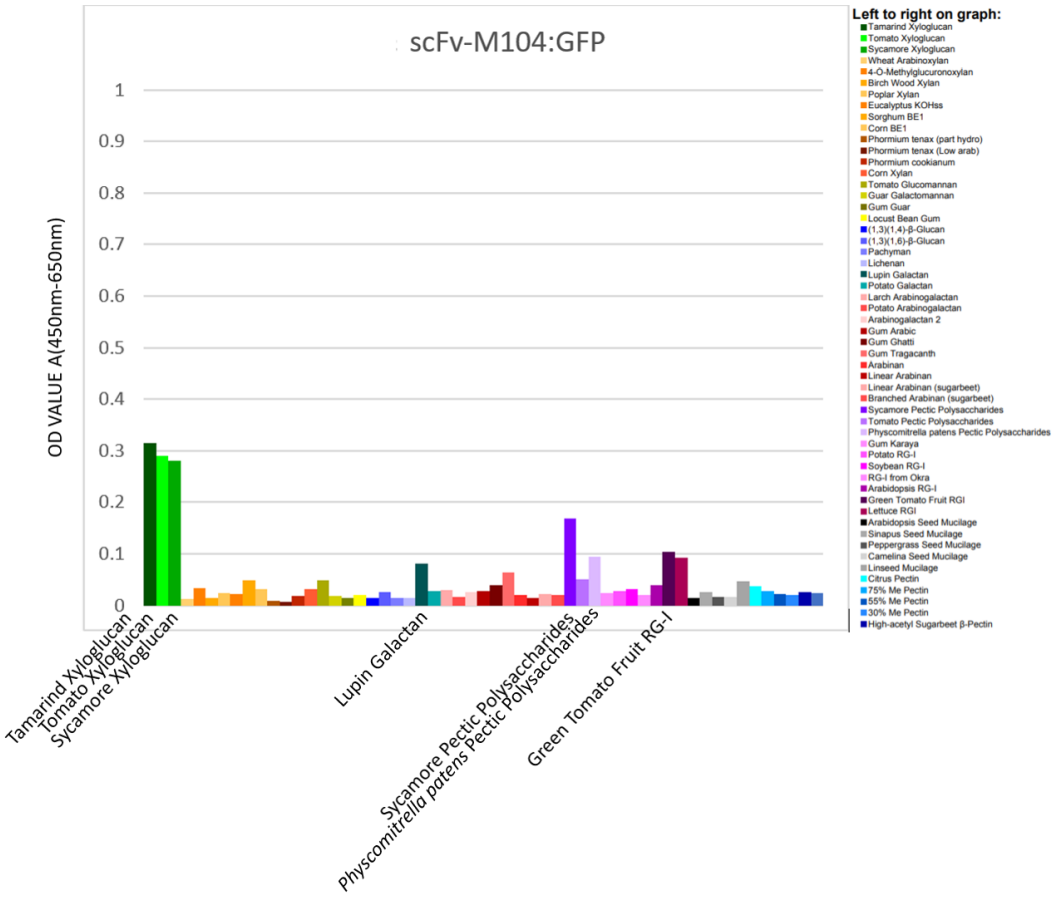

Figure 3.8 Binding specificity of scFv-M104:GFP toward 55 plant polysaccharides.

The specificity of scFv-M104:GFP is revealed by its polysaccharide recognition pattern in the ELISA. Each column reflects the binding strength of scFv-M104:GFP against an immobilized polysaccharide in the corresponding well. ELISA of each scFv was performed in triplicate and the values are the mean.

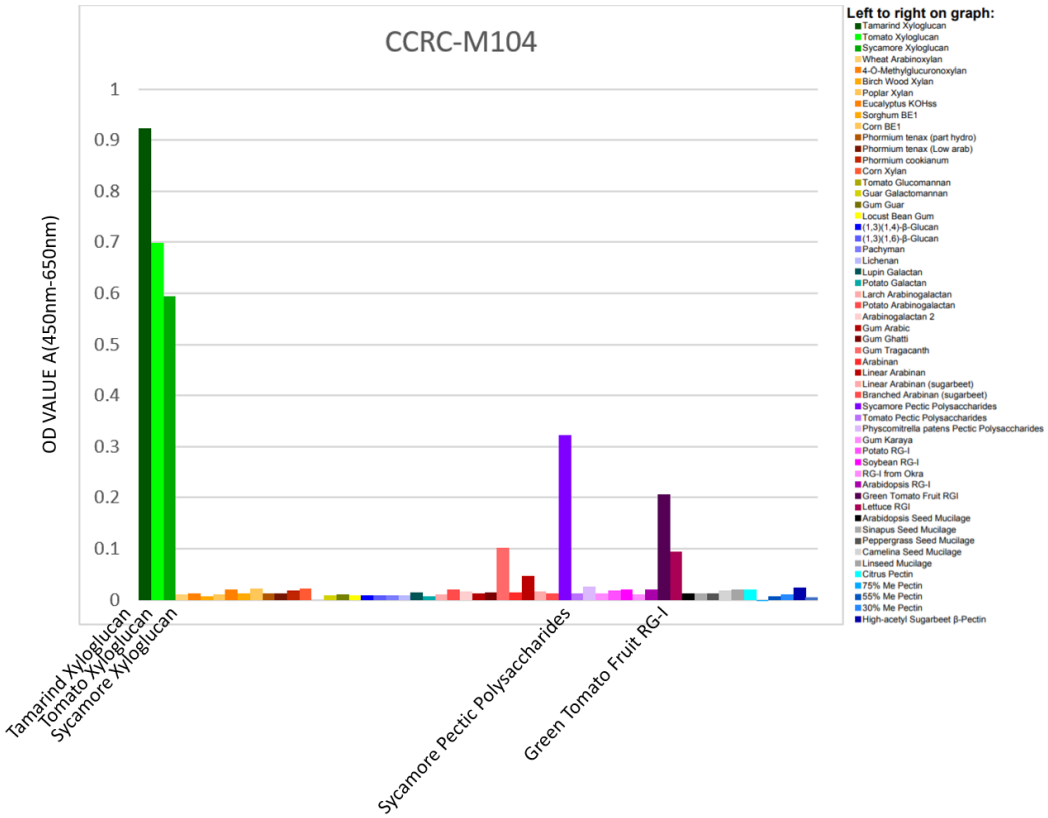

Figure 3.9 Binding specificity of CCRC-M104 toward 55 plant polysaccharides.

The specificity of CCRC-M104 is revealed by its polysaccharide recognition pattern through ELISA. Each column reflects the binding strength of CCRC-M104 against an immobilized polysaccharide in the corresponding well. ELISA of each CCRC parental antibody was performed once.

Xylan-binding Group (scFv-M116:GFP, scFv-M140:GFP, scFv-M144:GFP)

The ELISA results showed that the fluorescent protein GFP tagged scFv-M116:GFP had similar specific binding activities of CCRC-M116 for xylans. Like CCRC-M116, scFv-M116:GFP displayed binding capacity to several xylan preparations (Sorghum BE1, Corn BE1, *Phormium tenax* (Low arab), *Phormium cookianum*) (Figure 3.10, 3.11). In addition, scFv-M116:GFP showed cross-reactivity with a broad range of other arabinans and galactans; these

cross-reactivities were similar, but not identical to those exhibited by the parent antibody, CCRC-M116. Noticeably, the signal strength of scFv-M116:GFP was lower than CCRC-M116.

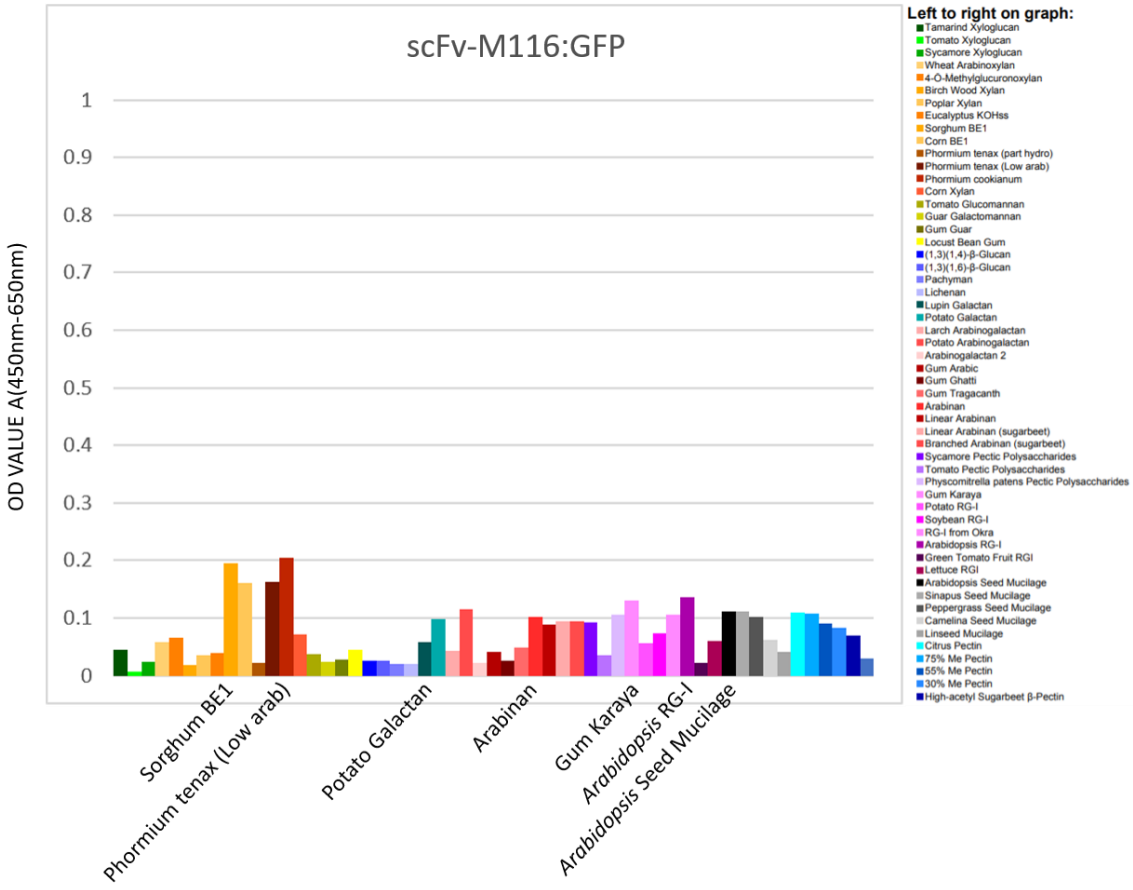

Figure 3.10 Binding specificity of scFv-M116:GFP toward 55 plant polysaccharides.

The specificity of scFv-M116:GFP is revealed by its polysaccharide recognition pattern in the ELISA. Each column reflects the binding strength of scFv-M116:GFP against an immobilized polysaccharide in the corresponding well. ELISA of each scFv was performed in triplicate and the values are the mean.

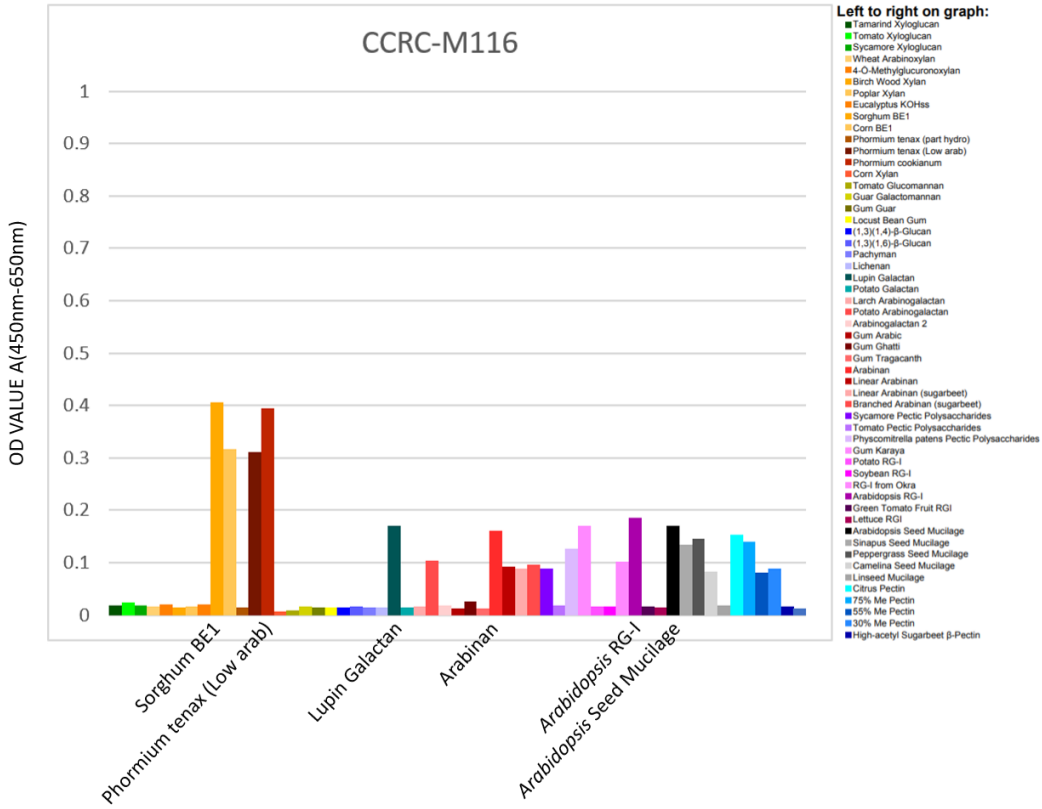

Figure 3.11 Binding specificity of CCRC-M116 toward 55 plant polysaccharides.

The specificity of CCRC-M116 is revealed by its polysaccharide recognition pattern through ELISA. Each column reflects the binding strength of CCRC-M116 against an immobilized polysaccharide in the corresponding well. ELISA of each CCRC parental antibody was performed once.

Previous study displayed that CCRC-M140 bound effectively to xylan preparations including wheat Arabinoxylan, 4-O-Methyl-D-glucurono-D-xylan, Birch Wood xylan, Poplar xylan and Eucalyptus KOH extract which is largely xylan (Pattathil, Avci et al. 2010) (Figure 3.13). However, the ELISA test showed that scFv-M140:GFP did not recognize any xylan preparation included in the panel, nor to any other polysaccharide (Figure 3.12). The inability of

scFv-M140:GFP to recognize polysaccharides most probably reflects variations in the structural differences between antibody and scFv, or an inherent instability of the scFv.

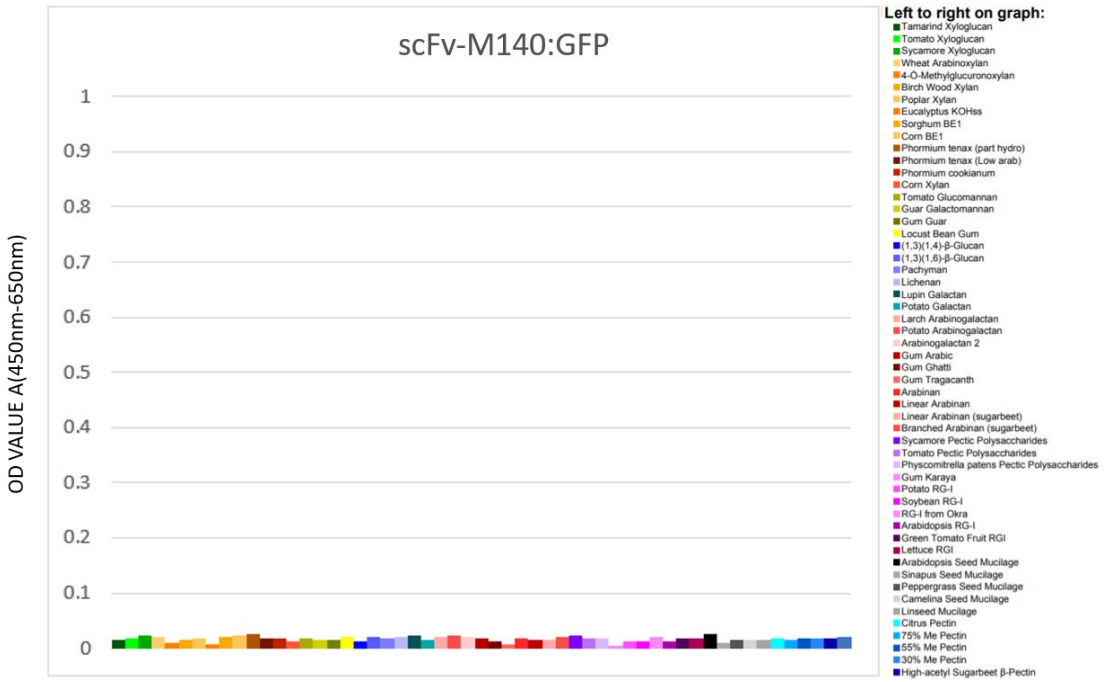

Figure 3.12 Binding specificity of scFv-M140:GFP toward 55 plant polysaccharides.

The specificity of scFv-M140:GFP is revealed by its polysaccharide recognition pattern in the ELISA. Each column reflects the binding strength of scFv-M140:GFP against an immobilized polysaccharide in the corresponding well. ELISA of each scFv was performed in triplicate and the values are the mean.

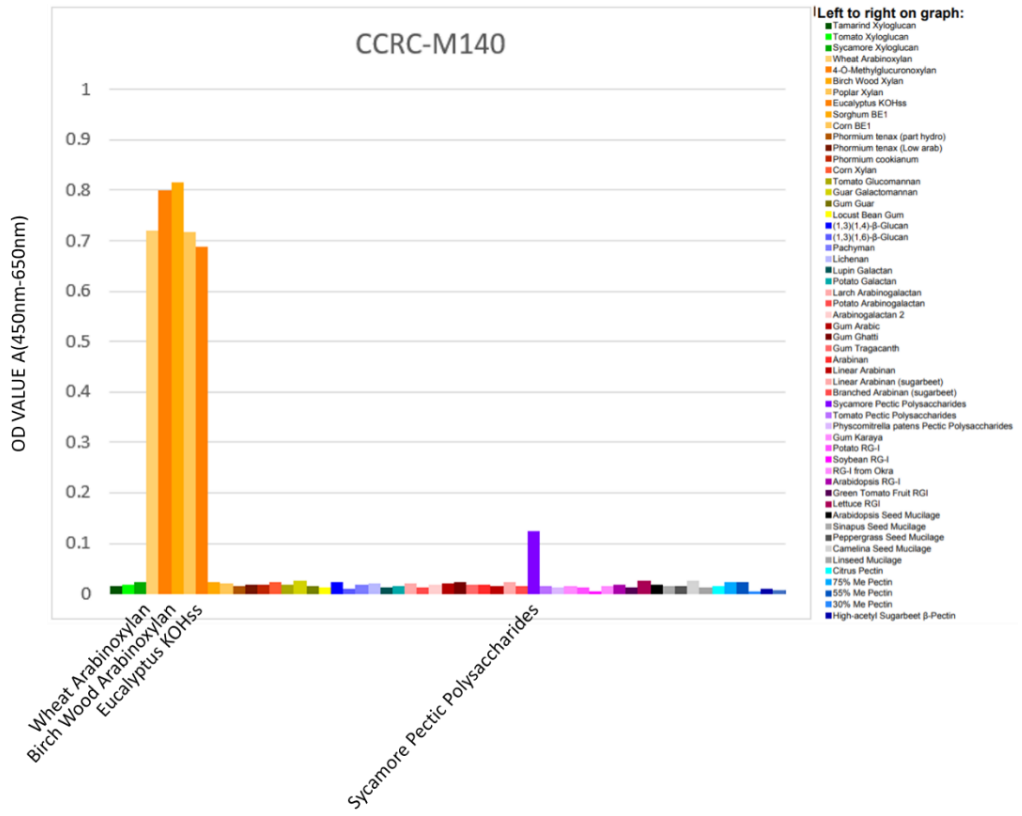

Figure 3.13 Binding specificity of CCRC-M140 toward 55 plant polysaccharides.

The specificity of CCRC-M140 is revealed by its polysaccharide recognition pattern through ELISA. Each column reflects the binding strength of CCRC-M140 against an immobilized polysaccharide in the corresponding well. ELISA of each CCRC parental antibody was performed once.

The ELISA results showed that the fluorescent protein GFP tagged scFv-M144:GFP had different specific binding partners of CCRC-M144 for xylans. Unlike CCRC-M144 which bound to Wheat Arabinoxylan, 4-O-Methylglucuronoxylan, Birch Wood Xylan, Poplar Xylan, Eucalyptus KOHss, Sorghum BE1 and Corn BE1(Figure 3.15), scFv-M144:GFP displayed binding capacity to 4-O-Methylglucuronoxylan, Birch Wood Xylan, *Arabidopsis* Seed Mucilage and Citrus Pectin (Figure 3.14). Noticeably, the signal strength of scFv-M144:GFP was lower

than CCRC-M144.

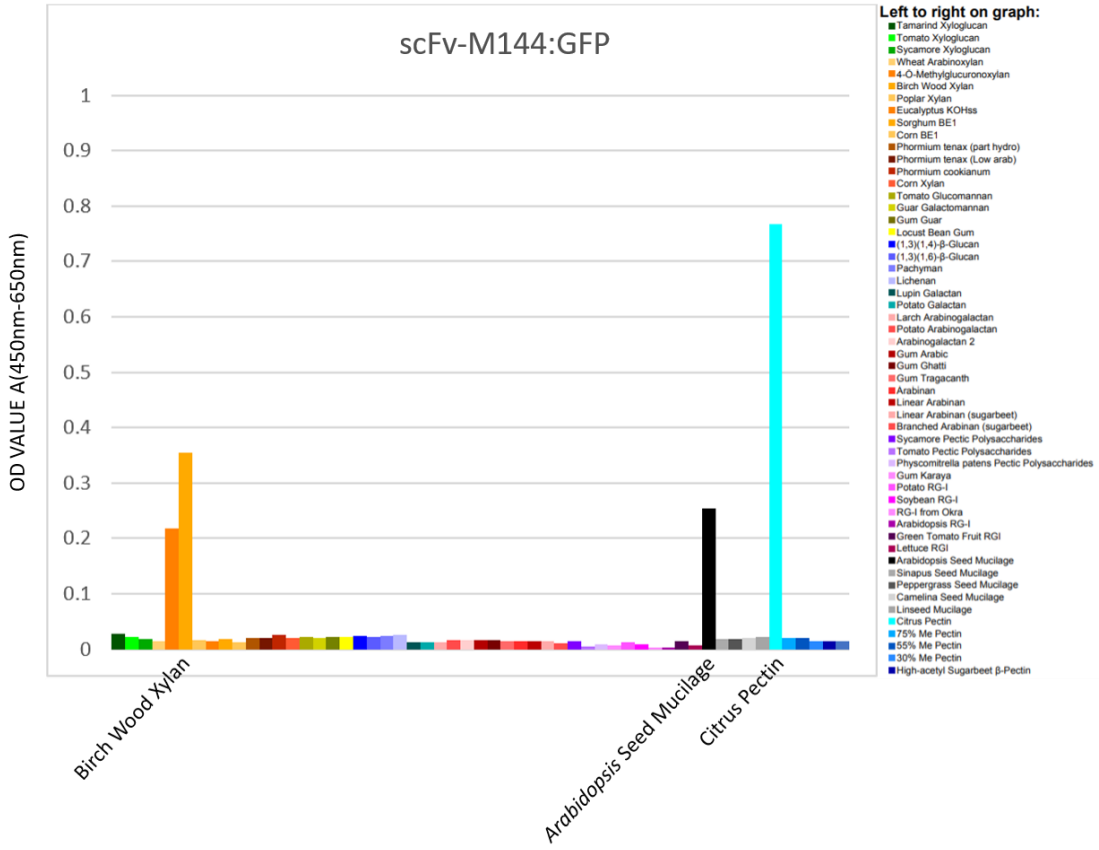

Figure 3.14 Binding specificity of scFv-M144:GFP toward 55 plant polysaccharides.

The specificity of scFv-M144:GFP is revealed by its polysaccharide recognition pattern in the ELISA. Each column reflects the binding strength of scFv-M144:GFP against an immobilized polysaccharide in the corresponding well. ELISA of each scFv was performed in triplicate and the values are the mean.

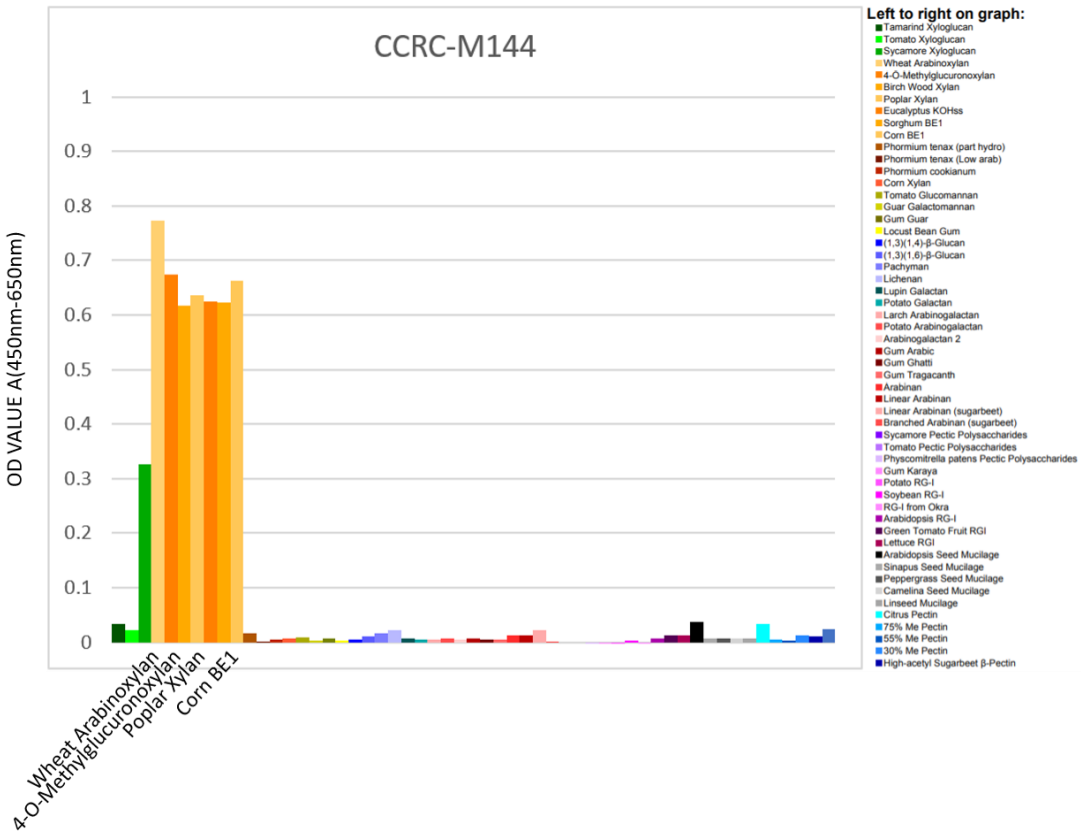

Figure 3.15 Binding specificity of CCRC-M144 toward 55 plant polysaccharides.

The specificity of CCRC-M144 is revealed by its polysaccharide recognition pattern through ELISA. Each column reflects the binding strength of CCRC-M144 against an immobilized polysaccharide in the corresponding well. ELISA of each CCRC parental antibody was performed once.

RG-I-binding Group (scFv-M14:GFP, scFv-M35:GFP, scFv-M134:GFP)

The ELISA results showed that scFv-M14:GFP had subtle differences in its binding activities from its parent antibody, CCRC-M14. Previous study showed that CCRC-M14 recognizes the backbone of RG-I (Ruprecht, Bartetzko et al. 2017), and will bind to a broad diversity of plant RG-I and mucilage preparations (Figures 3.17). The scFv-M14:GFP showed binding capacity to RG-I and seed mucilage from different species (Figures 3.16). Different from

CCRC-M14, the scFv-M14:GFP bound effectively to Citrus Pectin, 30% Me Pectin, High-acetyl Sugarbeet β-Pectin and Jatoba Xyloglucan of *Hymenaea courbaril*. Both scFv-M14:GFP and its parent antibody, CCRC-M14 bound to a broad range of arabinogalactan-containing polysaccharides. However, the specific binding intensities and patterns among the polysaccharides tested are not identical for scFv-M14:GFP and CCRC-M14. Additional testing would be required to resolve and understand these differences.

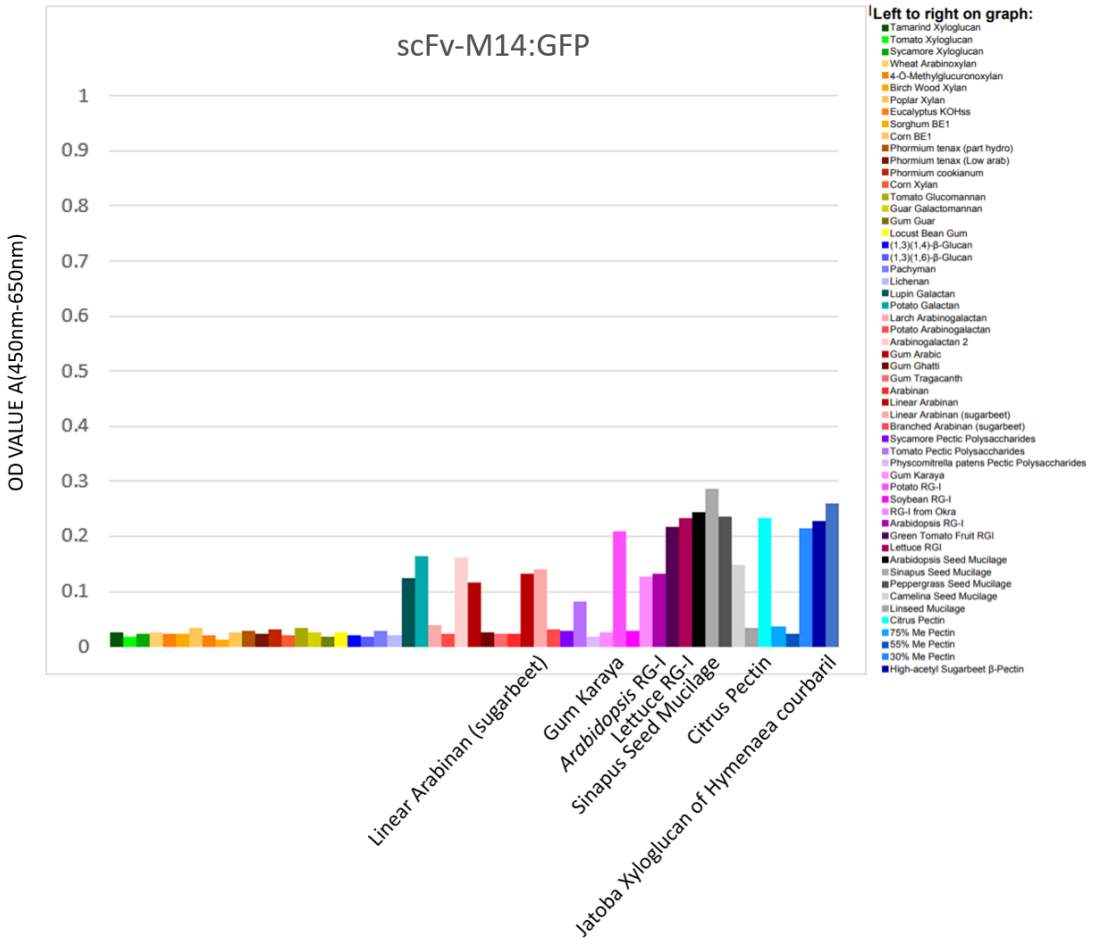

Figure 3.16 Binding specificity of scFv-M14:GFP toward 55 plant polysaccharides.

The specificity of scFv-M14:GFP is revealed by its polysaccharide recognition pattern in the ELISA. Each column reflects the binding strength of scFv-M14:GFP against an immobilized

polysaccharide in the corresponding well. ELISA of each scFv was performed in triplicate and the values are the mean.

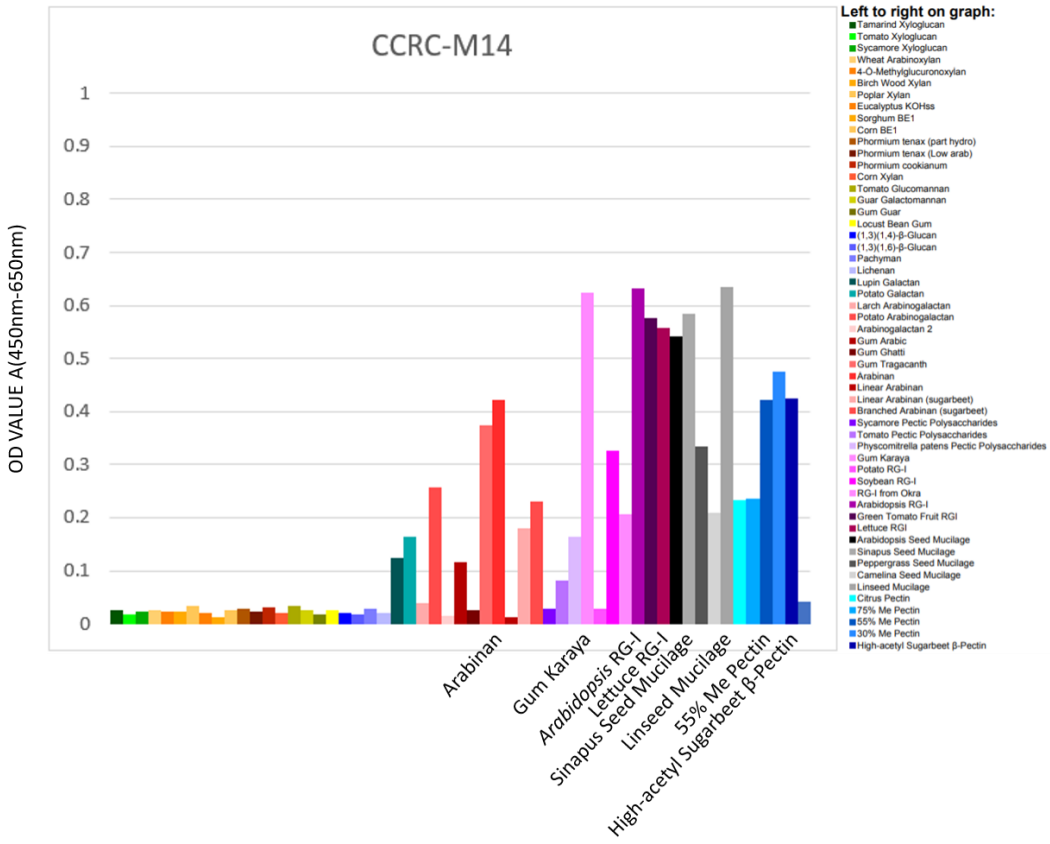

Figure 3.17 Binding specificity of CCRC-M14 toward 55 plant polysaccharides.

The specificity of CCRC-M14 is revealed by its polysaccharide recognition pattern through ELISA. Each column reflects the binding strength of CCRC-M14 against an immobilized polysaccharide in the corresponding well. ELISA of each CCRC parental antibody was performed once.

The ELISA results showed that the fluorescent protein GFP tagged scFv-M35:GFP had very low binding activity and very different binding activities from its parent antibody, CCRC-M35. Previous study showed that CCRC-M35 is specific for the backbone of RG-I (Ruprecht, Bartetzko et al. 2017) and binds to RG-I and seed mucilages from different species (Figures

3.19). However, scFv-M35:GFP showed binding capacity to RG-I and seed mucilage from different species, but did not bind to pectin preparations (e.g. sugar beet pectin) recognized by the parent antibody (Figures 3.18). Besides Soybean RG-I, *Arabidopsis* RG-I and Lettuce RG-I, it also bound effectively to Gum Ghatti. Unlike CCRC-M35 which bound to a broad range of arabinogalactan-containing polysaccharides, scFv-M35:GFP did not bind to these polysaccharides. One possible reason is that scFv-M35:GFP showed very weak signals compared to CCRC-M35, raising the possibility that scFv-M35:GFP is not active at all. Additional testing would be required to resolve and understand these differences.

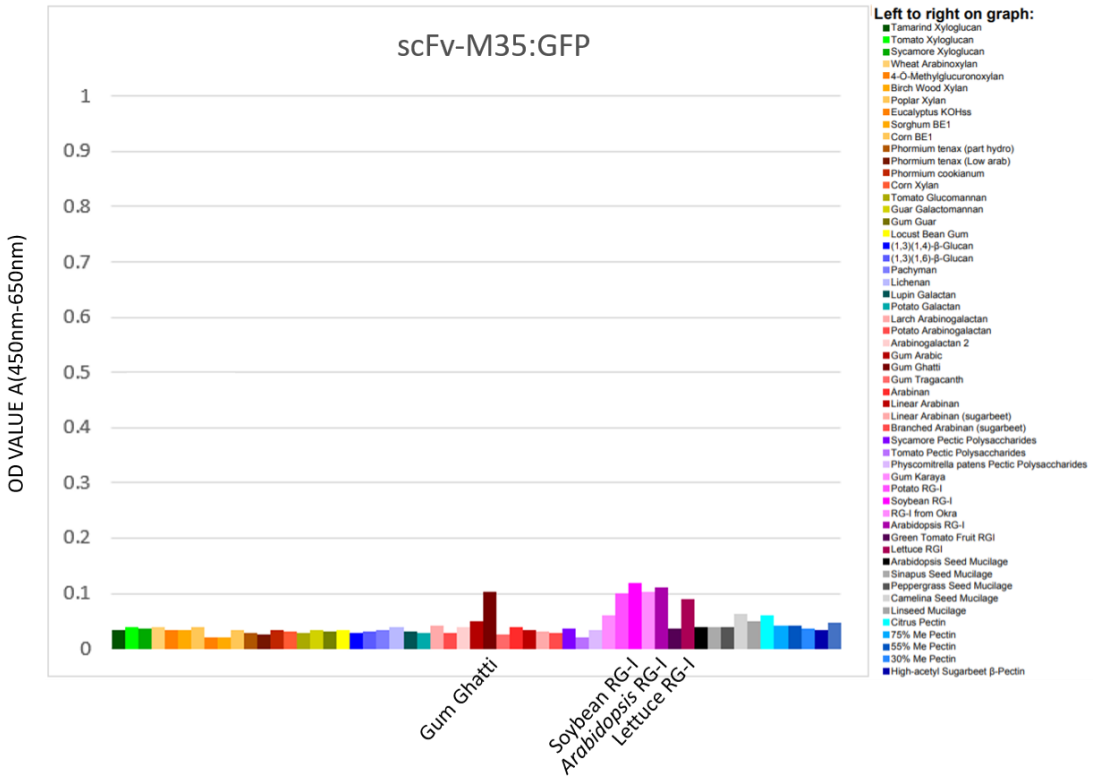

Figure 3.18 Binding specificity of scFv-M35:GFP toward 55 plant polysaccharides.

The specificity of scFv-M35:GFP is revealed by its polysaccharide recognition pattern in the ELISA. Each column reflects the binding strength of scFv-M35:GFP against an immobilized

polysaccharide in the corresponding well. ELISA of each scFv was performed in triplicate and the values are the mean.

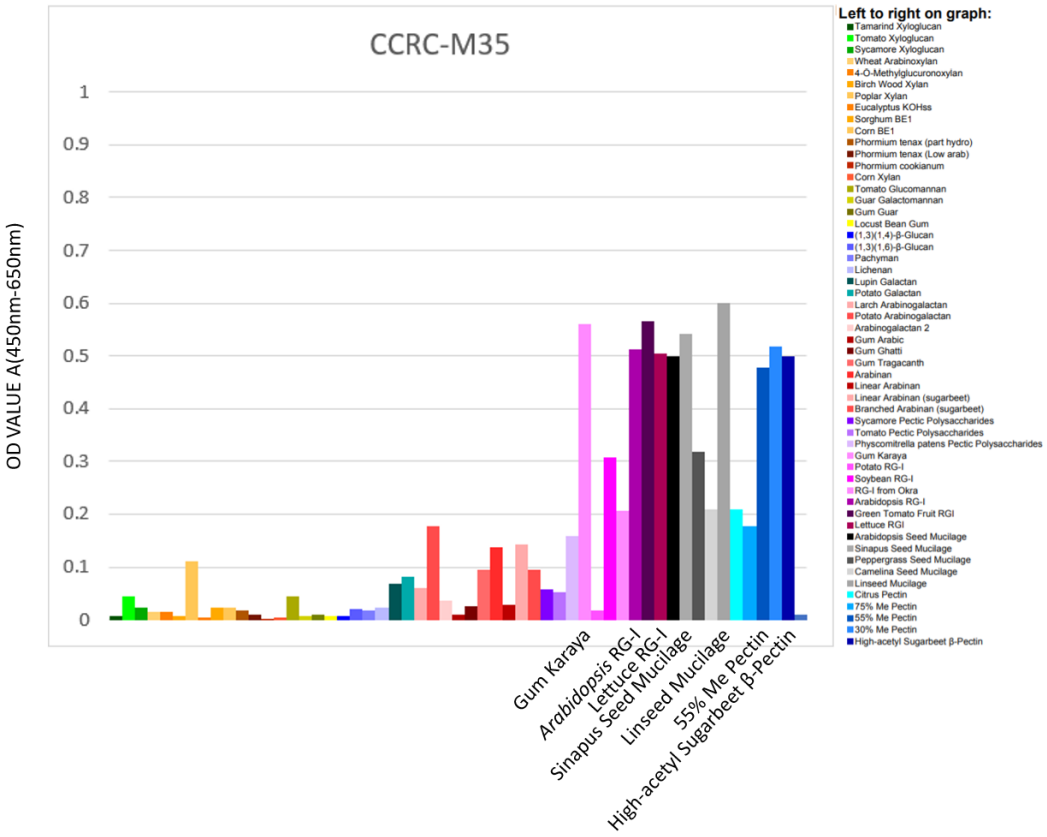

Figure 3.19 Binding specificity of CCRC-M35 toward 55 plant polysaccharides.

The specificity of CCRC-M35 is revealed by its polysaccharide recognition pattern through ELISA. Each column reflects the binding strength of CCRC-M35 against an immobilized polysaccharide in the corresponding well. ELISA of each CCRC parental antibody was performed once.

The ELISA results showed that the fluorescent protein GFP tagged scFv-M134:GFP had different binding activities from its parent antibody, CCRC-M134. Previous study showed that

CCRC-M134 bound to RG-I and seed mucilage from different species. The CCRC-M134 showed significant binding to Sycamore Maple Pectic Polysaccharides and Tomato Pectic Polysaccharides, which is mostly RG-I (Figures 3.21). It also bound effectively to Tomato Xyloglucan, Tomato Glucomannan, Larch Arabinogalactan, Gum Ghatti, Gum Tragacanth, Linear Arabinan, Lettuce RG-I and Sinapus Seed Mucilage. The binding pattern was probably because the structure of the RG-I side chain varies greatly among plants (Harholt, Suttangkakul et al. 2010). Compared to CCRC-M134, scFv-M134:GFP showed binding capacity to 4-O-Methyl-D-glucurono-D-xylan, Corn Xylan, Gum Guar, Branched Arabinan, *Physcomitrella patens* Pectic Polysaccharides, Soybean RG-I and Okra RG-I (Figure 3.20). Both scFv-M134:GFP and its parent antibody, CCRC-M134 bind to a broad range of arabinogalactan-containing polysaccharides. However, the specific binding intensities and patterns among the polysaccharides tested are not identical for scFv-134:GFP and CCRC-M134. Additional testing would be required to resolve and understand these differences.

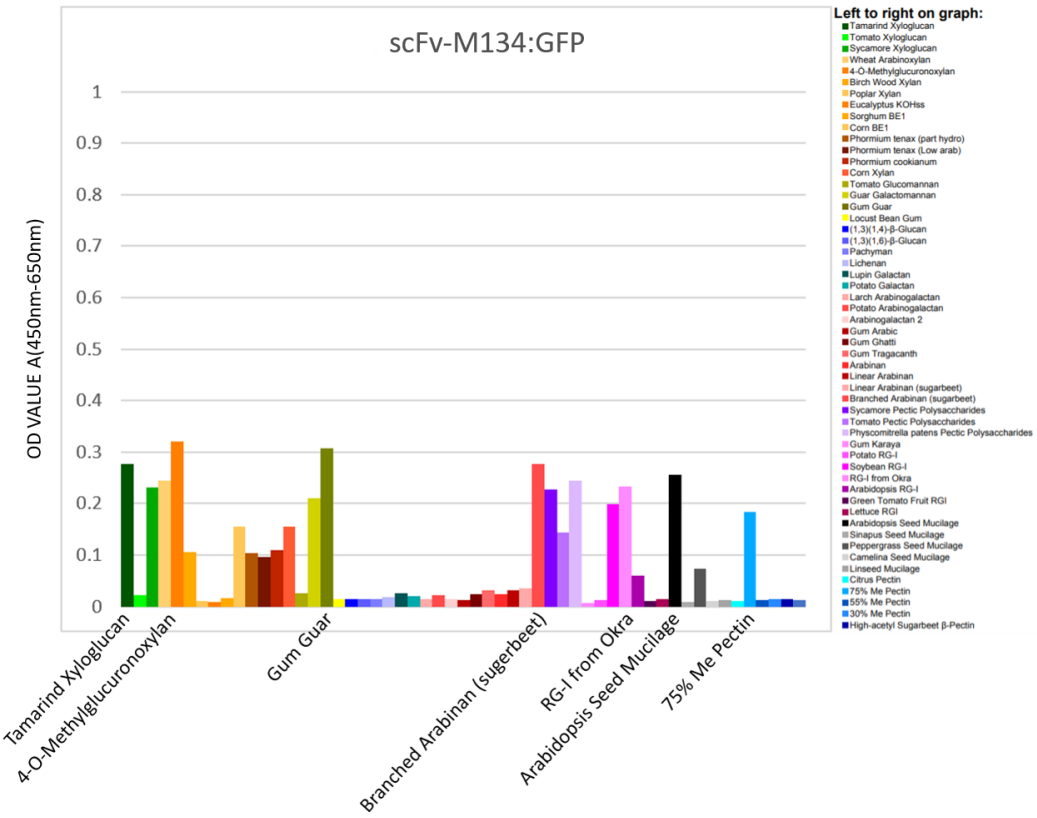

Figure 3.20 Binding specificity of scFv-M134:GFP toward 55 plant polysaccharides.

The specificity of scFv-M134:GFP is revealed by its polysaccharide recognition pattern in the ELISA. Each column reflects the binding strength of scFv-M134:GFP against an immobilized polysaccharide in the corresponding well. ELISA of each scFv was performed in triplicate and the values are the mean.

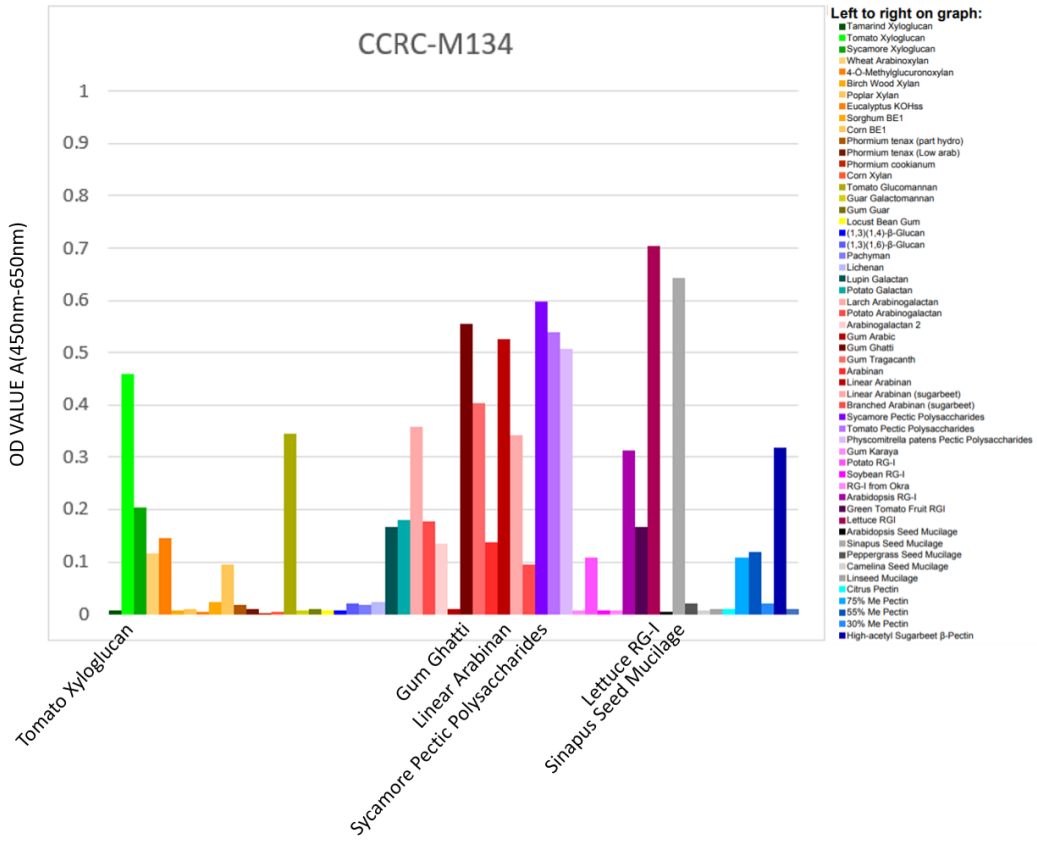

Figure 3.21 Binding specificity of CCRC-M134 toward 55 plant polysaccharides.

The specificity of CCRC-M134 is revealed by its polysaccharide recognition pattern through ELISA. Each column reflects the binding strength of CCRC-M134 against an immobilized polysaccharide in the corresponding well. ELISA of each CCRC parental antibody was performed once.

Linseed mucilage-binding Group (scFv-M141:GFP)

The ELISA results showed that the fluorescent protein GFP tagged scFv-M141:GFP had cross-reactivities not observed with its parent antibody, CCRC-M141. Previous study showed that CCRC-M141 bound exclusively to Linseed Mucilage (Figure 3.23). Compared to CCRC-M141, scFv-M141:GFP showed additional binding capacity to Corn BE1 and (1,3)(1,6)-β-

Glucan (Figure 3.22). At present, we cannot explain the additional cross-reactivity of scFv-M141:GFP with other polysaccharides besides the Linseed mucilage.

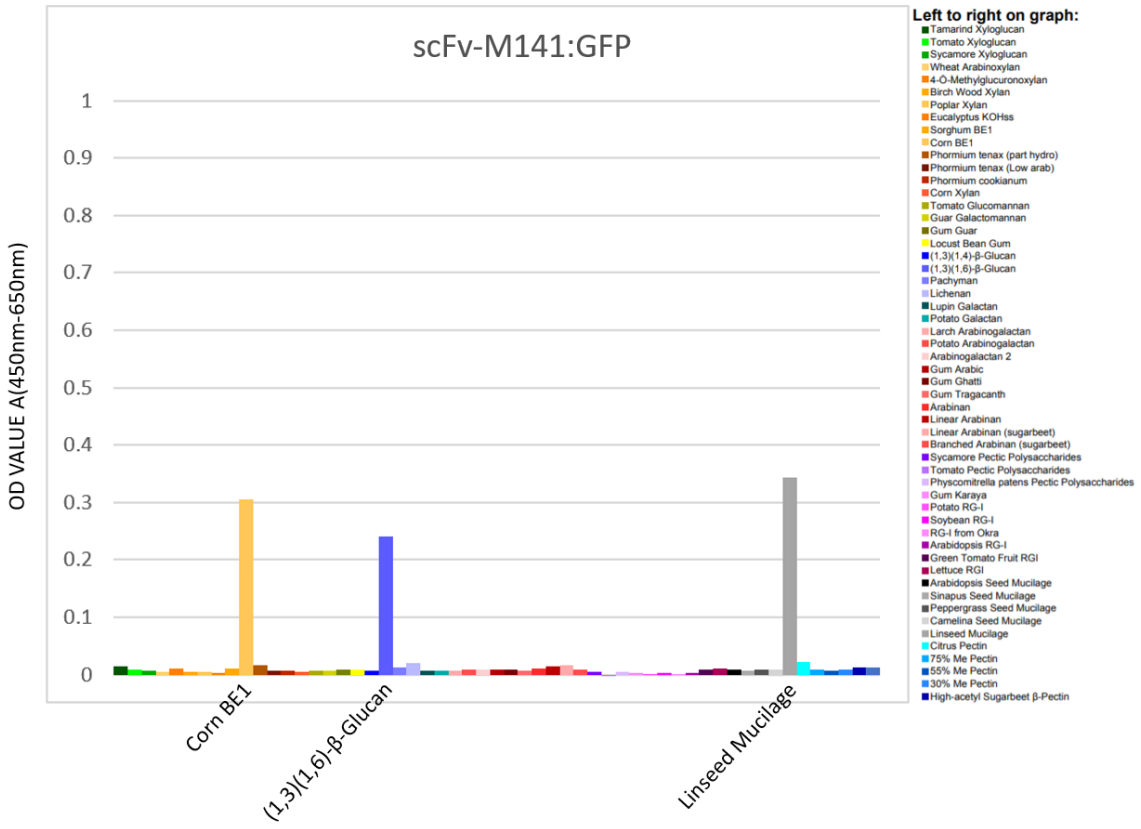

Figure 3.22 Binding specificity of scFv-M141:GFP toward 55 plant polysaccharides.

The specificity of scFv-M141:GFP is revealed by its polysaccharide recognition pattern in the ELISA. Each column reflects the binding strength of scFv-M141:GFP against an immobilized polysaccharide in the corresponding well. ELISA of each scFv was performed in triplicate and the values are the mean.

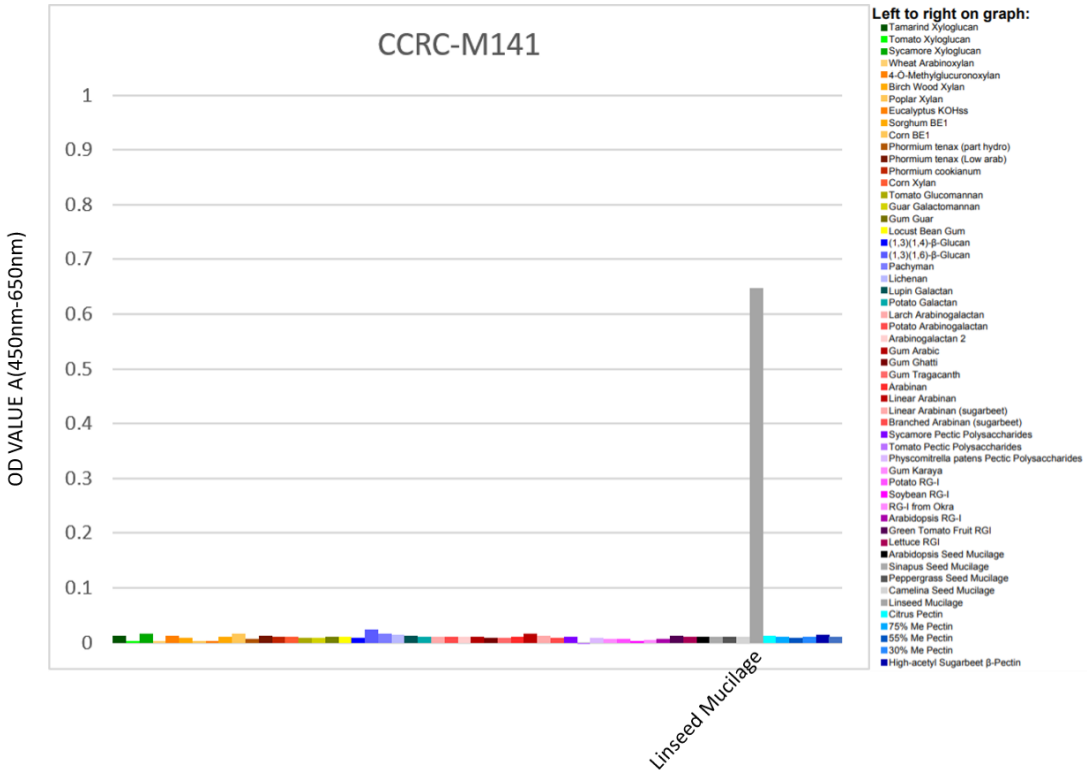

Figure 3.23 Binding specificity of CCRC-M141 toward 55 plant polysaccharides.

The specificity of CCRC-M141 is revealed by its polysaccharide recognition pattern through ELISA. Each column reflects the binding strength of CCRC-M141 against an immobilized polysaccharide in the corresponding well. ELISA of each CCRC parental antibody was performed once.

Physcomitrella patens pectic polysaccharides-binding Group (scFv-M98:GFP)

The ELISA results showed that the fluorescent protein GFP tagged scFv-M98:GFP had similar binding activities compared to its parent, CCRC-M98. Like CCRC-M98, scFv-M98:GFP bound to *Physcomitrella patens* Pectic Polysaccharides (Figure 3.24, 3.25). Noticeably, the signal strength of scFv-M98:GFP was lower than CCRC-M98.

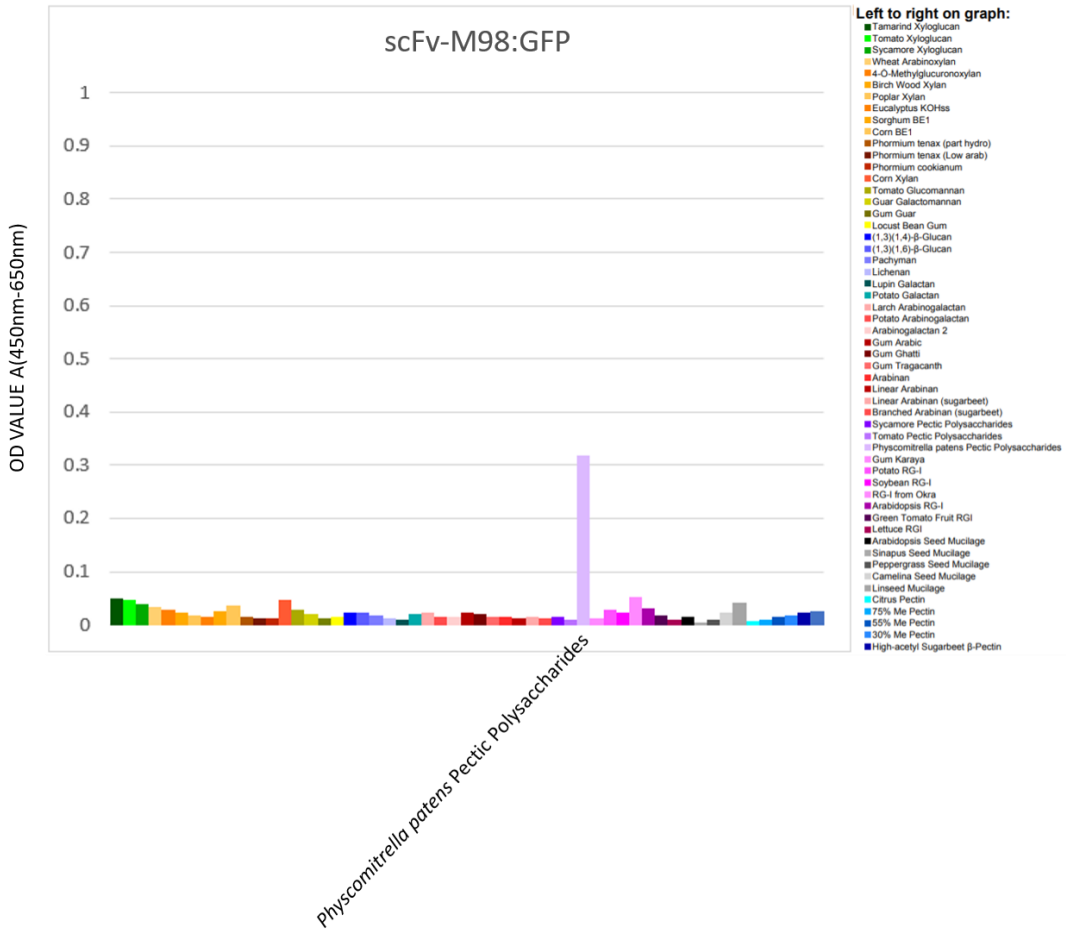

Figure 3.24 Binding specificity of scFv-M98 toward 55 plant polysaccharides.

The specificity of scFv-M98:GFP is revealed by its polysaccharide recognition pattern in the ELISA. Each column reflects the binding strength of scFv-M98:GFP against an immobilized polysaccharide in the corresponding well. ELISA of each scFv was performed in triplicate and the values are the mean.

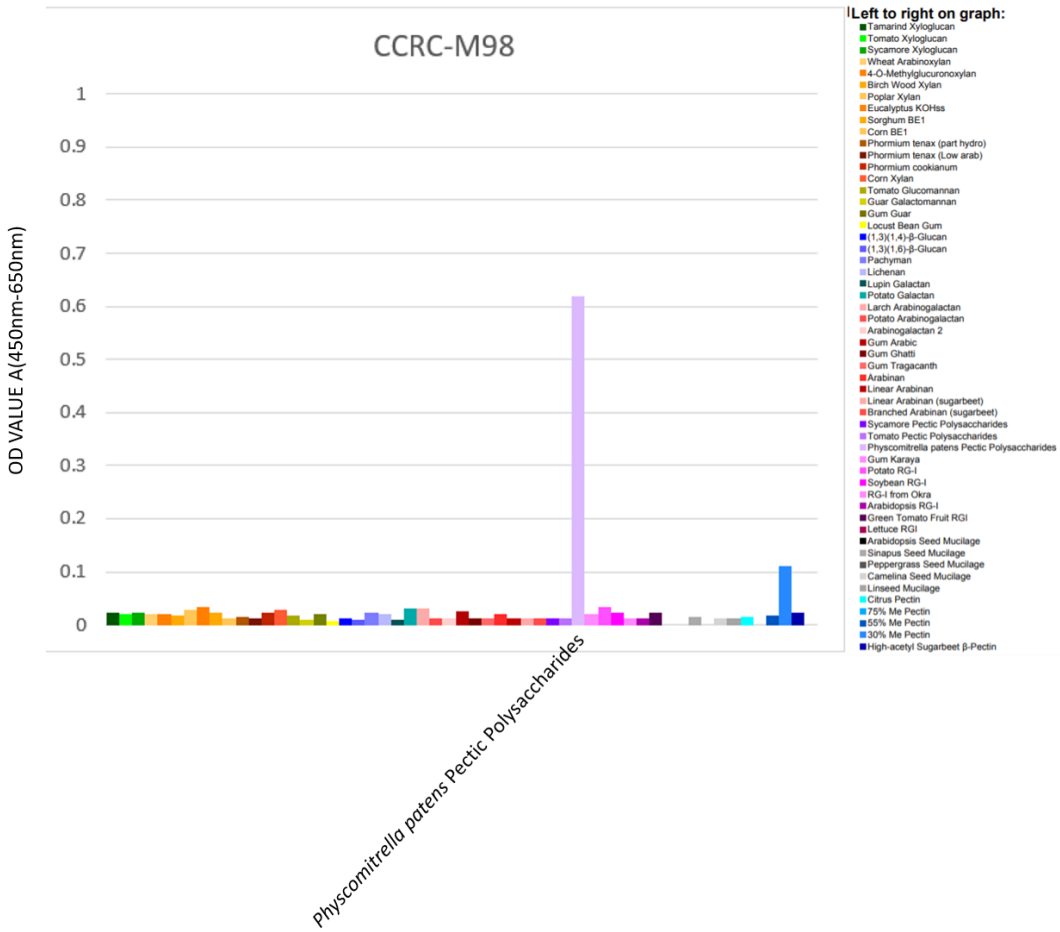

Figure 3.25 Binding specificity of CCRC-M98 toward 55 plant polysaccharides.

The specificity of CCRC-M98 is revealed by its polysaccharide recognition pattern through ELISA. Each column reflects the binding strength of CCRC-M98 against an immobilized polysaccharide in the corresponding well. ELISA of each CCRC parental antibody was performed once.

HG backbone-binding Group (scFv-M131:GFP)

The ELISA results showed that the fluorescent protein GFP tagged scFv-M131:GFP was actually more selective than its parent, CCRC-M131. Like CCRC-M131, scFv-M131:GFP bound to Soybean RG-I, Green Tomato Fruit RG-I, Peppergrass Seed Mucilage, 75% Me Pectin and

High-acetyl Sugarbeet β-Pectin (Figure 3.26, 3.27). However, CCRC-M131 also binds to several other pectic polysaccharide preparations that are not recognized by scFv-M131. Noticeably, the signal strength of scFv-M131:GFP was lower than CCRC-M131, and perhaps this explains why no signal was observed for several polysaccharides recognized by the parent antibody.

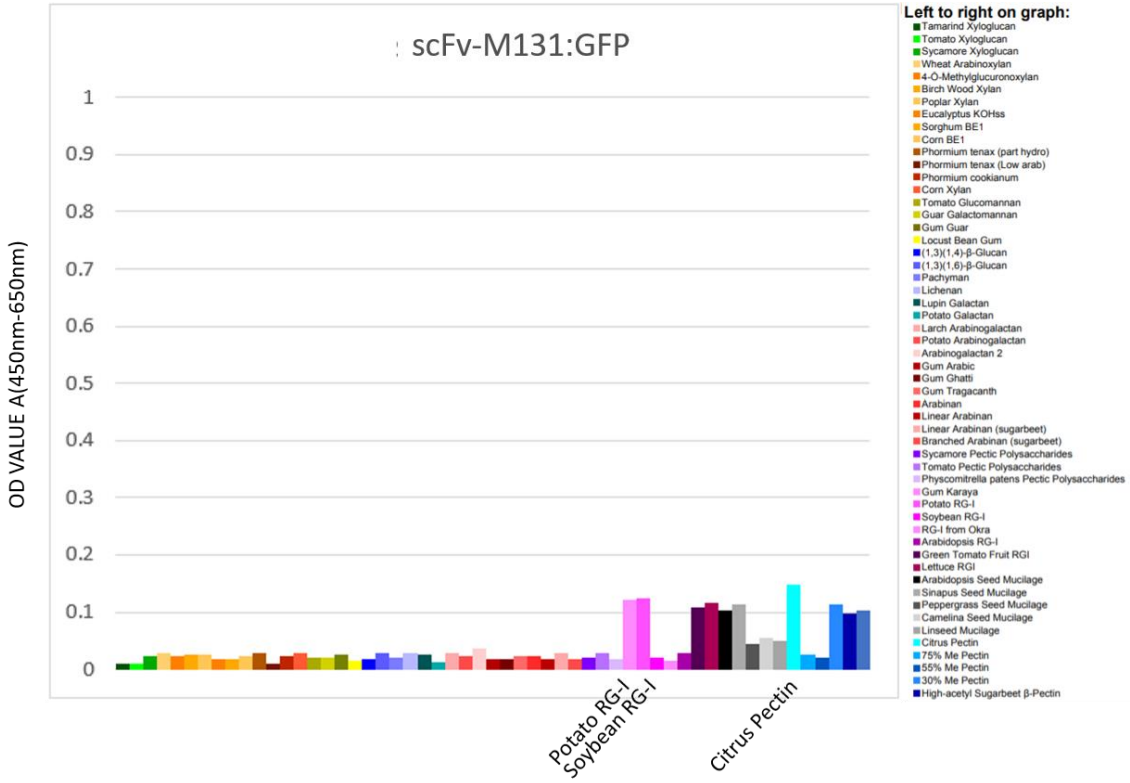

Figure 3.26 Binding specificity of scFv-M131:GFP toward 55 plant polysaccharides.

The specificity of scFv-M131:GFP is revealed by its polysaccharide recognition pattern in the ELISA. Each column reflects the binding strength of scFv-M131:GFP against an immobilized polysaccharide in the corresponding well. ELISA of each scFv was performed in triplicate and the values are the mean.

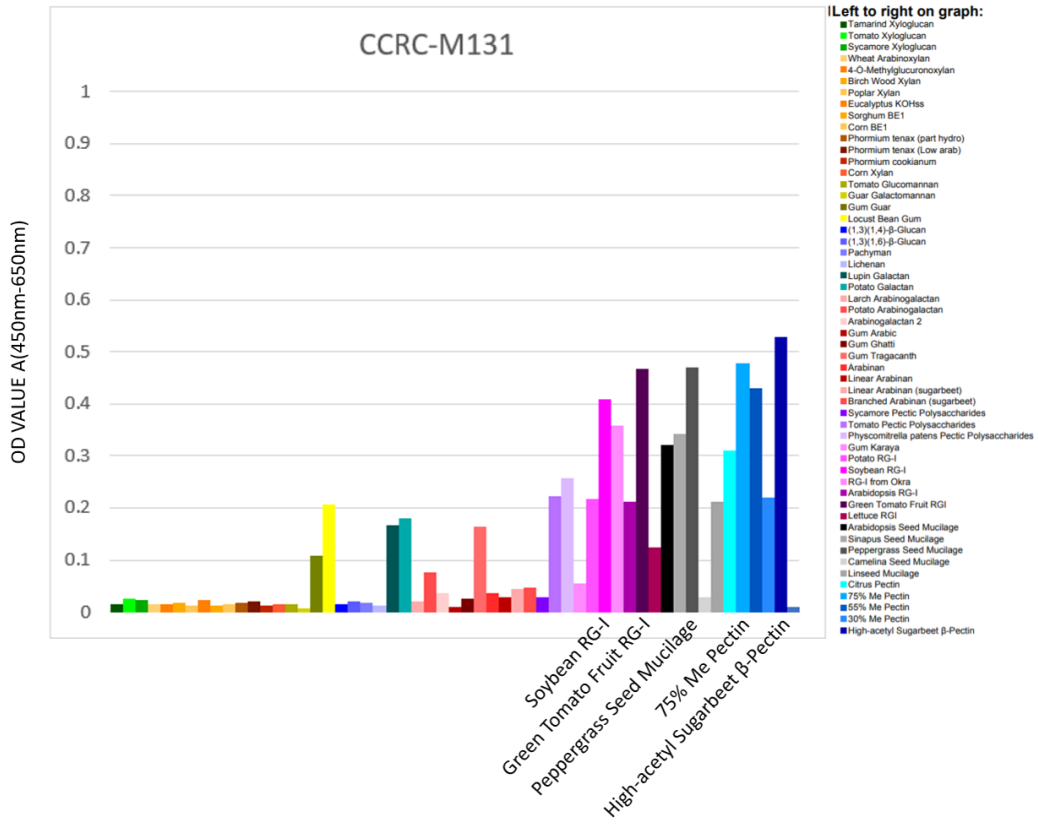

Figure 3.27 Binding specificity of CCRC-M131 toward 55 plant polysaccharides.

The specificity of CCRC-M131 is revealed by its polysaccharide recognition pattern through ELISA. Each column reflects the binding strength of CCRC-M131 against an immobilized polysaccharide in the corresponding well. ELISA of each CCRC parental antibody was performed once.

Direct labeling of fixed *Arabidopsis* root sections using tagged scFvs

Arabidopsis root sections were immunolabeled to measure the abilities of the twelve fluorescent protein-tagged scFvs (scFv-M1:GFP, scFv-M14:GFP, scFv-M35:GFP, scFv-M58:GFP, scFv-M98:GFP, scFv-M104:GFP, scFv-M106:GFP, scFv-M116:GFP, scFv-

M131:GFP, scFv-M134:GFP, scFv-M141:GFP, scFv-M144:GFP) to label plant cell walls (Figure 3.28). The four xyloglucan-binding scFv-M1:GFP, scFv-M58:GFP, scFv-M104:GFP and scFv-M106:GFP displayed binding mainly to cell walls of the epidermis and with root hairs. They also showed weaker binding to cell walls of cortex, endodermis, pericycle, parenchyme, phloem and xylem. The two xylan-binding scFv-M116:GFP and scFv-M144:GFP did not appear to label root sections and neither did their parent antibodies. The RG-I-binding scFv-M14:GFP, scFv-M35:GFP and scFv-M134:GFP appeared to label the cell walls of every tissue in the *Arabidopsis* root. The HG backbone-binding scFv-M131:GFP also displayed weak binding to the cell walls of every tissue in the *Arabidopsis* root. The *Physcomitrella patens* pectic polysaccharides-binding scFv-M98:GFP and the linseed mucilage-binding scFv-M141:GFP do not label any cell walls in the *Arabidopsis* root. Thus, results from labeling of fixed *Arabidopsis* root sections with GFP fusion scFvs confirmed that the xyloglucan-binding,RG-I-binding, and HG backbone-binding could recognize *Arabidopsis* cell walls when applied to tissue sections *in vitro*, and display labeling patterns very similar to those of their parent antibodies, although the labeling was weaker for the scFvs.

A

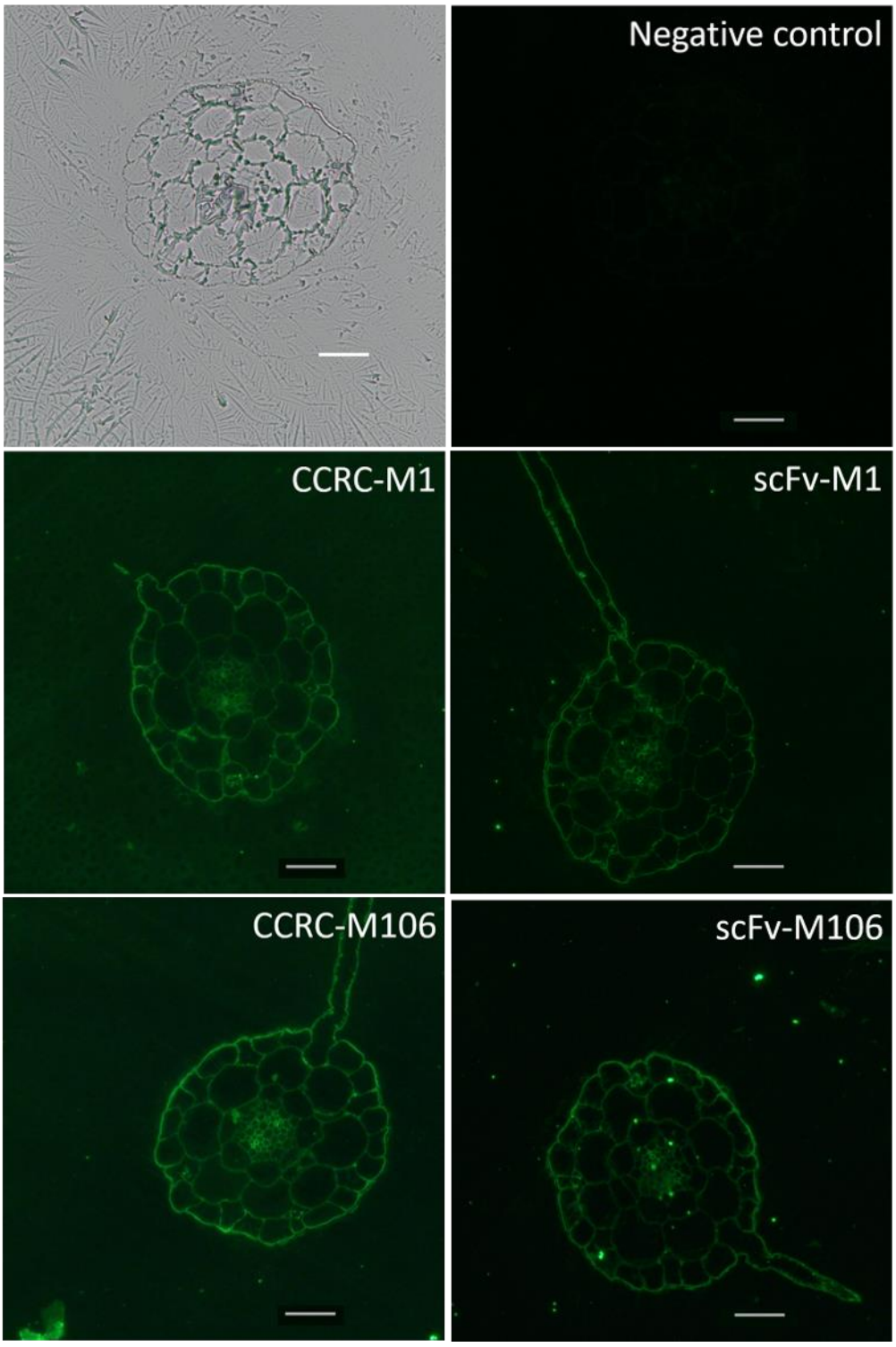

B

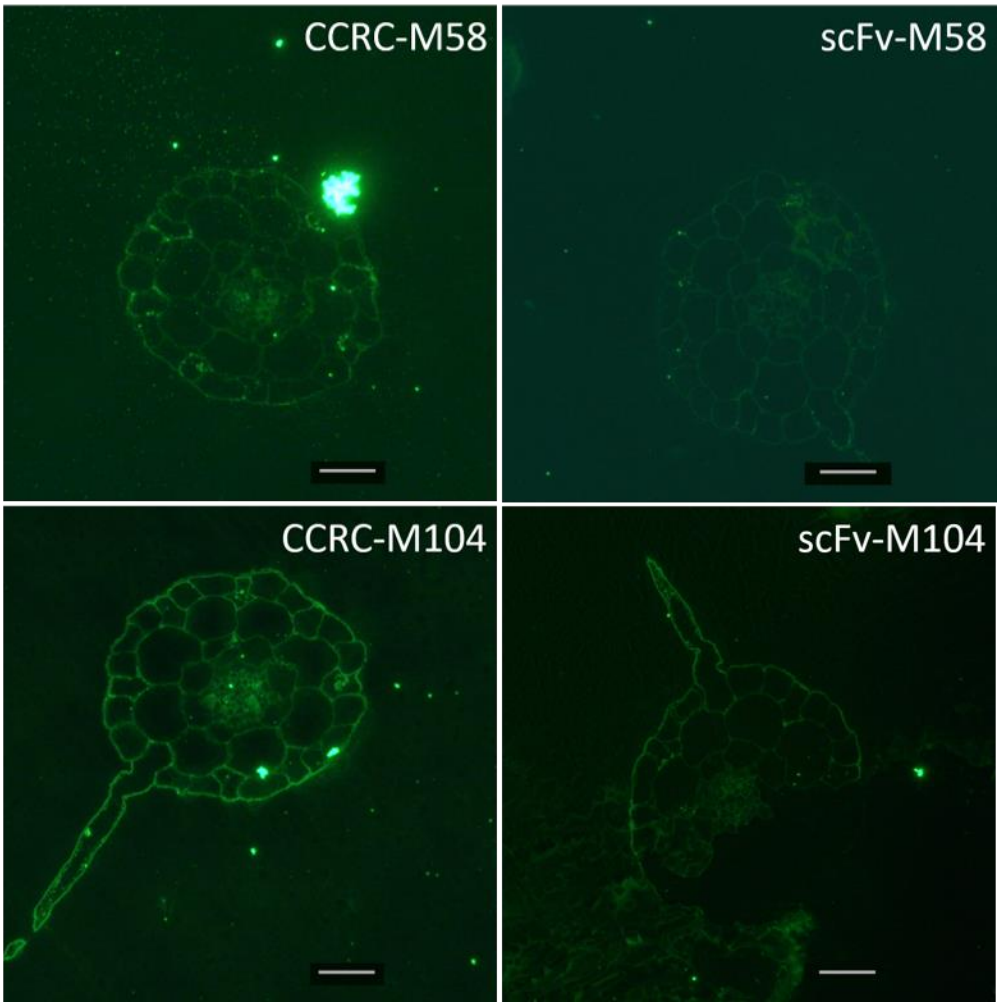

C

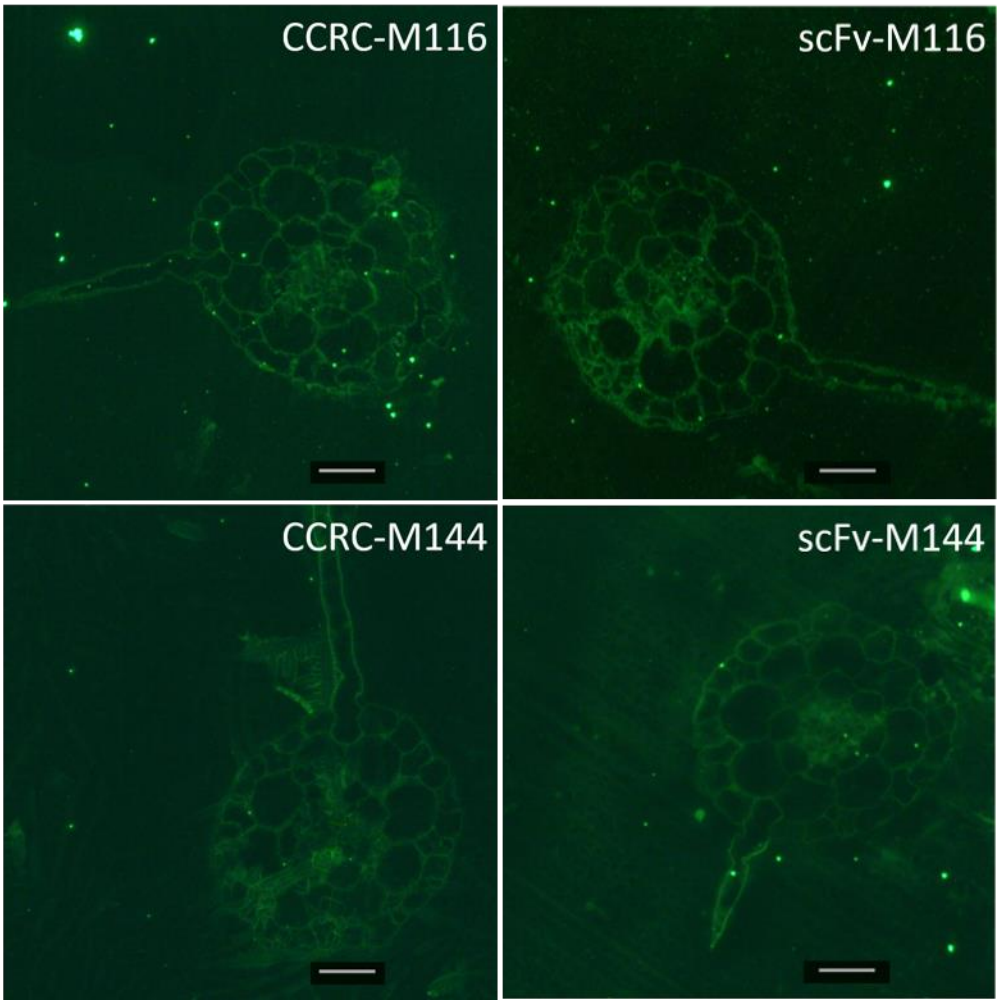

D

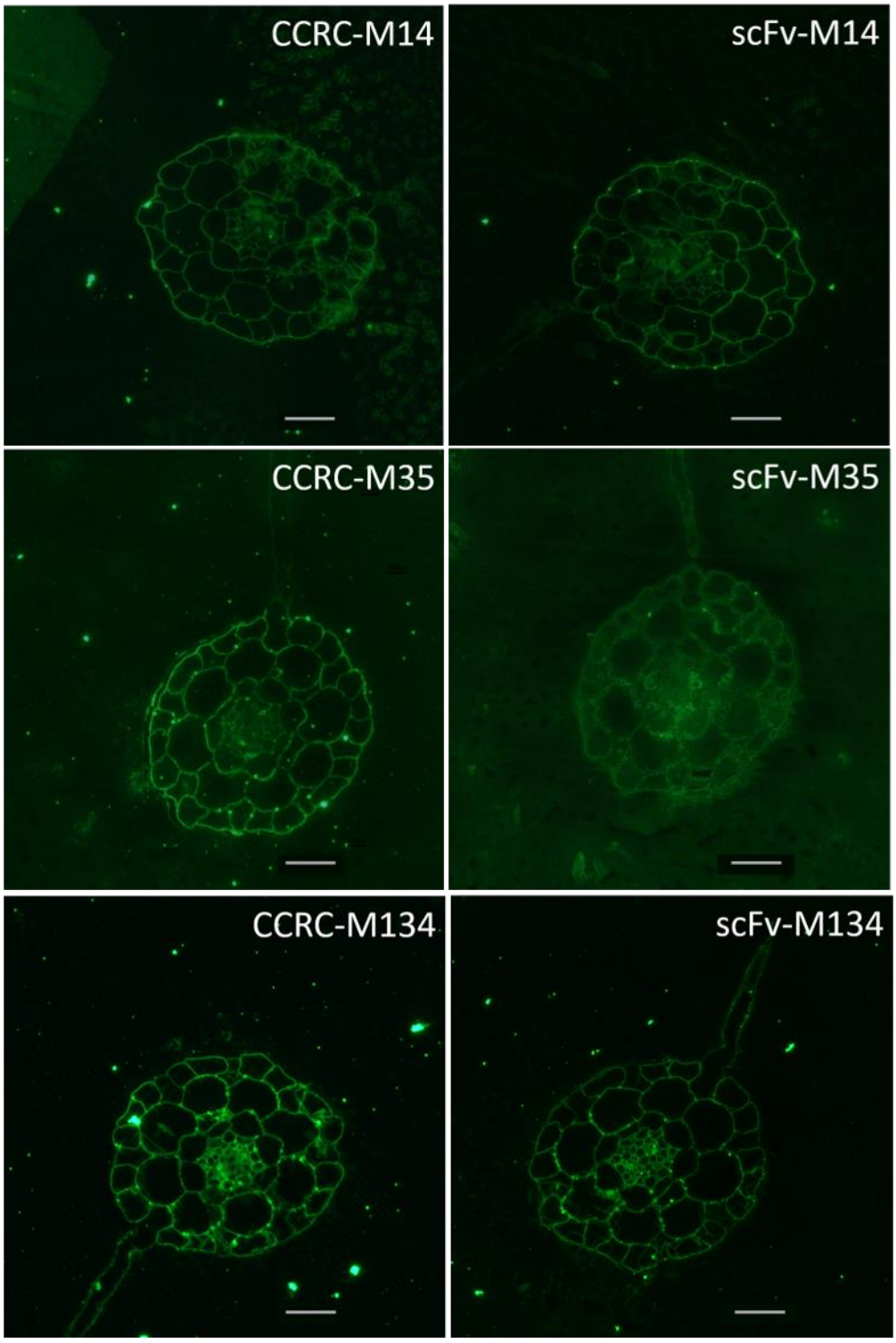

E

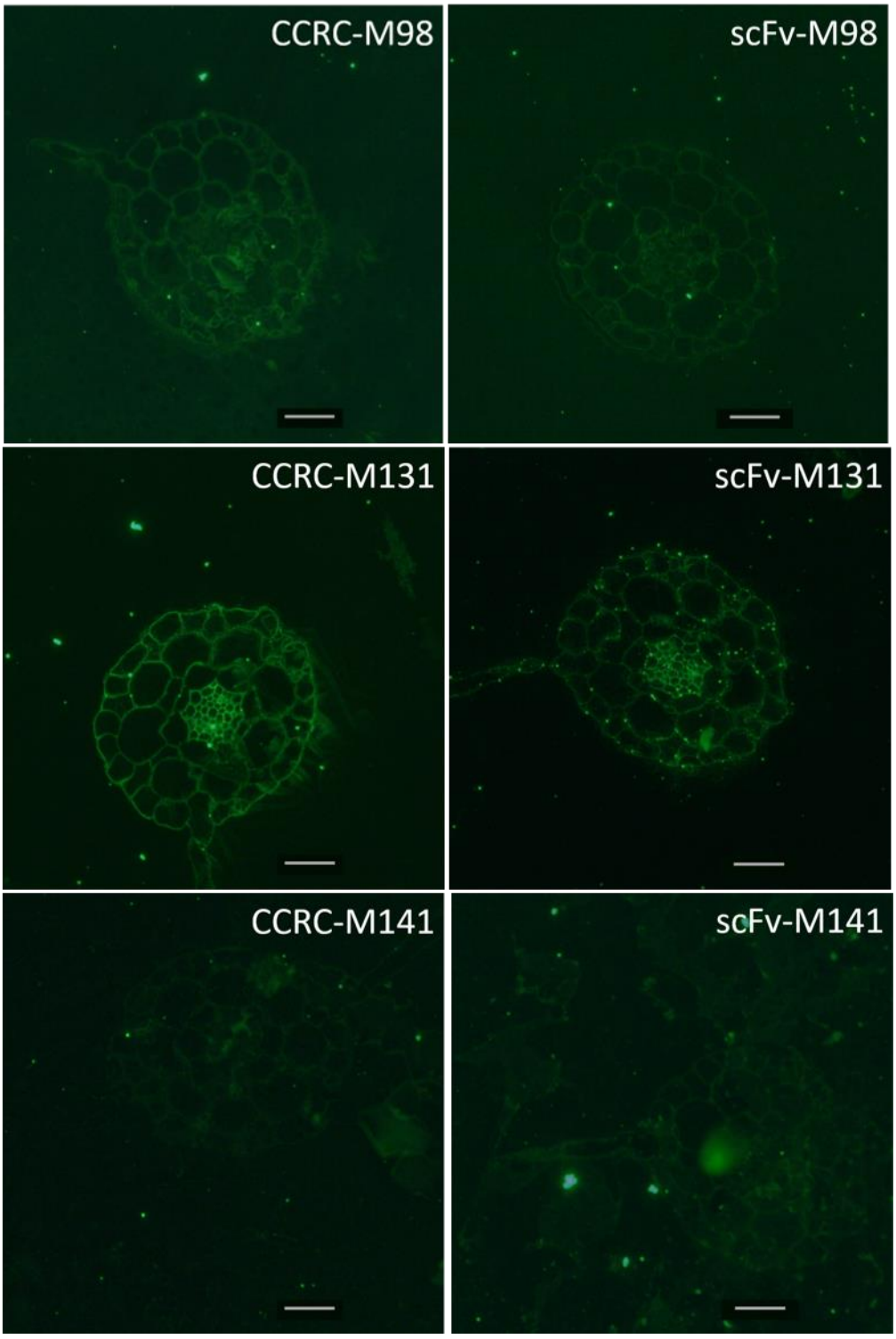

Figure 3.28 Labeling of *Arabidopsis* root sections *in vitro* with tagged scFv fusion proteins.

(A) Fucosylated xyloglucan binding group: scFv-M1:GFP, scfv-M106:GFP and their parent antibodies. Exposure time = 5s. Scale bar = 50µm.

(B) Non-fucosylated xyloglucan binding group: scFv-M58:GFP, scfv-M104:GFP and their parent antibodies. Exposure time: scFv-M58:GFP = 20s, others = 5s. Scale bar = 50µm.

(C) Xylan binding group: scFv-M116:GFP, scFv-M144:GFP and their parent antibodies. Exposure time = 10s. Scale bar = 50µm.

(D) RG-I binding group: scFv-M14:GFP, scFv-M35:GFP and scFv-M134:GFP and their parent antibodies. Exposure time: scFv-M35:GFP = 10s, others = 5s. Scale bar = 50µm.

(E) *Physcomitrella patens* pectic polysaccharides-binding scFv-M98:GFP, HG backbone-binding scFv-M131:GFP, Linseed mucilage-binding scFv-M141:GFP and their parent antibodies. Exposure time: CCRC-M141 and scFv-M141:GFP = 10s, others = 5s. Scale bar = 50µm.

Heterologous Expression of scFvs:YFP in *Arabidopsis*

The experimental design for the heterologous expression of fluorescent protein-tagged scFvs in *Arabidopsis* is outlined in Figure 3.15. In the pBI121 vector (Clontech), a fluorescent protein-tagged form of the xyloglucan-binding scFv-M1 and xylan-binding scFv-M140 was generated by fusing the gene encoding the yellow fluorescent protein (Nagai, Ibata et al. 2002). The full-length scFv-M1:YFP or scFv-M140:YFP gene was fused in frame with the *AtExpansin10* signal peptide (SP) coding sequence (Cho and Cosgrove 2000) at the 5'-end in order to target the translated fusion protein to the cell wall through the secretory pathway in *Arabidopsis*. The empty vector containing the *AtExpansin*10 signal peptide coding sequence

directly fused with YFP was produced as a negative control to verify that expression of the YFP protein itself does not bind to or affect the plant cell wall. After transformation, kanamycin antibiotic-resistant transgenic plants were selected and the expression of introduced genes was confirmed by Reverse Transcript (RT)-PCR analysis using total RNA harvested from stems. For each construct, three independent lines were isolated and selfed. T2 generations of these transgenic plants were screened for kanamycin resistance and examined by RT-PCR and fluorescence microscopy. Among the T2 plants, the introduced scFv-M1:YFP or scFv-M140:YFP or SP:YFP genes were stably inherited by confirmation of semi RT-PCR (Figure 3.29E). In our imaging analysis, transgenic plants were grown from seeds of one line of each transgenic plant expressing scFv-M1:YFP or scFv-M140:YFP or SP:YFP.

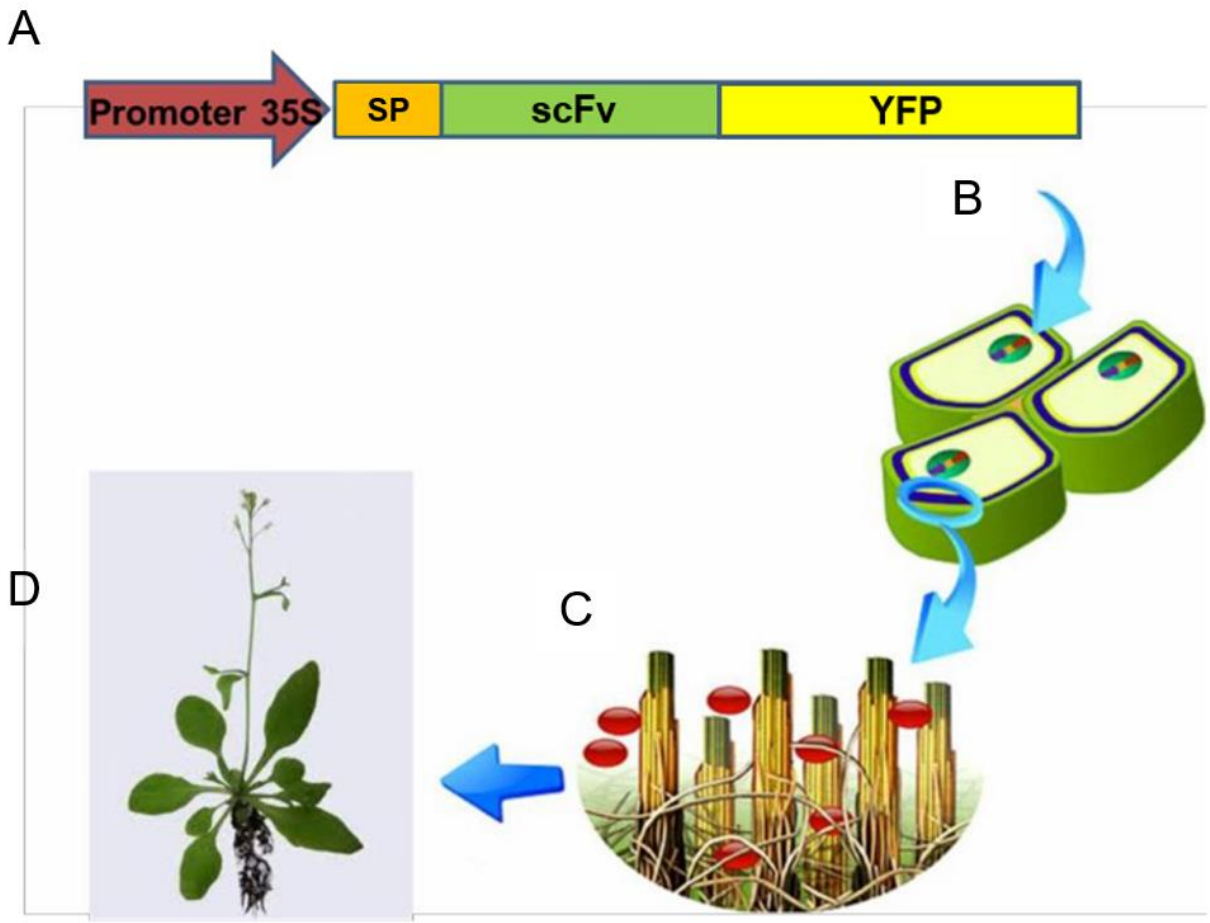

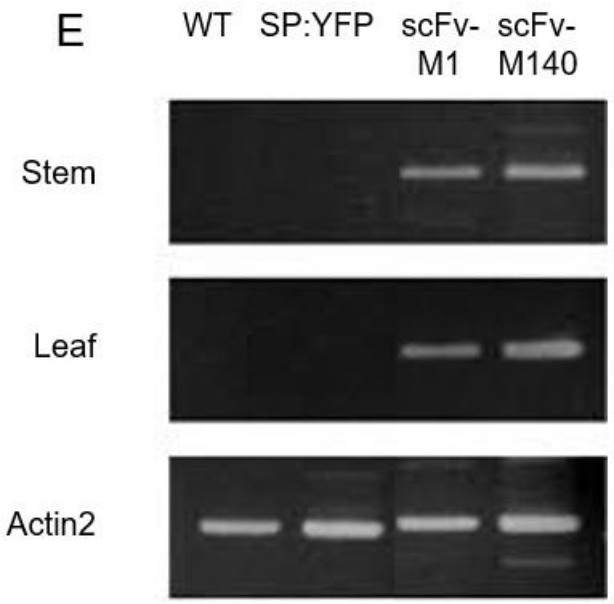

Figure 3.29 Outline of heterologous expression of scFv:YFP in transgenic plants

[Figure is modified from Figure 1 of (Abramson, Shoseyov et al. 2010)]

(A) Gene constructs consisting of a constitutive promoter (Cauliflower Mosaic Virus 35S promoter (red)), a cell wall targeting signal peptide (dark yellow), scFv gene (green), and yellow fluorescent protein (light yellow).

(B) Transformation of scFv:YFP gene into the plant genome.

(C) ScFv:YFP protein is then expressed and possibly secreted into the cell wall.

(D) Transgenic scFv:YFP plant is generated and expression of scFv:YFP protein is examined.

(E) Results of semi RT-PCR on t-DNA from T2.

Developmental Effects of Expressed scFv-M1:YFP in Transgenic Plants

Heterologous expression of scFv-M1:YFP yielded phenotypes different than wild type throughout plant growth and development. At week 2, the scFv-M1:YFP plants displayed hypoplasia, which showed an underdevelopment phenotype. The rosette leaves were smaller and

shorter compared to the control, average of which were approximately 37% in width and 49% in length. (Figure 3.30A, D, E). The rosette leaves eventually developed to a size of approximately 23% in width and 31% in length (Figures 3.30B, D, E). They began to wither when the scFv-M1:YFP plants started bolting. The bolting time of scFv-M1:YFP was 1 week earlier than wild type plants. The average height of the mature stem was 4.7cm, which was approximately 10.2% of the average height of wild type plants (Figures 3.30B). 2 weeks after bolting the scFv-M1:YFP died without any seed yielded. (Figures 3.30C).

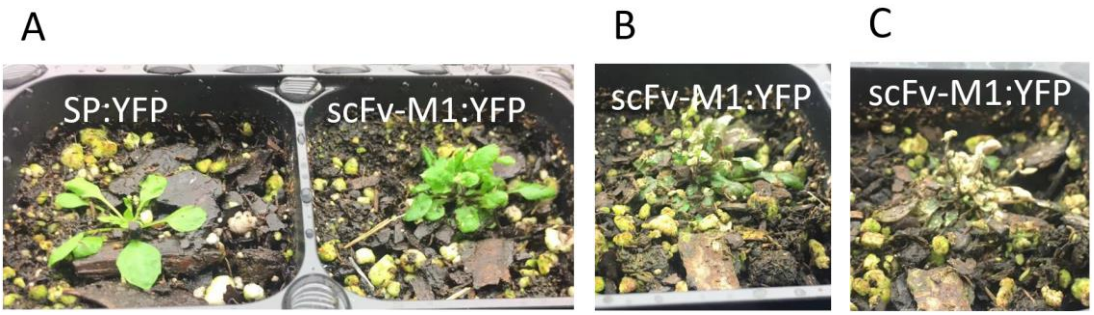

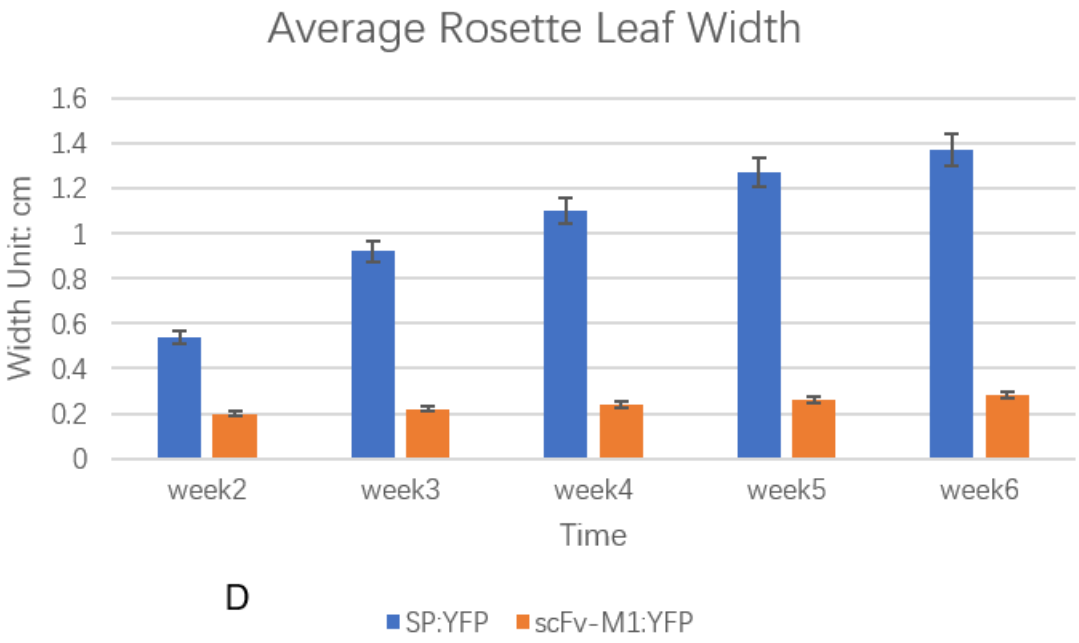

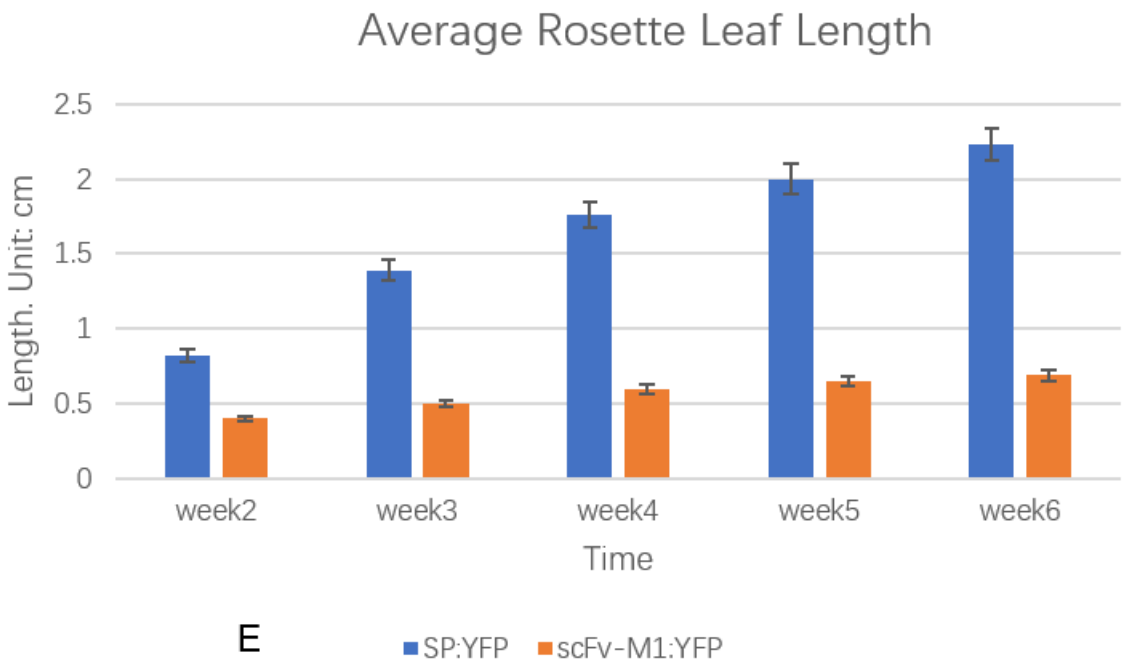

Figure 3.30 Phenotypic characterization of transgenic scFv-M1:YFP plants

(A) Growth of SP:YFP (left) and scFv-M1:YFP (right) at week 2.

(B) Growth of scFv-M1:YFP at 3-days after bolting.

(C) Growth of scFv-M1:YFP at 2 weeks after bolting.

(D) Average width of the rosettes ± error (n=3 for wild type, n=3 for transgenic scFv-M1:YFP plants).

(E) Average length of the rosettes ± error (n=3 for wild type, n=3 for transgenic scFv-M1:YFP plants).

Heterologous Expression and Developmental Effects of Expressed scFv-M140:YFP in Transgenic Plants

Weekly measurements of the growth of rosettes and inflorescence stems were conducted for transgenic scFv-M140:YFP plants to observe the developmental effects of the expressed

scFv-M140:YFP along with wild type plants. Heterologous expression of scFv-M140:YFP yielded phenotypes different than wild type in plant cotyledon shape and size, rosette size and standing of stem. Cotyledon in the transgenic plants was developed at the same time, while the size was only 34% of wild type individuals when fully open at week 1 (Figure 3.31A, F, G). Between the week 2 and 3, the first pair of rosette leaves emerged at the same time as wild type. However, the shape of rosette leaves was only half as the part from tip to the middle of lamina was missing. (Figure 3.31B). The rosette leaves eventually developed to a smaller size, which was 31~73% of the wild type plants at week 6 (Figure 3.31C, F, G). scFv-M140:YFP plants started bolting at the same time as wild type plants at week 4/5. When reaching ~20cm at week 6, the inflorescence stems started to show a small degree from vertical (Figure 3.31C). The degree increased with the development of the inflorescence stem. When the inflorescence stem height reached ~25 cm, the degree was 30~45° (Figures 3.31D). After the inflorescence stem height was over 30cm, the degree was ~90°, which means the stem was lodging (Figures 3.31E).

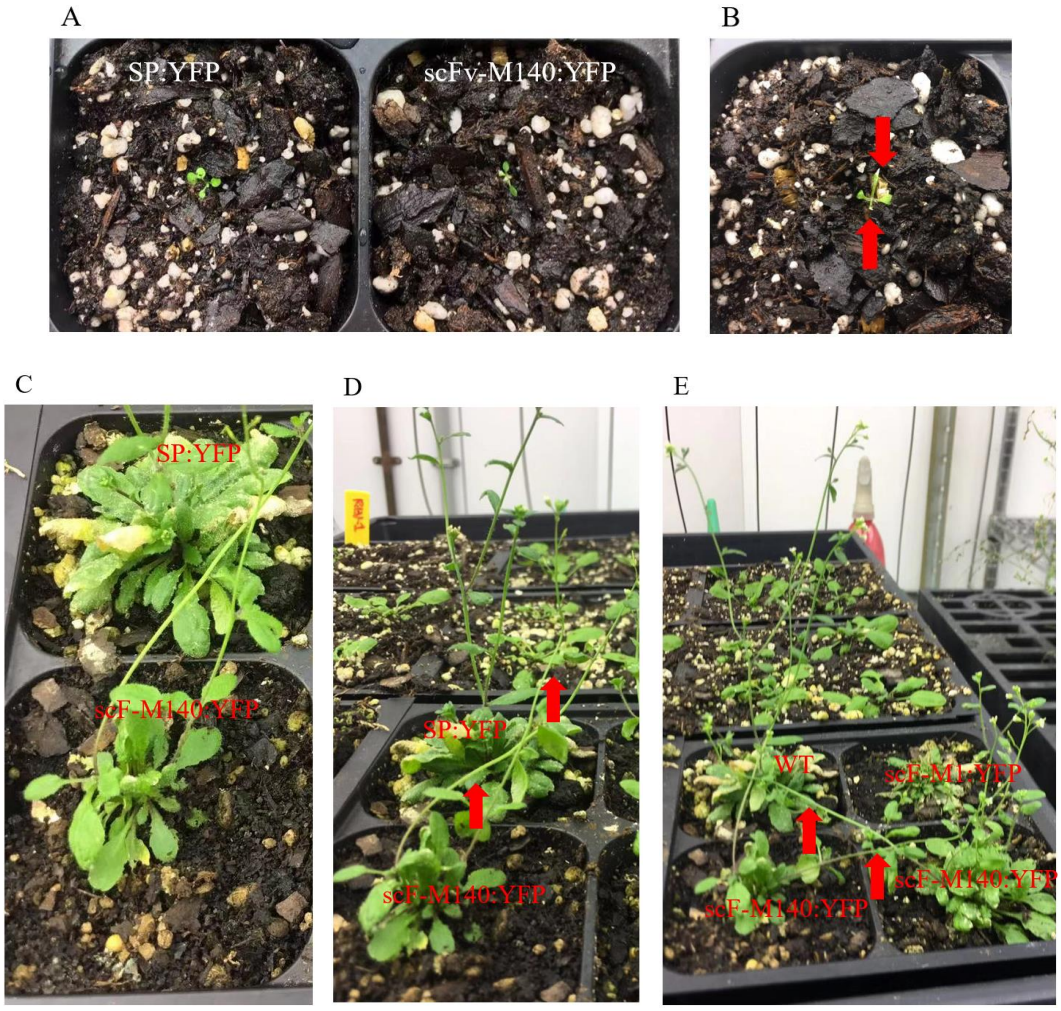
A
SP:YFP
scFv-M140:YFP
B
C
SP:YFP
scF-M140:YFP
D
SP:YFP
scF-M140:YFP
E
WT
scF-M140:YFP
scF-M140:YFP
scF-M140:YFP

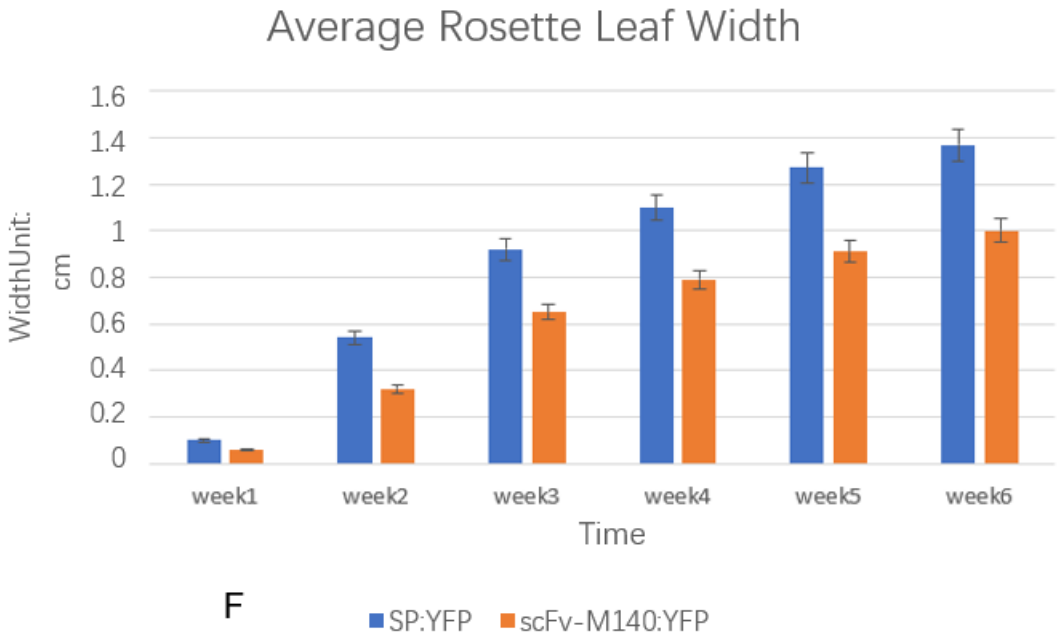
Average Rosette Leaf Width
WidthUnit: cm
1.6
1.4
1.2
1
0.8
0.6
0.4
0.2
0
week1
week2
week3
week4
week5
week6
Time
SP:YFP
scFv-M140:YFP

F

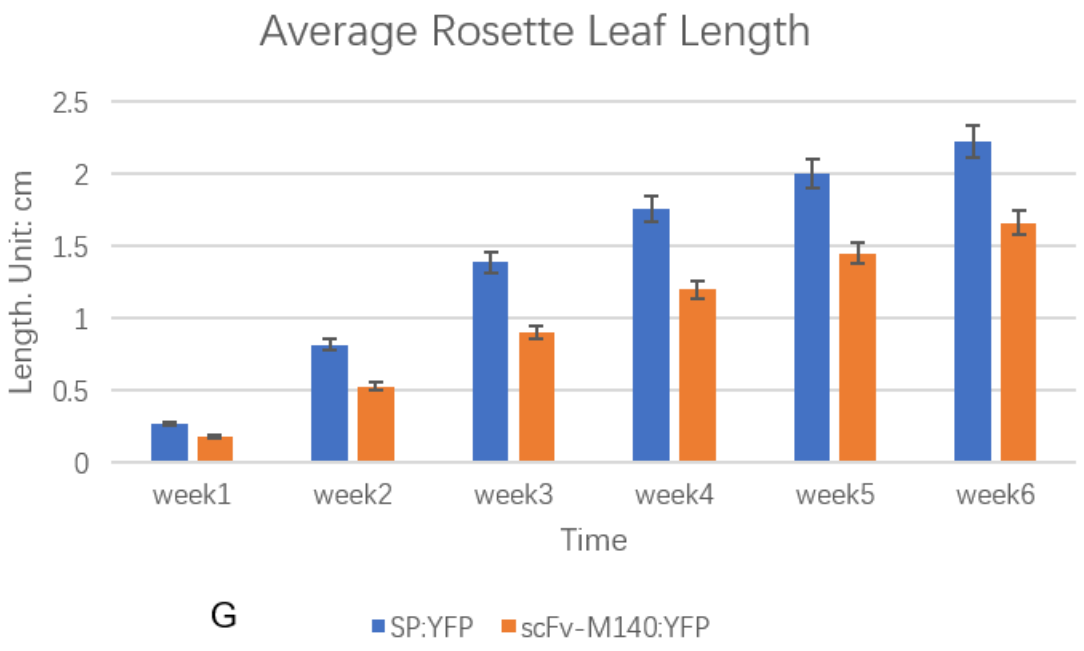

Figure 3.31 Phenotypic characterization of transgenic scFv-M140:YFP plants

(A) Growth of SP:YFP (left) and scFv-M140:YFP (right) at week 1.

(B) The first pair of rosette leaves of scFv-M140:YFP.

(C) The rosette leaves of scFv-M140:YFP at week 6.

(D) The inflorescence stem of scFv-M140:YFP reached ~25 cm tall. Red arrows point to the inclined stem.

(E) The inflorescence stem of scFv-M140:YFP reached ~30 cm tall. Red arrows point to the inclined stem.

(F) Average width of the rosettes ± error (n=3 for wild type, n=3 for transgenic scFv-M140 :YFP plants).

(G) Average width of the rosettes ± error (n=3 for wild type, n=3 for transgenic scFv-M140 :YFP plants).

CHAPTER IV

DISCUSSION

ScFvs have been proven to be a powerful tool in both scientific and medical areas. However, previous studies have found that the solubility of ScFvs varied based on the expression systems and the amino acid sequence (Ahmad, Yeap et al. 2012). Currently, there are three main expression systems for scFvs: *E. coli*, *Pichia pastoris* (Ahmad, Hirz et al. 2014) and mammalian cells. Since *E. coli* is a well-established expression system, there are many molecular tools and protocols developed for the high-level production of heterologous proteins (Baneyx 1999). However, there are reports that *E. coli* is not a good expression host for scFvs. The expression of scFv antibodies in bacterial hosts sometimes causes the aggregation of recombinant proteins due to inappropriate folding. These aggregates, which are named inclusion bodies, need to refold into their proper structure to obtain a functional protein. This refolding process is costly, laborious and time-consuming (Guo, You et al. 2003, Baneyx and Mujacic 2004, Guo, Li et al. 2006). Dr. Fangfang Fu from Hahn Lab had tried to express several scFvs using *E. coli* (BL21). Different conditions were tested, including IPTG, incubation time, temperature, shaking protocol, medium additives (Mg^{2+}, sucrose) and pH. While Dr. Fu was successful with a few scFvs, most expressed recombinant scFvs were insoluble (personal communication), even under conditions that were deemed helpful in previous reports (Sina, Farajzadeh et al. 2015).

We also tried *Pichia pastoris* as expression system for scFvs (data not shown). *P. pastoris*, currently reclassified as *Komagataella pastoris*, is a methylotrophic yeast widely used for expressing heterologous proteins since the 1980's (Cregg, Vedvick et al. 1993). Compared to

E. coli, it has the capabilities of eukaryotic post-translational modifications. Previous study revealed that because of correct proteolytic processing, folding, disulfide bond formation and glycosylation, some protein which were expressed as inactive inclusion bodies in bacterial expression systems could be expressed as biologically functional molecules in *P. pastoris* (Higgins 2001). We utilized pPICZα A vector (purchased from Thermo), which carries *AOX1* gene for controlling expression of GOI relying on methanol (Ellis, Brust et al. 1985, Tschopp, Brust et al. 1987, Koutz, Davis et al. 1989) and α-factor signal from *Saccharomyces cerevisiae*. It has been claimed that *P. pastoris* is more suitable for expression of antibodies such as IgG than mammalian cells because of the mannose-rich glycan glycosylation and amino acid residue from α-factor pre-pro sequence left at the N-termini of both chains (Schaefer and Pluckthun 2012). We tried different conditions, including temperature, shaking RPM, incubation span, and methanol concentration. However, we did not detect any signal of recombinant scFv in Western Blotting tests for any scFv construct that we tested.

HEK293 is another popular expression system for over 25 years. It is able to carry out most of the post-translational folding and processing required to generate active protein because of its biochemical machinery (Thomas and Smart 2005). We tried to express the scFvs using HEK293 and pSecTag2A expression vector, which was also purchased from Thermo. The pSecTag2A carries the N-terminal V-J2-C region of the mouse Ig kappa-chain for efficient secretion of recombinant proteins, and C-terminal 6x polyhistidine for rapid purification with nickel-chelating resin. However, we did not detect any his-tag signal from Western Blotting on the medium. Then we switched to pGEc2-DEST and collected the expressed scFvs successfully from the medium. We compared the sequences between pSecTag2A and pGEc2-DEST. The

pSecTag2A contains an amino acid sequence of DAAQPARRAVR, which pGEc2-DEST does not carry. From our data this region of DAAQPARRAVR possibly affects the solubility and/or secretion. There was no previous study on this amino acid or the sequence between signal peptide and gene of interest, so it needs further investigation.

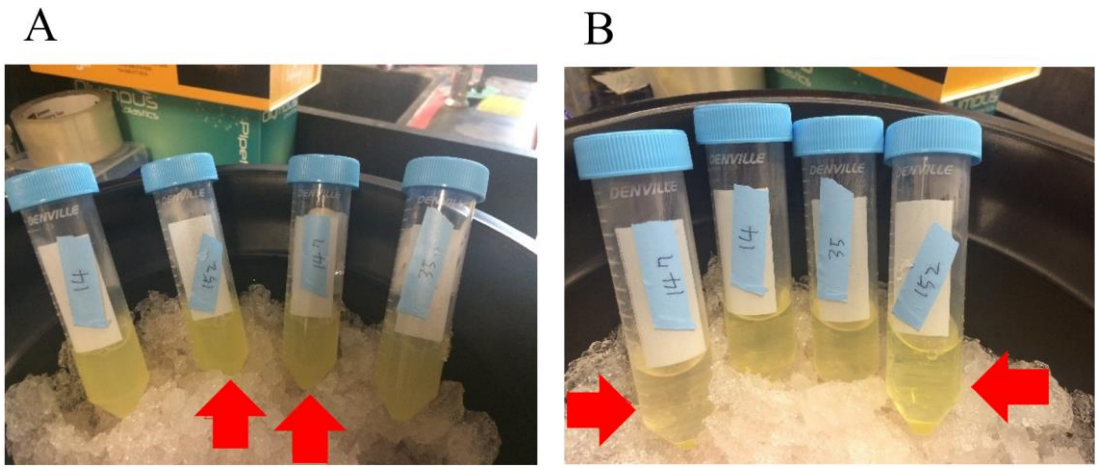

Figure 4.1 Example of insecretable scFvs.

(A) before centrifuge and (B) after centrifuge. It is clear that the cell+medium of scFv-M147:GFP and scFv-M152:GFP (pointed by the red arrows in A) looked green but the medium-only of scFv-M147:GFP and scFv-M152:GFP (pointed by the red arrows in B) looked less green. As a matter of fact, neither of them had fluorescence signal (Table 3.2)

Antibodies are composed of Fab and Fc domains. The Fab has V_H and CH_1 together with the V_L and CL_1, while Fc has the CH_2 and CH_3 domains. ScFv is either V_H-linker-V_L or V_L-linker-V_H. ScFvs are believed to have the same affinity and specificity for antigens as their full-size parent mAbs, and they are preferred for molecular research due to their much smaller size (Bird, Hardman et al. 1988, McCafferty, Griffiths et al. 1990, Hoogenboom, Griffiths et al. 1991). However, previous research also reported that since scFvs have weaker affinity than the

whole antibody molecules because they are the 'shorter version of antibodies' (Cai, Fu et al. 2013). In our project, the scFvs demonstrated differences in binding specificity and/or affinity *in vitro* compared to the parent antibodies. The most different one is scFv-M140:GFP, which did not bind to any polysaccharides in the ELISA test, while its parent antibody is highly selective for xylans. We proposed two possible reasons. The first possible reason is that the scFv is unstable in free solution and either denatures or is degraded. I will discuss this possibility below. The second possible reason is multivalency vs monovalency. The parent antibodies have two recognition sites in the case of an IgG or five recognition sites in the case of an IgM, while the scFvs only have one. So it is common that antibodies usually have higher avidity (also known as functional affinity) compared to the scFvs (Rudnick and Adams 2009). Thus, for the same amount of antigen, antibody could yield much stronger signal than scFv.

In our previous ELISAs, we added 10X the amount of scFvs compared to their parent antibodies in order to get similar signal strength. In the latest ELISA test, we added the same amount of scFvs. After comparison, we noticed that some binding peaks observed with the 10X amount of scFvs were not present in the 1X ELISAs. For example, Figure 4.2 shows the results with scFv-M58:GFP and scFv-M106:GFP. Compared with Figures 3.4 and 3.6, it is clear that the 10X ELISAs gave additional peaks compared with the 1X ELISA. So the greater amount of scFvs could cause non-specific reactions. However, there are still some scFvs displaying unexpected binding compared with their parent antibodies even at 1X, such as scFv-M1:GFP and scFv-M141:GFP. Since we are the pioneer in this area, there were few publications on the specificity or affinity of scFv on polysaccharides. There was one report pointing out that an scFv did not have specificity on binding to DNA (Kim, Kim et al. 2006). So we think that the binding

pattern of scFv to carbohydrate needs further investigation. The amount of scFv raised another question. The 1X amount of scFvs yields signals, some of which were only a little stronger than background. In order to make results more convincing, it needs more work to find the balance point between yielding strong signal and not producing non-specific binding activities, which we believe has significance for future research on scFv.

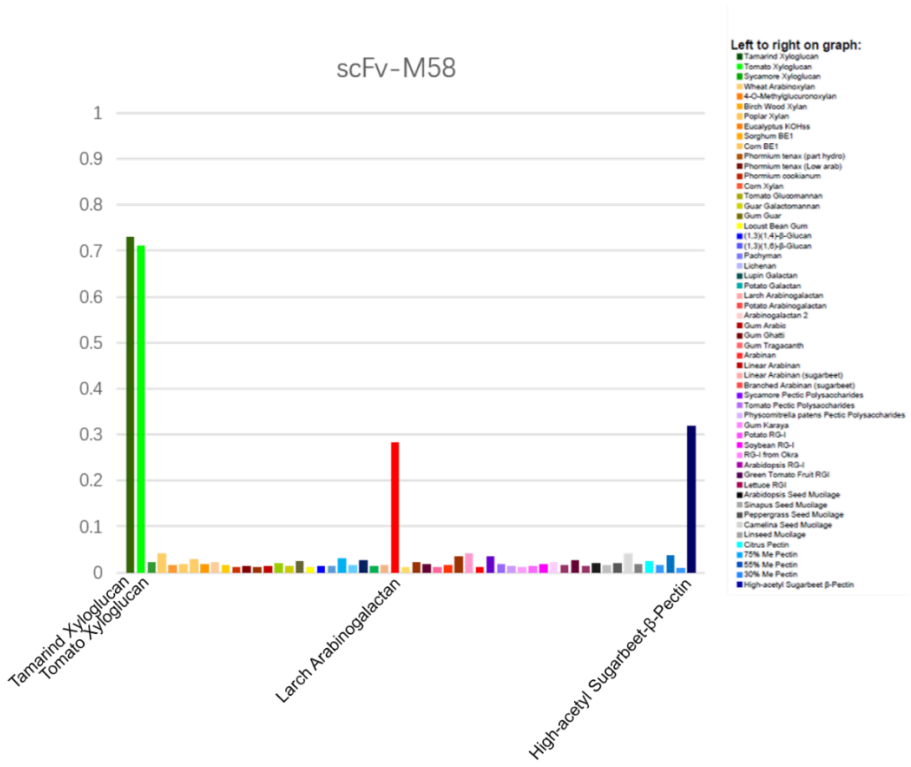

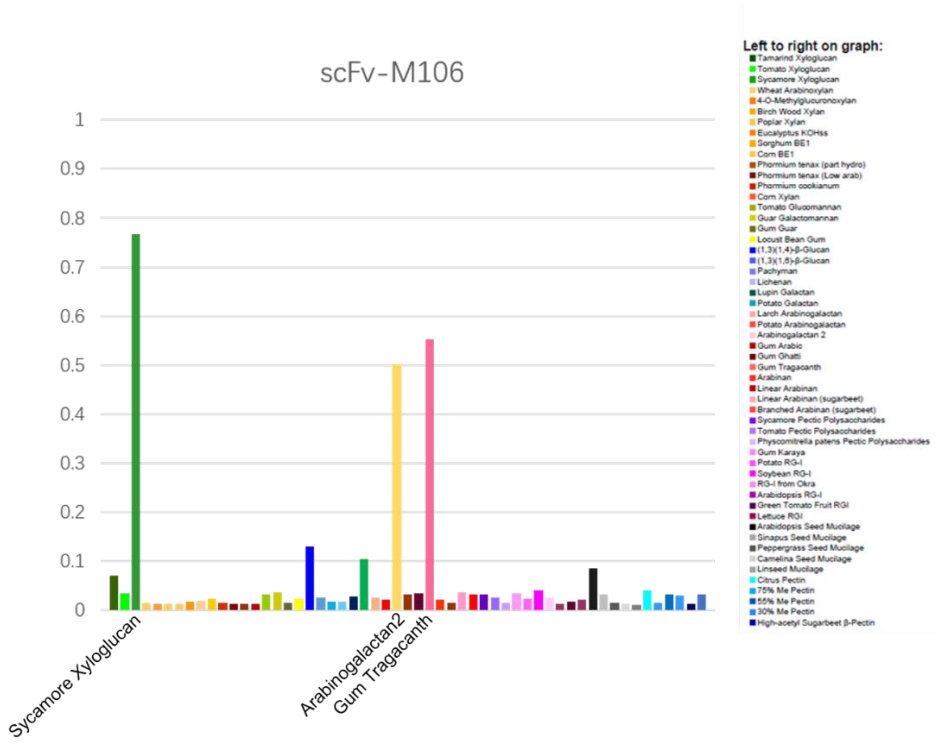

Figure 4.2 Binding specificity of scFv-M58:GFP and scFv-M106:GFP toward 55 plant polysaccharides.

The added scFv amount was 10X compared to their parent antibodies.

ScFv is known for its low stability (Glockshuber, Malia et al. 1990). Previous studies have revealed that there are many methods to make it more stable (Chowdhury and Vasmatzis 2003, Reiter, Brinkmann et al. 1996). In our experiments, we found the solution buffer of scFv played significant role in keeping it stable. The TBS is able to keep scFv-M58:GFP active for over several months, while PBS could only keep the activity for ~3 days (Figure 4.3). However, scFv-M70:GFP was a special case. We could not detect its activity when it was in PBS (data not shown). In TBS its activity could be detected within only ~2 days. It was not surprising to us because previous study found the half-life of scFvs could be as low as 0.6 h (Zhang 2013). Like

other scFvs, the scFv-M70:GFP has four cysteines forming two disulfide bonds, one of which is in V_H domain and the other is in V_L domain. And its length of 789 bp makes it not special compared to other scFvs (714 bp ~ 864 bp). Thus, there is no obvious reason for its instability. We did not investigate this instability further in this report. The reason causing its super instability requires further investigation.

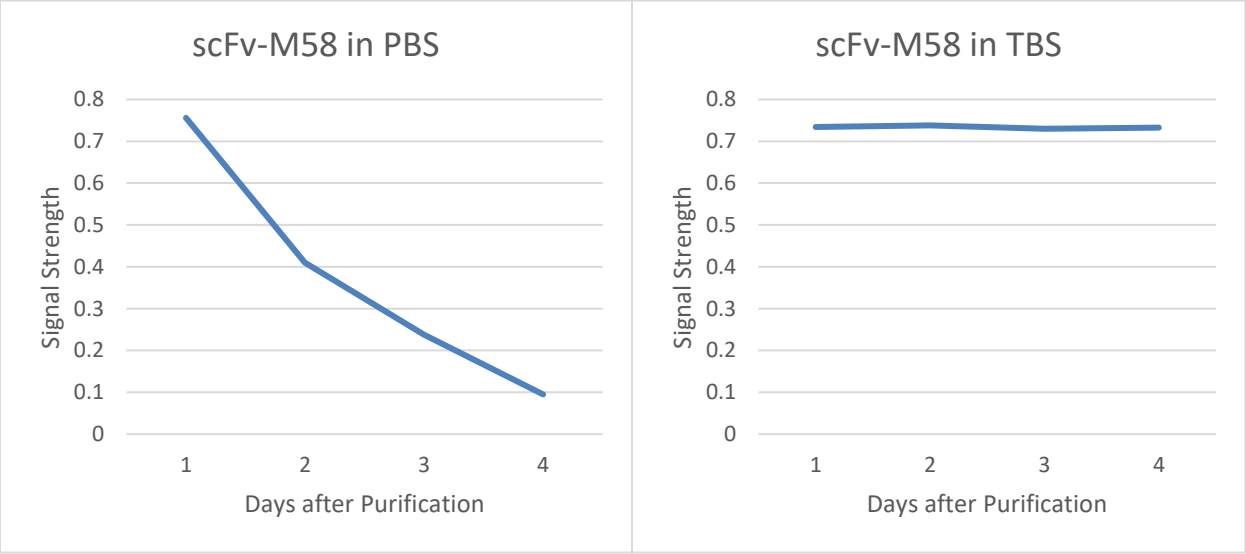

Figure 4.3 Binding activity of scFv-M58 toward Tamarind Xyloglucan. Added amount = 50ul, ~0.5mg/ml.

The transgenic scFv-M1:YFP plants was unable to develop to maturity and set seed, and exhibited altered growth even during seedling and vegetative growth. The plants died right after the inflorescence emerged. So we still have question brought by this abnormal process: how did it happen? This is more challenging to find out because there is no chance to do the sectioning to observe the binding distribution of scFv-M1:YFP *in vivo*. And we did not get a chance to collect the seeds for G3 because no seed was produced. Thus, further detailed investigation will be needed to get a further understanding of how scFv-M1:YFP works *in vivo*.

The transgenic scFv-M140:YFP displayed traits of lodging. It is still unclear why the scFv-M140:GFP could not bind to any polysaccharides in *vitro* while it impacted the growth of plant. One possible explanation is that the plant cell processed the scFv-M140:YFP on its post-translation modification in a correct way, leading to an active scFv *in planta,* while the HEK293-6E cells did not process and fold the protein correctly. Isolation and structure study of scFv-M140:YFP could help us get a deeper understanding. Another possible explanation is that the YFP affected the folding of scFv-M140 less that GFP, although there is no evidence to support this idea. Previous study showed that the reduced xylan in plant could lead to smaller leaves and lower stem (Lao, Long et al. 2003). From the data that have been obtained to date, it is not possible to conclude whether or not binding of scFv-M140:YFP to xylan, if it occurs in the transgenic plants, is responsible for the observed phenotypes. The third possible explanation is the instability mentioned above. Given ELISA was tested on scFv-M140:GFP about one week after purification, there is a chance that scFv-M140:GFP lost its activities before we observed it.

There is large desire for tools to document cell wall structure in relation to plant development, and to reveal further understanding of polysaccharide functions. Currently, the main method is to employ immunohistochemical techniques *in vitro* on fixed tissues in order to discern cell wall structures and to locate polysaccharides in plant cells, tissues and organs. However, the native configurations of polysaccharides *in vivo* are still largely unknown, and substantial effort is required to demonstrate that *in vitro* characteristics of polysaccharides are precise reflections of the structures and behaviors *in vivo*. In the Hahn Lab, we have created new methods and obtained results which show that there is hope to assay the effects of genetic, developmental, and environmental variation on polysaccharides

biosynthesis by tagging the polysaccharides *in vivo*. Several antibodies of CCRC series of antibodies have been expressed *in vivo,* including those described here. Furthermore, Dr. Tiantian Zhang in the Hahn lab was able to demonstrate that heterologous expression of a tagged xylan-binding CBM, CBM2b-1-2:mCherry, could be used for *in vivo* tracking of xylans (Zhang et al., in preparation). In addition, Dr. Zhang also showed that expression of the cellulose-directed CBM, CBM3a:mCherry, *in planta* provided some insight into the negative impact of this CBM on cell wall integrity and plant fitness (Zhang et al., in preparation). Thus, there is hope that a broad collection of *Arabidopsis* plants expressing diverse microbial CBMs, antibodies and/or single-chain antibody fragments (scFvs) that target plant cell wall polysaccharide structures may serve as polysaccharide-selective agents to learn about and alter cell wall structure for the future.

REFERENCES

Abramson, M., O. Shoseyov and Z. Shani (2010). "Plant cell wall reconstruction toward improved lignocellulosic production and processability." Plant Science **178**: 61-72.

Ahmad, M., M. Hirz, H. Pichler and H. Schwab (2014). "Protein expression in Pichia pastoris: recent achievements and perspectives for heterologous protein production." Appl Microbiol Biotechnol **98**(12): 5301-5317.

Ahmad, Z. A., S. K. Yeap, A. M. Ali, W. Y. Ho, N. B. Alitheen and M. Hamid (2012). "scFv antibody: principles and clinical application." Clin Dev Immunol **2012**: 980250.

Albersheim, P. (1976). The primary cell wall. Plant Biochemistry. J. BONNER and J. E. VARNER. New York, Academic Press**:** 225-274.

Anders, N., M. D. Wilkinson, A. Lovegrove, J. Freeman, T. Tryfona, T. K. Pellny, T. Weimar, J. C. Mortimer, K. Stott, J. M. Baker, M. Defoin-Platel, P. R. Shewry, P. Dupree and R. A. Mitchell (2012). "Glycosyl transferases in family 61 mediate arabinofuranosyl transfer onto xylan in grasses." Proc Natl Acad Sci U S A **109**(3): 989-993.

Argos, P. (1990). "An investigation of oligopeptides linking domains in protein tertiary structures and possible candidates for general gene fusion." J Mol Biol **211**(4): 943-958.

Atwell, J. L., K. A. Breheney, L. J. Lawrence, A. J. McCoy, A. A. Kortt and P. J. Hudson (1999). "scFv multimers of the anti-neuraminidase antibody NC10: length of the linker between VH and VL domains dictates precisely the transition between diabodies and triabodies." Protein Eng **12**(7): 597-604.

Bajpai, P. (1997). "Microbial xylanolytic enzyme system: properties and applications." Adv

Appl Microbiol **43**: 141-194.

Bajpai, P. (2014). Xylanolytic Enzymes, Academic Press.

Baneyx, F. (1999). "Recombinant protein expression in Escherichia coli." Curr Opin Biotechnol **10**(5): 411-421.

Baneyx, F. and M. Mujacic (2004). "Recombinant protein folding and misfolding in Escherichia coli." Nat Biotechnol **22**(11): 1399-1408.

Bartley, L. E., M. L. Peck, S. R. Kim, B. Ebert, C. Manisseri, D. M. Chiniquy, R. Sykes, L. Gao, C. Rautengarten, M. E. Vega-Sanchez, P. I. Benke, P. E. Canlas, P. Cao, S. Brewer, F. Lin, W. L. Smith, X. Zhang, J. D. Keasling, R. E. Jentoff, S. B. Foster, J. Zhou, A. Ziebell, G. An, H. V. Scheller and P. C. Ronald (2013). "Overexpression of a BAHD acyltransferase, OsAt10, alters rice cell wall hydroxycinnamic acid content and saccharification." Plant Physiol **161**(4): 1615-1633.

Bauer, W. D., K. W. Talmadge, K. Keegstra and P. Albersheim (1973). "The Structure of Plant Cell Walls: II. The Hemicellulose of the Walls of Suspension-cultured Sycamore Cells." Plant physiology **51**(1): 174-187.

Bent, A. (2006). "Arabidopsis thaliana floral dip transformation method." Methods Mol Biol **343**: 87-103.

Bernard, P. (1996). "Positive selection of recombinant DNA by CcdB." Biotechniques **21**(2): 320-323.

Bernard, P. and M. Couturier (1992). "Cell killing by the F plasmid CcdB protein involves poisoning of DNA-topoisomerase II complexes." J Mol Biol **226**(3): 735-745.

Bird, R. E., K. D. Hardman, J. W. Jacobson, S. Johnson, B. M. Kaufman, S. M. Lee, T. Lee, S. H. Pope, G. S. Riordan and M. Whitlow (1988). "Single-chain antigen-binding proteins."

Science **242**(4877): 423-426.

Brown, D. M., F. Goubet, V. W. Wong, R. Goodacre, E. Stephens, P. Dupree and S. R. Turner (2007). "Comparison of five xylan synthesis mutants reveals new insight into the mechanisms of xylan synthesis." Plant J **52**(6): 1154-1168.

Brummell, D. A., A. Camirand and G. A. Maclachlan (1990). "Differential distribution of xyloglucan glycosyl transferases in pea Golgi dictyosomes and secretory vesicles." J. Cell Sci. **96**: 705–710.

Buchanan, B. B., W. Gruissem and R. L. Jones (2000). Biochemistry and Molecular Biology of Plants. Rockville, MD USA, American Society of Plant Biologists.

Buckeridge, M. S. (2010). "Seed cell wall storage polysaccharides: models to understand cell wall biosynthesis and degradation." Plant Physiol **154**(3): 1017-1023.

Bush, M. S. and M. C. McCann (2002). "Pectic epitopes are differentially distributed in the cell walls of potato (Solanum tuberosum) tubers." Physiol. Plant **107**: 201-213.

C. A. Janeway, P. T., M. Walport, M. J. Shlomchik (2001). Immunobiology. New York, Garland Science.

Cai, Z., T. Fu, Y. Nagai, L. Lam, M. Yee, Z. Zhu and H. Zhang (2013). "scFv-based "Grababody" as a general strategy to improve recruitment of immune effector cells to antibody-targeted tumors." Cancer Res **73**(8): 2619-2627.

Calzas, C., P. Lemire, G. Auray, V. Gerdts, M. Gottschalk and M. Segura (2015). "Antibody response specific to the capsular polysaccharide is impaired in Streptococcus suis serotype 2-infected animals." Infect Immun **83**(1): 441-453.

Carpita, N. C. (1996). "Structure and Biogenesis of the Cell Walls of Grasses." Annu Rev Plant Physiol Plant Mol Biol **47**: 445-476.

Carpita, N. C. and D. M. Gibeaut (1993). "Structural models of primary cell walls in flowering plants: consistency of molecular structure with the physical properties of the walls during growth." Plant J **3**(1): 1-30.

Chaudhary, V. K., J. K. Batra, M. G. Gallo, M. C. Willingham, D. J. FitzGerald and I. Pastan (1990). "A rapid method of cloning functional variable-region antibody genes in Escherichia coli as single-chain immunotoxins." Proc Natl Acad Sci U S A **87**(3): 1066-1070.

Chaudhary, V. K., C. Queen, R. P. Junghans, T. A. Waldmann, D. J. FitzGerald and I. Pastan (1989). "A recombinant immunotoxin consisting of two antibody variable domains fused to Pseudomonas exotoxin." Nature **339**(6223): 394-397.

Chevalier, L., S. Bernard, Y. Ramdani, R. Lamour, M. Bardor, P. Lerouge, M. L. Follet-Gueye and A. Driouich (2010). "Subcompartment localization of the side chain xyloglucan-synthesizing enzymes within Golgi stacks of tobacco suspension-cultured cells." Plant J **64**(6): 977-989.

Chiniquy, D., V. Sharma, A. Schultink, E. E. Baidoo, C. Rautengarten, K. Cheng, A. Carroll, P. Ulvskov, J. Harholt, J. D. Keasling, M. Pauly, H. V. Scheller and P. C. Ronald (2012). "XAX1 from glycosyltransferase family 61 mediates xylosyltransfer to rice xylan." Proc Natl Acad Sci U S A **109**(42): 17117-17122.

Cho, H. T. and D. J. Cosgrove (2000). "Altered expression of expansin modulates leaf growth and pedicel abscission in Arabidopsis thaliana." Proc Natl Acad Sci U S A **97**(17): 9783-9788.

Choo, A. B., R. D. Dunn, K. W. Broady and R. L. Raison (2002). "Soluble expression of a functional recombinant cytolytic immunotoxin in insect cells." Protein Expr Purif **24**(3): 338-347.

Chou, Y. H., G. Pogorelko and O. A. Zabotina (2012). "Xyloglucan xylosyltransferases XXT1,

XXT2, and XXT5 and the glucan synthase CSLC4 form Golgi-localized multiprotein complexes." Plant Physiol **159**(4): 1355-1366.

Chowdhury, P. S. and G. Vasmatzis (2003). "Engineering scFvs for improved stability." Methods Mol Biol **207**: 237-254.

Clackson, T., H. R. Hoogenboom, A. D. Griffiths and G. Winter (1991). "Making antibody fragments using phage display libraries." Nature **352**(6336): 624-628.

Coloma, M. J., A. Hastings, L. A. Wims and S. L. Morrison (1992). "Novel Vectors for the Expression of Antibody Molecules Using Variable Regions Generated by Polymerase Chain Reaction. ." J. Imm. Methods **152**: 89-104.

Cosgrove, D. J. (2001). "Plant cell walls: wall-associated kinases and cell expansion." Current biology **11**(14): R558-559.

Cregg, J. M., T. S. Vedvick and W. C. Raschke (1993). "Recent advances in the expression of foreign genes in Pichia pastoris." Biotechnology (N Y) **11**(8): 905-910.

Dai, K., H. Zhu and C. Ruan (2003). "Generation and characterization of recombinant single chain Fv antibody that recognizes platelet glycoprotein Ibalpha." Thromb Res **109**(2-3): 137-144.

Davis, J., F. Brandizzi, A. H. Liepman and K. Keegstra (2010). "Arabidopsis mannan synthase CSLA9 and glucan synthase CSLC4 have opposite orientations in the Golgi membrane." Plant J **64**(6): 1028-1037.

Deng, C., M. A. O'Neill, M. G. Hahn and W. S. York (2009). "Improved procedures for the selective chemical fragmentation of rhamnogalacturonans." Carbohydr Res **344**(14): 1852-1857.

Deng, X. K., L. A. Nesbit and K. J. Morrow, Jr. (2003). "Recombinant single-chain variable fragment antibodies directed against Clostridium difficile toxin B produced by use of an optimized phage display system." Clin Diagn Lab Immunol **10**(4): 587-595.

Drouhet, E. and J. Latge (1988). Techniques Available to Prepare Monoclonal Antibodies Directed Toward Fungal Polysaccharide Antigens. **New York, USA, Plenum Press.**

Ebringerova, A., Heinze, T. (2000). "Xylan and xylan derivatives—biopolymers with valuable properties, 1. Naturally occurring xylans structures, isolation procedures and properties." Macromol. Rapid Commun. **21**: 542-556.

Ellis, S. B., P. F. Brust, P. J. Koutz, A. F. Waters, M. M. Harpold and T. R. Gingeras (1985). "Isolation of alcohol oxidase and two other methanol regulatable genes from the yeast Pichia pastoris." Mol Cell Biol **5**(5): 1111-1121.

Finlay, W. J., I. Shaw, J. P. Reilly and M. Kane (2006). "Generation of high-affinity chicken single-chain Fv antibody fragments for measurement of the Pseudonitzschia pungens toxin domoic acid." Appl Environ Microbiol **72**(5): 3343-3349.

Freshour, G., C. P. Bonin, W. D. Reiter, P. Albersheim, A. G. Darvill and M. G. Hahn (2003). "Distribution of fucose-containing xyloglucans in cell walls of the mur1 mutant of Arabidopsis." Plant Physiol **131**(4): 1602-1612.

Galeffi, P., A. Lombardi, I. Pietraforte, F. Novelli, M. Di Donato, M. Sperandei, A. Tornambe, R. Fraioli, A. Martayan, P. G. Natali, M. Benevolo, M. Mottolese, F. Ylera, C. Cantale and P. Giacomini (2006). "Functional expression of a single-chain antibody to ErbB-2 in plants and cell-free systems." J Transl Med **4**: 39.

Glockshuber, R., M. Malia, I. Pfitzinger and A. Pluckthun (1990). "A comparison of strategies to stabilize immunoglobulin Fv-fragments." Biochemistry **29**(6): 1362-1367.

Gottschalk, M., J. Xu, C. Calzas and M. Segura (2010). "Streptococcus suis: a new emerging or an old neglected zoonotic pathogen?" Future Microbiol **5**(3): 371-391.

Gram, H., L. A. Marconi, C. F. Barbas, 3rd, T. A. Collet, R. A. Lerner and A. S. Kang

(1992). "In vitro selection and affinity maturation of antibodies from a naive combinatorial immunoglobulin library." Proc Natl Acad Sci U S A **89**(8): 3576-3580.

Griffiths, A. D. and A. R. Duncan (1998). "Strategies for selection of antibodies by phage display." Curr Opin Biotechnol **9**(1): 102-108.

Guo, J. Q., Q. M. Li, J. Y. Zhou, G. P. Zhang, Y. Y. Yang, G. X. Xing, D. Zhao, S. Y. You and C. Y. Zhang (2006). "Efficient recovery of the functional IP10-scFv fusion protein from inclusion bodies with an on-column refolding system." Protein Expr Purif **45**(1): 168-174.

Guo, J. Q., S. Y. You, L. Li, Y. Z. Zhang, J. N. Huang and C. Y. Zhang (2003). "Construction and high-level expression of a single-chain Fv antibody fragment specific for acidic isoferritin in Escherichia coli." J Biotechnol **102**(2): 177-189.

Hahn, M. G., A. Darvill, P. Albersheim, C. Bergmann, J.-J. Cheong, A. Koller and V.-M. Lò (1992). Preparation and characterization of oligosaccharide elicitors of phytoalexin accumulation. Oxford,UK, Oxford University Press.

Harholt, J., A. Suttangkakul and H. Vibe Scheller (2010). "Biosynthesis of pectin." Plant Physiol **153**(2): 384-395.

Hayashi, T. (1989). "Xyloglucans in the primary cell wall." Annu. Rev. Plant. Physiol. **40**: 139–168.

Hayashi, T., T. Koyama and K. Matsuda (1988). "Formation of UDP-Xylose and Xyloglucan in Soybean Golgi Membranes." Plant Physiol **87**(2): 341-345.

He, J., G. Zhou, K. D. Liu and X. Y. Qin (2002). "Construction and preliminary screening of a human phage single-chain antibody library associated with gastric cancer." J Surg Res **102**(2): 150-155.

Hervé, C., S. E. Marcus and J. P. Knox (2010). Monoclonal Antibodies, Carbohydrate-Binding

Modules, and the Detection of Polysaccharides in Plant Cell Walls. Berlin, Germany, Springer Science.

Higgins, D. R. (2001). "Overview of protein expression in Pichia pastoris." Curr Protoc Protein Sci Chapter 5: Unit5 7.

Ho, M., S. Nagata and I. Pastan (2006). "Isolation of anti-CD22 Fv with high affinity by Fv display on human cells." Proc Natl Acad Sci U S A **103**(25): 9637-9642.

Hoogenboom, H. R., A. D. Griffiths, K. S. Johnson, D. J. Chiswell, P. Hudson and G. Winter (1991). "Multi-subunit proteins on the surface of filamentous phage: methodologies for displaying antibody (Fab) heavy and light chains." Nucleic Acids Res **19**(15): 4133-4137.

Hu, X., R. O'Dwyer and J. G. Wall (2005). "Cloning, expression and characterisation of a single-chain Fv antibody fragment against domoic acid in Escherichia coli." J Biotechnol **120**(1): 38-45.

Huston, J. S., M. Mudgett-Hunter, M. S. Tai, J. McCartney, F. Warren, E. Haber and H. Oppermann (1991). "Protein engineering of single-chain Fv analogs and fusion proteins." Methods Enzymol **203**: 46-88.

Ishii, T. (1997). "O-acetylated oligosaccharides from pectins of potato tuber cell walls." Plant Physiol **113**(4): 1265-1272.

J. S. Huston, D. L., M. Mudgett-Hunter, M. S. Tai, J. Novotný, M. N. Margolies, R. J. Ridge, R. E. Bruccoleri, E. Haber, R. Crea (1988). "Protein engineering of antibody binding sites: recovery of specific activity in an anti-digoxin single-chain Fv analogue produced in Escherichia coli." PNAS **85**(16): 5879-5883.

Jia, Z., Q. Qin, A. G. Darvill and W. S. York (2003). "Structure of the xyloglucan produced by suspension-cultured tomato cells." Carbohydr Res **338**(11): 1197-1208.

Joseleau, J. P., N. Cartier, G. Chambat, A. Faik and K. Ruel (1992). "Structural features and biological activity of xyloglucans from suspension-cultured plant cells." Biochimie **74**(1): 81-88.

Keegstra, K., K. W. Talmadge, W. D. Bauer and P. Albersheim (1973). "The Structure of Plant Cell Walls: III. A Model of the Walls of Suspension-cultured Sycamore Cells Based on the Interconnections of the Macromolecular Components." Plant physiology **51**(1): 188-197.

Kim, Y. R., J. S. Kim, S. H. Lee, W. R. Lee, J. N. Sohn, Y. C. Chung, H. K. Shim, S. C. Lee, M. H. Kwon and Y. S. Kim (2006). "Heavy and light chain variable single domains of an anti-DNA binding antibody hydrolyze both double- and single-stranded DNAs without sequence specificity." J Biol Chem **281**(22): 15287-15295.

Knox, J. P. (1997). "The use of antibodies to study the architecture and developmental regulation of plant cell walls." Int Rev Cytol **171**: 79-120.

Knox, J. P. (2008). "Revealing the structural and functional diversity of plant cell walls." Curr Opin Plant Biol **11**(3): 308-313.

Kobayashi, N., M. Ohtoyo, E. Wada, Y. Kato, N. Mano and J. Goto (2005). "Generation of a single-chain Fv fragment for the monitoring of deoxycholic acid residues anchored on endogenous proteins." Steroids **70**(4): 285-294.

Komalavilas, P. and A. J. Mort (1989). "The acetylation at O-3 of galacturonic acid in the rhamnose-rich region of pectins." Carbohydr. Rev. **189**: 261-272.

Koutz, P., G. R. Davis, C. Stillman, K. Barringer, J. Cregg and G. Thill (1989). "Structural comparison of the Pichia pastoris alcohol oxidase genes." Yeast **5**(3): 167-177.

Lao, N. T., D. Long, S. Kiang, G. Coupland, D. A. Shoue, N. C. Carpita and T. A. Kavanagh (2003). "Mutation of a family 8 glycosyltransferase gene alters cell wall carbohydrate composition and causes a humidity-sensitive semi-sterile dwarf phenotype in Arabidopsis." Plant

Mol Biol **53**(5): 647-661.

Lau, J. M., M. McNeil, A. G. Darvill and P. Albersheim (1985). "Structure of the backbone of rhamnogalacturonan I, a pectic polysaccharide in the primary cell walls of plants." Carbohydr. Res. **137**: 111-125.

Lee, C., M. A. O'Neill, Y. Tsumuraya, A. G. Darvill and Z. H. Ye (2007). "The irregular xylem9 mutant is deficient in xylan xylosyltransferase activity." Plant Cell Physiol **48**(11): 1624-1634.

Lee, C., Q. Teng, R. Zhong, Y. Yuan, M. Haghighat and Z. H. Ye (2012). "Three Arabidopsis DUF579 domain-containing GXM proteins are methyltransferases catalyzing 4-o-methylation of glucuronic acid on xylan." Plant Cell Physiol **53**(11): 1934-1949.

Lin-Chao, S., W. T. Chen and T. T. Wong (1992). "High copy number of the pUC plasmid results from a Rom/Rop-suppressible point mutation in RNA II." Mol Microbiol **6**(22): 3385-3393.

Luo, D., N. Mah, M. Krantz, K. Wilde, D. Wishart, Y. Zhang, F. Jacobs and L. Martin (1995). "Vl-linker-Vh orientation-dependent expression of single chain Fv-containing an engineered disulfide-stabilized bond in the framework regions." J Biochem **118**(4): 825-831.

Marks, J. D., H. R. Hoogenboom, T. P. Bonnert, J. McCafferty, A. D. Griffiths and G. Winter (1991). "By-passing immunization. Human antibodies from V-gene libraries displayed on phage." J Mol Biol **222**(3): 581-597.

McCafferty, J., A. D. Griffiths, G. Winter and D. J. Chiswell (1990). "Phage antibodies: filamentous phage displaying antibody variable domains." Nature **348**(6301): 552-554.

McNeil, M., A. G. Darvill and P. Albersheim (1980). "Structure of Plant Cell Walls: X. Rhamnogalacturonan I, a structurally complex pectic polysaccharide in the walls of suspension-

cultured sycamore cells." Plant physiology **66**(6): 1128-1134.

McNeil, M., A. G. Darvill, S. C. Fry and P. Albersheim (1984). "Structure and function of the primary cell walls of plants." Annual review of biochemistry **53**: 625-663.

Mikolajczyk, M. G., N. F. Concepcion, T. Wang, D. Frazier, B. Golding, C. E. Frasch and D. E. Scott (2004). "Characterization of antibodies to capsular polysaccharide antigens of Haemophilus influenzae type b and Streptococcus pneumoniae in human immune globulin intravenous preparations." Clin Diagn Lab Immunol **11**(6): 1158-1164.

Mollet, J. C., C. Leroux, F. Dardelle and A. Lehner (2013). "Cell Wall Composition, Biosynthesis and Remodeling during Pollen Tube Growth." Plants (Basel) **2**(1): 107-147.

Moore, P. J. and L. A. Staehelin (1988). "Immunogold localization of the cell-wall-matrix polysaccharides rhamnogalacturonan I and xyloglucan during cell expansion and cytokinesis inTrifolium pratense L.; implication for secretory pathways." Planta **174**(4): 433-445.

Mortimer, J. C., G. P. Miles, D. M. Brown, Z. Zhang, M. P. Segura, T. Weimar, X. Yu, K. A. Seffen, E. Stephens, S. R. Turner and P. Dupree (2010). "Absence of branches from xylan in Arabidopsis gux mutants reveals potential for simplification of lignocellulosic biomass." Proc Natl Acad Sci U S A **107**(40): 17409-17414.

Nagai, T., K. Ibata, E. S. Park, M. Kubota, K. Mikoshiba and A. Miyawaki (2002). "A variant of yellow fluorescent protein with fast and efficient maturation for cell-biological applications." Nat Biotechnol **20**(1): 87-90.

Niklas, K. J., E. D. Cobb and A. J. Matas (2017). "The evolution of hydrophobic cell wall biopolymers: from algae to angiosperms." J Exp Bot **68**(19): 5261-5269.

O'Neill, M. A., P. Albersheim and A. Darvill (1990). The pectic polysaccharides of primary cell walls, in Methods in Plant Biochemistry. London, Academic Press.

Oikawa, A., H. J. Joshi, E. A. Rennie, B. Ebert, C. Manisseri, J. L. Heazlewood and H. V. Scheller (2010). "An integrative approach to the identification of Arabidopsis and rice genes involved in xylan and secondary wall development." PLoS One **5**(11): e15481.

Oomen, R. J., C. H. Doeswijk-Voragen, M. S. Bush, J. P. Vincken, B. Borkhardt, L. A. van den Broek, J. Corsar, P. Ulvskov, A. G. Voragen, M. C. McCann and R. G. Visser (2002). "In muro fragmentation of the rhamnogalacturonan I backbone in potato (Solanum tuberosum L.) results in a reduction and altered location of the galactan and arabinan side-chains and abnormal periderm development." The Plant journal **30**(4): 403-413.

Pauly, M. and H. V. Scheller (2000). "O-Acetylation of plant cell wall polysaccharides: identification and partial characterization of a rhamnogalacturonan O-acetyl-transferase from potato suspension-cultured cells." Planta **210**(4): 659-667.

Pattathil, S., U. Avci, D. Baldwin, A. G. Swennes, J. A. McGill, Z. Popper, T. Bootten, A. Albert, R. H. Davis, C. Chennareddy, R. Dong, B. O'Shea, R. Rossi, C. Leoff, G. Freshour, R. Narra, M. O'Neil, W. S. York and M. G. Hahn (2010). "A comprehensive toolkit of plant cell wall glycan-directed monoclonal antibodies." Plant Physiol **153**(2): 514-525.

Pattathil, S., U. Avci, T. Zhang, C. L. Cardenas and M. G. Hahn (2015). "Immunological Approaches to Biomass Characterization and Utilization." Front Bioeng Biotechnol **3**: 173.

Pauly, M. and K. Keegstra (2016). "Biosynthesis of the Plant Cell Wall Matrix Polysaccharide Xyloglucan." Annu Rev Plant Biol **67**: 235-259.

Pena, M. J., A. G. Darvill, S. Eberhard, W. S. York and M. A. O'Neill (2008). "Moss and liverwort xyloglucans contain galacturonic acid and are structurally distinct from the xyloglucans synthesized by hornworts and vascular plants." Glycobiology **18**(11): 891-904.

Pennell, R. I. and K. Roberts (1995). "Monoclonal antibodies to cell-specific cell surface

carbohydrates in plant cell biology and development." Methods Cell Biol **49**: 123-141.

Perrin, R. M., A. E. DeRocher, M. Bar-Peled, W. Zeng, L. Norambuena, A. Orellana, N. V. Raikhel and K. Keegstra (1999). "Xyloglucan fucosyltransferase, an enzyme involved in plant cell wall biosynthesis." Science **284**(5422): 1976-1979.

Piston, F., C. Uauy, L. Fu, J. Langston, J. Labavitch and J. Dubcovsky (2010). "Down-regulation of four putative arabinoxylan feruloyl transferase genes from family PF02458 reduces ester-linked ferulate content in rice cell walls." Planta **231**(3): 677-691.

Ravn, P., A. Danielczyk, K. B. Jensen, P. Kristensen, P. A. Christensen, M. Larsen, U. Karsten and S. Goletz (2004). "Multivalent scFv display of phagemid repertoires for the selection of carbohydrate-specific antibodies and its application to the Thomsen-Friedenreich antigen." J Mol Biol **343**(4): 985-996.

Reiter, Y., U. Brinkmann, B. Lee and I. Pastan (1996). "Engineering antibody Fv fragments for cancer detection and therapy: disulfide-stabilized Fv fragments." Nat Biotechnol **14**(10): 1239-1245.

Rennie, E. A., S. F. Hansen, E. E. Baidoo, M. Z. Hadi, J. D. Keasling and H. V. Scheller (2012). "Three members of the Arabidopsis glycosyltransferase family 8 are xylan glucuronosyltransferases." Plant Physiol **159**(4): 1408-1417.

Rennie, E. A. and H. V. Scheller (2014). "Xylan biosynthesis." Curr Opin Biotechnol **26**: 100-107.

Ridley, B. L., M. A. O'Neill and D. Mohnen (2001). "Pectins: structure, biosynthesis, and oligogalacturonide-related signaling." Phytochemistry **57**(6): 929-967.

Robbins, J. B., J. C. Parke, Jr., R. Schneerson and J. K. Whisnant (1973). "Quantitative measurement of "natural" and immunization-induced Haemophilus influenzae type b capsular

polysaccharide antibodies." Pediatr Res **7**(3): 103-110.

Rudnick, S. I. and G. P. Adams (2009). "Affinity and avidity in antibody-based tumor targeting." Cancer Biother Radiopharm **24**(2): 155-161.

Ruprecht, C., M. P. Bartetzko, D. Senf, P. Dallabernadina, I. Boos, M. C. F. Andersen, T. Kotake, J. P. Knox, M. G. Hahn, M. H. Clausen and F. Pfrengle (2017). "A Synthetic Glycan Microarray Enables Epitope Mapping of Plant Cell Wall Glycan-Directed Antibodies." Plant Physiol **175**(3): 1094-1104.

Rydahl, M. G., S. K. Krac Un, J. U. Fangel, G. Michel, A. Guillouzo, S. Genicot, J. Mravec, J. Harholt, C. Wilkens, M. S. Motawia, B. Svensson, O. Tranquet, M. C. Ralet, B. Jorgensen, D. S. Domozych and W. G. T. Willats (2017). "Development of novel monoclonal antibodies against starch and ulvan - implications for antibody production against polysaccharides with limited immunogenicity." Sci Rep **7**(1): 9326.

Sakai, K., Y. Shimizu, T. Chiba, A. Matsumoto-Takasaki, Y. Kusada, W. Zhang, M. Nakata, N. Kojima, K. Toma, A. Takayanagi, N. Shimizu and Y. Fujita-Yamaguchi (2007). "Isolation and characterization of phage-displayed single chain antibodies recognizing nonreducing terminal mannose residues. 1. A new strategy for generation of anti-carbohydrate antibodies." Biochemistry **46**(1): 253-262.

Schaefer, J. V. and A. Pluckthun (2012). "Engineering aggregation resistance in IgG by two independent mechanisms: lessons from comparison of Pichia pastoris and mammalian cell expression." J Mol Biol **417**(4): 309-335.

Selvendran, R. R. and M. A. O'Neill (1985). Isolation and analysis of cell walls from plant material. Methods of Biochemical Analysis. D. Glick. New York, J. Wiley and Sons**:** 25-133.

Shadidi, M. and M. Sioud (2001). "An anti-leukemic single chain Fv antibody selected from a

synthetic human phage antibody library." Biochem Biophys Res Commun **280**(2): 548-552.

Sina, M., D. Farajzadeh and S. Dastmalchi (2015). "Effects of Environmental Factors on Soluble Expression of a Humanized Anti-TNF-alpha scFv Antibody in Escherichia coli." Adv Pharm Bull **5**(4): 455-461.

Somerville, C. (2007). "Biofuels." Curr Biol **17**(4): R115-119.

Stephen, A. M., G. O. Phillips and P. A. Williams (2006). Food Polysaccharides and Their Applications. Boca Raton, FL, CRC Press.

Stevenson, T. T., A. G. Darvill and P. Albersheim (1988). "Structural features of the plant cell-wall polysaccharide rhamnogalacturonan-II." Carbohydrate Research **182**(2): 207-226.

Stevenson, T. T., M. McNeil, A. G. Darvill and P. Albersheim (1986). "Structure of Plant Cell Walls : XVIII. An Analysis of the Extracellular Polysaccharides of Suspension-Cultured Sycamore Cells." Plant Physiol **80**(4): 1012-1019.

Talmadge, K. W., K. Keegstra, W. D. Bauer and P. Albersheim (1973). "The Structure of Plant Cell Walls: I. The Macromolecular Components of the Walls of Suspension-cultured Sycamore Cells with a Detailed Analysis of the Pectic Polysaccharides." Plant physiology **51**(1): 158-173.

Thomas, P. and T. G. Smart (2005). "HEK293 cell line: a vehicle for the expression of recombinant proteins." J Pharmacol Toxicol Methods **51**(3): 187-200.

Tschopp, J. F., P. F. Brust, J. M. Cregg, C. A. Stillman and T. R. Gingeras (1987). "Expression of the lacZ gene from two methanol-regulated promoters in Pichia pastoris." Nucleic Acids Res **15**(9): 3859-3876.

Urbanowicz, B. R., M. J. Pena, S. Ratnaparkhe, U. Avci, J. Backe, H. F. Steet, M. Foston, H. Li, M. A. O'Neill, A. J. Ragauskas, A. G. Darvill, C. Wyman, H. J. Gilbert and W. S. York

(2012). "4-O-methylation of glucuronic acid in Arabidopsis glucuronoxylan is catalyzed by a domain of unknown function family 579 protein." Proc Natl Acad Sci U S A **109**(35): 14253-14258.

Willats, W. G., L. McCartney, W. Mackie and J. P. Knox (2001). "Pectin: cell biology and prospects for functional analysis." Plant molecular biology **47**(1-2): 9-27.

Wong, D. (2008). "Enzymatic deconstruction of backbone structures of the ramified regions in pectins." The protein journal **27**(1): 30-42.

Wu, A. M., E. Hornblad, A. Voxeur, L. Gerber, C. Rihouey, P. Lerouge and A. Marchant (2010). "Analysis of the Arabidopsis IRX9/IRX9-L and IRX14/IRX14-L pairs of glycosyltransferase genes reveals critical contributions to biosynthesis of the hemicellulose glucuronoxylan." Plant Physiol **153**(2): 542-554.

York, W. S., L. K. Harvey, R. Guillen, P. Albersheim and A. G. Darvill (1993). "Structural analysis of tamarind seed xyloglucan oligosaccharides using beta-galactosidase digestion and spectroscopic methods." Carbohydr Res **248**: 285-301.

York, W. S. and M. A. O'Neill (2008). "Biochemical control of xylan biosynthesis - which end is up?" Curr Opin Plant Biol **11**(3): 258-265.

Zablackis, E., J. Huang, B. Muller, A. G. Darvill and P. Albersheim (1995). "Characterization of the cell-wall polysaccharides of Arabidopsis thaliana leaves." Plant Physiol **107**(4): 1129-1138.

Zeng, W., N. Jiang, R. Nadella, T. L. Killen, V. Nadella and A. Faik (2010). "A glucurono(arabino)xylan synthase complex from wheat contains members of the GT43, GT47, and GT75 families and functions cooperatively." Plant Physiol **154**(1): 78-97.

Zhang, G. F. and L. A. Staehelin (1992). "Functional compartmentation of the Golgi apparatus

of plant cells : immunocytochemical analysis of high-pressure frozen- and freeze-substituted sycamore maple suspension culture cells." Plant Physiol **99**(3): 1070-1083.

Zhang, H. (2013). "Empowering scFv with effector cell functions for improved anticancer therapeutics." Oncoimmunology 2(6): e24439.

Zhang, J. L., J. J. Gou, Z. Y. Zhang, Y. X. Jing, L. Zhang, R. Guo, P. Yan, N. L. Cheng, B. Niu and J. Xie (2006). "Screening and evaluation of human single-chain fragment variable antibody against hepatitis B virus surface antigen." Hepatobiliary Pancreat Dis Int **5**(2): 237-241.